THE UNIVERSITY *of* EDINBURGH

Atmospheric Profiles of CO_2 as Integrators of Regional Scale Exchange

Thomas Luke Smallman

Doctor of Philosophy
University of Edinburgh
2014

Abstract

The global climate is changing due to the accumulation of greenhouse gases (GHGs) in the atmosphere, primarily due to anthropogenic activity. The dominant GHG is CO_2 which originates from combustion of fossil fuels, land use change and management. The terrestrial biosphere is a key driver of climate and biogeochemical cycles at regional and global scales. Furthermore, the response of the Earth system to future drivers of climate change will depend on feedbacks between biogeochemistry and climate. Therefore, understanding these processes requires a mechanistic approach in any model simulation framework. However ecosystem processes are complex and non-linear and consequently models need to be validated against observations at multiple spatial scales.

In this thesis the weather research and forecasting model (WRF) has been coupled to the mechanistic terrestrial ecosystem model soil-plant-atmosphere (SPA), creating WRF-SPA. The thesis is split into three main chapters:

i. WRF-SPA model development and validation at multiple spatial scales, scaling from surface fluxes of CO_2 and energy to aircraft profiles and tall tower observations of atmospheric CO_2 concentrations.

ii. Investigation of ecosystem contributions to observations of atmospheric CO_2 concentrations made at tall tower Angus, Dundee, Scotland using ecosystem specific CO_2 tracers at seasonal and interannual time scales.

iii. An assessment of detectability of a policy relevant national scale afforestation by observations made at a tall tower. Detectability of changes in atmospheric CO_2 concentrations was assessed through a comparison of a control simulation, using current day forest extent, and an experimentally afforested simulation using WRF-SPA.

WRF-SPA performs well at both site and regional scales, accurately simulating aircraft profiles of CO_2 concentration magnitudes (error $<^{+}_{-}$ 4 ppm), indicating appropriate source sink distribution and realistic atmospheric transport. Hourly observations made at tall tower Angus were also well simulated by WRF-SPA (R^2 = 0.67, RMSE = 3.5 ppm, bias = 0.58 ppm). Analysis of CO_2 tracers at tall tower Angus show an increase in the seasonal error between WRF-SPA simulated atmospheric CO_2 and observations, which coincides with simulated cropland harvest. WRF-SPA does not simulate uncultivated land associated with agriculture, which in Scotland represents $\sim$36 % of agricultural holdings. Therefore, uncultivated land components may provide an explanation for the increase in model-data error. Interannual variation in weather is indicated to have a greater impact on ecosystem specific contributions to atmospheric CO_2 concentrations at Angus than variation in surface activity.

In a model experiment, afforestation of Scotland was simulated to test the impact on Scotland's carbon balance. The changes were shown to be potentially detectable by observations made at tall tower Angus. Afforestation results in a reduction in atmospheric CO_2 concentrations by up to 0.6 ppm at seasonal time scales at tall tower Angus. Detection of changes in forest surface net CO_2 uptake flux due to afforestation was improved through the use of a network of tall towers (R^2 = 0.83) compared to tall tower Angus alone (R^2 = 0.75).

Lay Abstract

The global climate is changing due to the accumulation of greenhouse gases (GHGs) in the atmosphere, primarily due to human activity. The dominant GHG is CO_2 which originates from burning of fossil fuels, land use change and management. Vegetation on the land surface is a key driver of climate and biogeochemical cycles (e.g. the carbon cycle) at regional and global scales. Furthermore, the response of the Earth system to future drivers of climate change will depend on feedbacks between biogeochemistry (e.g. photosynthesis) and climate. Therefore, understanding these processes requires a mechanistic approach in any model simulation framework. However ecosystem processes are complex and non-linear and consequently models need to be validated against observations at multiple spatial scales.

In this thesis the weather research and forecasting model (WRF) has been coupled to the soil-plant-atmosphere (SPA) land surface model, creating WRF-SPA. The thesis is split into three main chapters:

i. WRF-SPA model development and validation at multiple spatial scales, scaling from surface fluxes of CO_2, water and heat to aircraft profiles and tall tower observations of atmospheric CO_2 concentrations.

ii. Investigation of ecosystem contributions to observations of atmospheric CO_2 concentrations made at tall tower Angus, Dundee, Scotland using ecosystem specific CO_2 tracers at seasonal and interannual time scales.

iii. An assessment of detectability of a policy relevant national scale afforestation by observations made at a tall tower. Detectability of changes in atmospheric CO_2 concentrations was assessed through a comparison of a control simulation, using current day forest extent, and an experimentally afforested simulation using WRF-SPA.

WRF-SPA performs well at both site and regional scales, accurately simulating aircraft profiles of CO_2 concentration magnitudes (error $< \pm 4$ ppm), indicating appropriate source sink distribution and realistic atmospheric transport. Hourly observations made at tall tower Angus were also well simulated by WRF-SPA (R^2 = 0.67, RMSE = 3.5 ppm, bias = 0.58 ppm). Analysis of CO_2 tracers at tall tower Angus show an increase in the seasonal error between WRF-SPA simulated CO_2 and observations, which coincides with simulated cropland harvest. WRF-SPA does not simulate uncultivated land associated with agriculture, which in Scotland represents $\sim$36 % of agricultural holdings. Therefore, uncultivated land components may provide an explanation for the increase in model-data error. Interannual variation in weather is indicated to have a greater impact on ecosystem specific contributions to atmospheric CO_2 concentrations at Angus than variation in surface activity.

In a model experiment, afforestation of Scotland was simulated to test the impact on Scotland's carbon balance. The changes were shown to be potentially detectable by observations made at tall tower Angus. Afforestation results in a reduction in atmospheric CO_2 concentrations by up to 0.6 ppm at seasonal time scales at tall tower Angus. Detection of changes in forest surface net CO_2 uptake flux due to afforestation was improved through the use of a network of tall towers (R^2 = 0.83) compared to tall tower Angus alone (R^2 = 0.75).

Declaration

I declare that this thesis was composed by myself and that the work contained therein is my own, except where explicitly stated otherwise in the text.

Thomas Luke Smallman

Acknowledgements

After nearly four years of working on this PhD, for which three of those the model didn't work, there is a mountain of people who I owe my thanks to. First I would like to thank my supervisors John Moncrieff and Mat Williams who made the project what it was. In addition to John and Mat there have been many people who heve helped me out over my time here including: Tim Hill, Anthony Bloom, Georgios Xenakis, Cecile Menard and Lucy Rowland to name but a few. These people, and many more have been available to talk things through with and provide a little extra advice.

I would also like to thank Bronwen Whitney, John Carson, Iain McNicol, Tom Maxfield, Luke Ridley, Sam Jones, Amber Annette and so many other people who have made my time in Edinburgh outside of work what it has been. Thank you for the many trips to the pub, hiking, cycling, road trips, Thai boxing, climbing, gigs and 'cultural stuff'. Without these people the last four years would have been so much harder to get through.

Finally I'm grateful to my family whom have always allowed me to go off on tangents and continue shifting where my interests were headed. But also to Rachel who has made my time here so very enjoyable, I couldn't imagine being in Edinburgh without you being here too!

“The best laid schemes o’ mice an’ men Gang aft a-gley....”

Robert Burns’ poem ‘To a Mouse’, 1786

Contents

List of Figures

Chapter 1

Introduction: land-atmosphere exchange of CO_2

The Earth's climate is changing, and anthropogenic activity is shown to be the key driver of observed and predicted future change (IPCC, 2007). The global mean annual air temperature has increased by $0.76^{+}_{-}0.19$°C (1906–2005), but the observed rate of warming has not been constant. The rate of warming accelerated in the latter half of the 20^{th} century and is expected to continue accelerating into the 21^{st} century. Furthermore, anthropogenic emission of CO_2 and other greenhouse gases (GHGs), which drive climate change, are also expected to continue increasing at an accelerated rate into the 21^{st} century. There remains considerable uncertainty in the predictions of future climate change, but all predictions expect a warming ranging between 2.0°C and 4.5°C by 2100 (Figure 1.1) (Friedlingstein et al., 2006; IPCC, 2007). Due to the global importance of the impacts of climate change, e.g. on ecosystem services, and continuing uncertainty of its prediction, extensive research has been undertaken into the drivers and feedbacks of historical, current and predicted global climate change (e.g. Canadell et al., 2007; Sitch et al., 2008; Friedlingstein and Prentice, 2010; Qian et al., 2010; Kaplan et al., 2012).

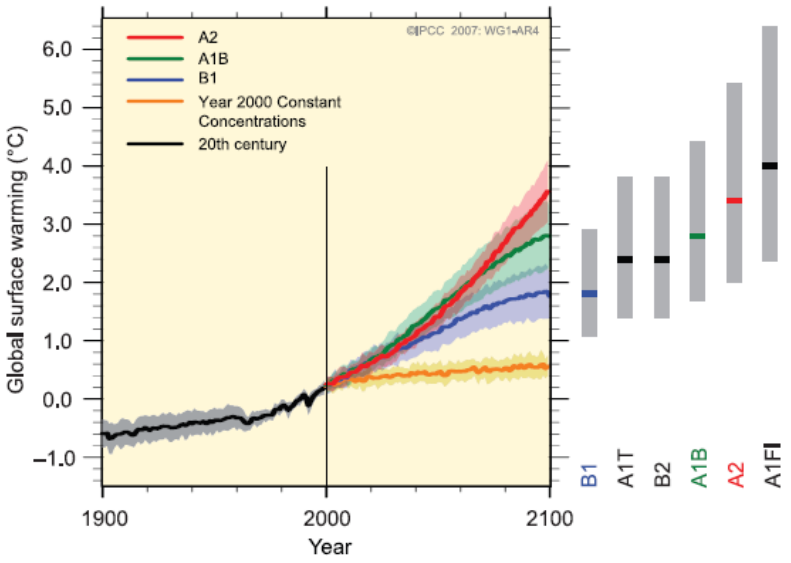

Figure 1.1: Simulated change in global mean air temperature with uncertainty estimates, from IPCC emissions scenarios (IPCC, 2007). Shows that while the range of possible future warming remains large there is agreement that there will be warming, due to accumulation of greenhouse gases in the atmosphere.

1.1 History of atmospheric CO_2 observation and investigation

Historical changes in air temperature and atmospheric CO_2 concentrations can be determined through analysis of ice cores (e.g. Petit et al., 1999; Jouzel et al., 2007). A strong correlation has been found between air temperature and atmospheric CO_2 concentrations over the last ∼650,000 years through examination of glacial / inter-glacial cycles in ice cores. However historical changes in CO_2 lag changes in air temperature by up to several thousand years (IPCC, 2007). Furthermore, during the glacial / inter-glacial cycles, atmospheric CO_2 concentrations have been bound between 180–300 ppm (Figure 1.2) (Petit et al., 1999).

The glacial / inter-glacial cycles of the last 650,000 years have been driven by changes in the Earth's orbit around the sun collectively called the Milankovitch cycles. The Milankovitch cycles consist of three separate cycles which describe changes in the Earth's orbit around the sun (eccentricity, precession and obliquity). These cycles alter the amount of solar radiation incident on the surface resulting in changes to the Earth's net radiation balance and ultimately affecting global mean temperature (Hays et al.,

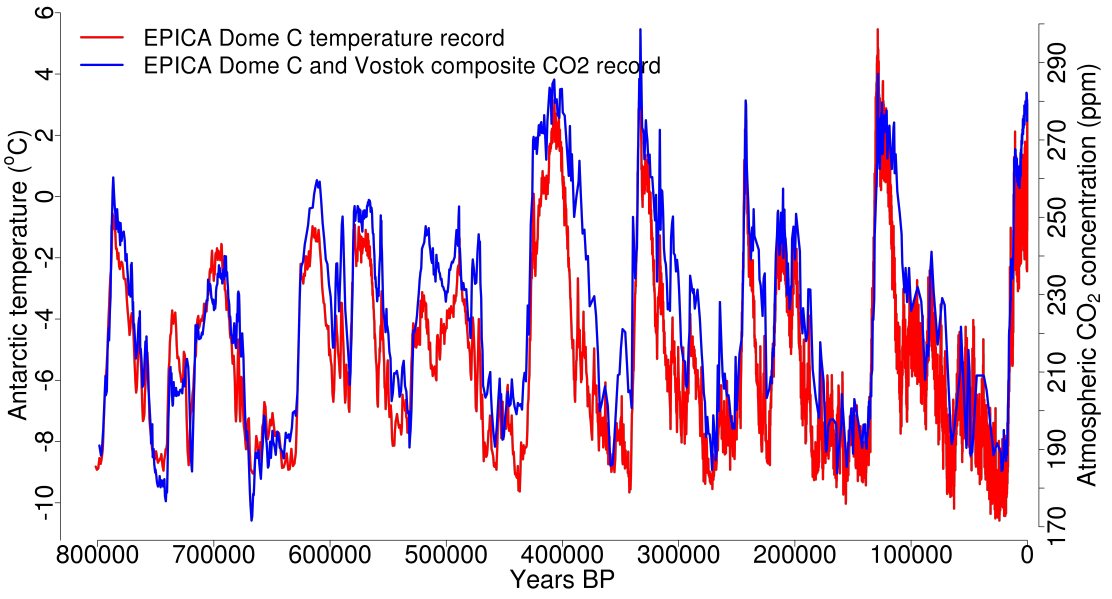

Figure 1.2: Surface air temperature and atmospheric CO_2 record for the last 800,000 years. Shows close correlation between temperature and atmospheric CO_2 concentrations glacial / inter-glacial cycles. Temperature and atmospheric CO_2 estimates are composite records from EPICA Dome C (Jouzel et al., 2007; Luthi et al., 2008).

1976; Kawamura et al., 2007). The global mean temperature change from glacial to inter-glacial periods are typically between 4°C to 10°C (Jouzel et al., 2007). The most recent inter-glacial transition was a warming of between 4°C to 7°C which compared to a predicted future warming by 2100 of between 2.0°C and 4.5 °C (IPCC, 2007), highlights that predicted anthropogenic warming is of a similar magnitude to that of a glacial / inter-glacial transition.

Due to recent warming the current mean air temperature for the northern hemisphere is likely to be the warmest it has been for at least 1,000 years (Cook et al., 2004). Furthermore global mean air temperatures are currently the warmest they have been since 1850 (e.g. Brohan et al., 2006); the majority of the observed increase occurred during the latter half of the 20^{th} century. Moreover, unlike during a transition from a glacial to inter-glacial period, the current increase in atmospheric CO_2 concentrations preceded the observed increase of temperature. Atmospheric CO_2 concentrations began increasing in $\sim$1750, coinciding with the onset of the industrial revolution in the northern hemisphere (IPCC, 2007). Current global average atmospheric CO_2 concentration far exceed those seen for the last $\sim$650,000 years (IPCC, 2007), reaching $\sim$393 ppm by

March 2013 (http://www.esrl.noaa.gov/gmd/ccgg/trends/, accessed 21/05/2013).

The potential for increasing atmospheric CO_2 concentration, and other GHGs, to drive global climate change is not a recent discovery. The ability of CO_2 and other GHGs to trap infra-red energy in the Earth's atmosphere, therefore resulting in warming, was first noted in the 1820s Joseph Fourier. However it was not until the late 19^{th} century that the effects of increased atmospheric CO_2 concentrations on global air temperature was calculated empirically (Arrhenius, 1896). Arrhenius calculated that doubling atmospheric CO_2 concentrations would lead to $\sim$5°C increase in mean global air temperature and hypothesised that changes in atmospheric CO_2 concentrations are linked to transition between glacial and interglacial periods. Furthermore, he correctly calculated that the effects of warming would not be uniform across latitudinal gradients, with more extreme warming towards the poles.

1.2 Contemporary measurement of CO_2

The prospect of global warming was not taken seriously until the first continuous measurements of atmospheric CO_2 concentrations from the Mauna Loa observatory, beginning in 1958, showed a long term increase (Keeling, 1960). The observed increase in atmospheric CO_2 concentrations were then attributed to anthropogenic emissions, primarily through burning of fossil fuels but also land use change and management (IPCC, 2007; Keeling et al., 2011). Furthermore, the rate of increase in atmospheric CO_2 concentrations has continued to accelerate, since these first observations, throughout the latter half of the 20^{th} and early 21^{st} century. The annual rate of atmospheric CO_2 accumulation has increased from $\sim$0.8 ppm in (1964–1971 average) (Keeling et al., 1976) to 1.9 ppm in 2005 (IPCC, 2007). In addition to the long term increase, seasonality in CO_2 concentrations was also observed. Seasonal reductions in atmospheric CO_2 concentrations coincides with summer in the northern hemisphere (Figure 1.3) (Keeling, 1960; Keeling et al., 1976, 2011).

The seasonal cycle observed in atmospheric CO_2 concentrations is due to photosyn-

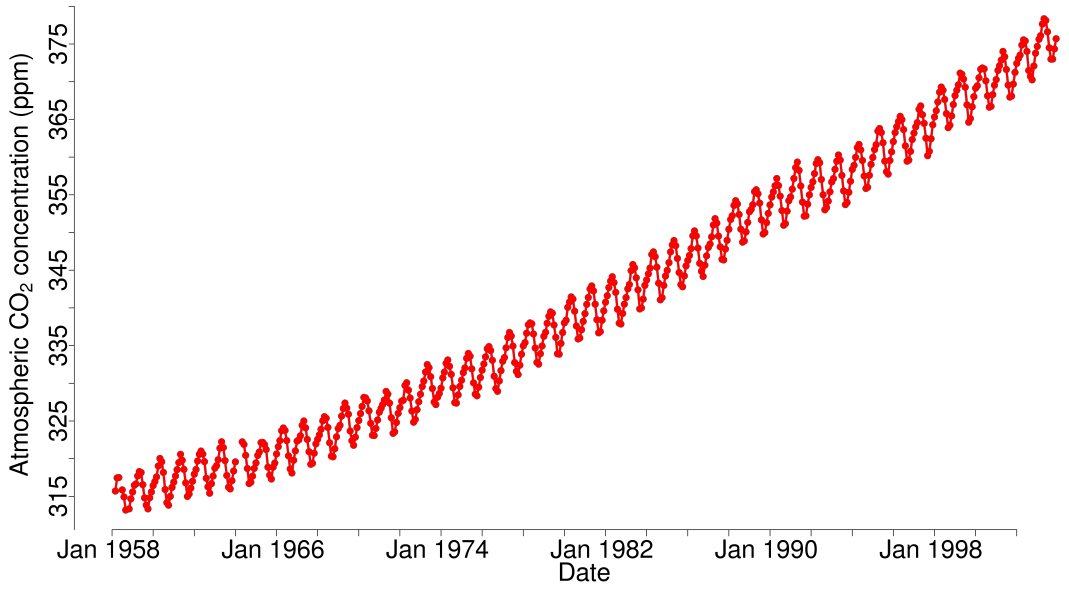

Figure 1.3: Monthly mean observations of seasonally varying atmospheric CO_2 concentrations from the Mauna Loa observatory. Seasonal reduction in atmospheric CO_2 coincides with the summer growing season in the northern hemisphere. Data from Keeling and Whorf (2005).

thetic activity of the terrestrial ecosystem, particularly of the northern hemisphere (Junge and Czeplak, 1968). Since the northern hemisphere has a larger land area than the southern hemisphere, there is proportionately greater photosynthetic activity during the northern hemisphere's growing season, resulting in a reduction in global atmospheric CO_2 concentration (i.e. the land surface is a net sink of CO_2) during the northern summer. Correspondingly during the northern hemisphere's winter, when respiratory processes dominate over photosynthesis, atmospheric CO_2 concentration increase (i.e. the land surface is a net source of CO_2). Despite seasonal variation of the terrestrial ecosystem being either a source or sink of CO_2, the global terrestrial biosphere is currently a net sink of CO_2 at annual time scales (Canadell et al., 2007).

1.3 Role of the terrestrial ecosystem

Exchange and feedbacks between the land surface and the atmosphere are highly complex processes and non-linear feedbacks occur at differing spatial and temporal scales, mediated through biogeochemical and biogeophysical processes that are typically linked

to ecosystem phenology (e.g. canopy height, rooting depth and leaf area index) (Bonan, 2008). Originally terrestrial ecosystems were considered to be passive, responding to changes in climate only (e.g. Koppen, 1936). In the 1970s it was first noted that the land surface can also drive climate through feedbacks (Charney, 1975). Charney (1975) showed that the high albedo of the Sahel desert relative to adjacent areas generates a thermal gradient resulting in horizontal advection of warm air which reduces precipitation locally and reinforces desert conditions. Since then further research has highlighted the complex and highly important role that the terrestrial land surface plays in global climate (e.g. Betts et al., 2007; Bonan, 2008; Friedlingstein and Prentice, 2010).

Currently the terrestrial ecosystem consumes a significant fraction of CO_2 from anthropogenic emissions (Canadell et al., 2007). However, the terrestrial ecosystem is complex, where some ecosystems are sinks of CO_2 and others are sources (Janssens et al., 2005; Thomson and van Oijen, 2007; Peters et al., 2010). Furthermore the terrestrial ecosystem is highly sensitive to disturbance (including human management) and variation in weather and climate (Sitch et al., 2008; Stoy et al., 2009; Peters et al., 2010), causing the fraction of anthropogenic CO_2 which the land consumes to vary significantly at interannual time scales (Figure 1.4) (Canadell et al., 2007). Therefore terrestrial ecosystems which are currently net sinks of CO_2 could in the future become sources or vice versa. To understand this better requires an improved understanding of the drivers of variability of sources and sinks such as changes in human management or in response to climate change (Friedlingstein et al., 2006; Thomson and van Oijen, 2007).

Land use change and management are often considered as a means of mitigating against the effects of anthropogenic emissions of CO_2 (IPCC, 2007). Afforestation and reforestation are commonly considered as part of mitigation strategies to increase terrestrial sequestration of CO_2, therefore reducing the accumulation of CO_2 in the atmosphere (IPCC, 2007; Kaplan et al., 2012). Arora and Montenegro (2011) predicted that 100 % afforestation of current cropland area would to lead to a small cooling effect on global mean temperature ($\leq$0.45°C, i.e. a reduction in the predicted warming not a net cooling), however 100 % afforestation is highly unrealistic. A 'more realistic' afforestation

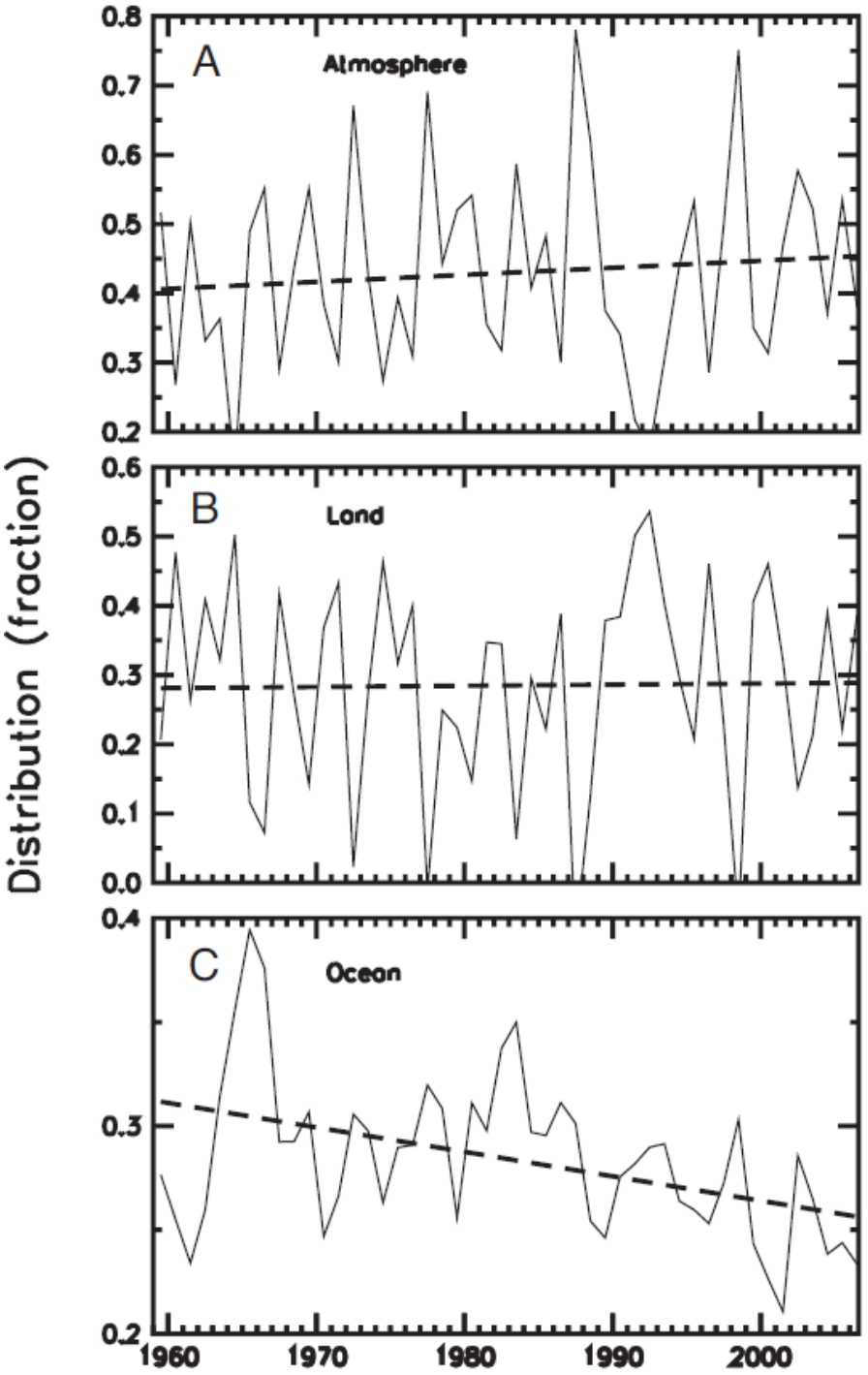

Figure 1.4: Fraction of anthropogenic CO_2 originating from fossil fuel combustion, land use and land cover change which remains in either (A) the atmosphere, (B) the terrestrial ecosystem and (C) the ocean. Shows considerable interannual variation in the fraction remaining in the atmosphere and consumed by the land surface, while there is comparatively little variation in ocean sequestration. Figure from Canadell et al. (2007).

of 50 % of global agricultural land was simulated to have a cooling effect of 0.25°C. The simulated cooling was mediated through an increase in global CO_2 sequestra-

tion and an increase in evapotranspiration, particularly at low latitudes. The simulated cooling is small compared to the effect of historical deforestation and agricultural expansion which are simulated to have resulted in a net cooling effect on mean global air temperature of 1-2°C through increased land surface albedo (Bala et al., 2007; Betts et al., 2007; Davin and de Noblet-Ducoudre, 2010; Kaplan et al., 2012). However, given that the simulated response of the land surface to increasing atmospheric CO_2 and climate change remains highly uncertain (Figure 1.5), the response of the land surface due to land use and land cover change (LULCC) should be closely examined (Friedlingstein et al., 2006; Sitch et al., 2008; Friedlingstein and Prentice, 2010; Qian et al., 2010). Moreover previous modelling studies which have investigated the impact of afforestation and deforestation have tended to consider global or large latitudinal scale LULCC (e.g. Betts et al., 2007; Arora and Montenegro, 2011). Policy relevant afforestation is unlikely to cover a majority of available agricultural land, resulting in a globally averaged impact that is likely to be smaller in magnitude than those simulated by e.g. Arora and Montenegro (2011). Therefore the regional impact of policy relevant afforestation on atmospheric CO_2 concentrations and surface meteorological variables remains to be investigated.

The effectiveness of mitigation strategies through LULCC needs to be assessed using reliable and robust methodologies. Methods for monitoring CO_2 sequestration associated with land use change such as afforestation include periodical forest inventories (Forestry Commission Scotland, 2009), Earth observation (EO) using radar backscatter of above ground biomass (which can be related to carbon stocks) (Le Toan et al., 2011; ESA, 2012) and model based atmospheric inversion of atmospheric CO_2 concentrations to infer surface CO_2 source sink distribution and magnitude (ICOS, 2012). Forest inventories are labour intensive and EO estimates of above ground biomass fail to account for changes in below ground carbon stocks, which represent a significant carbon store (Bradley et al., 2005). Furthermore the response of soil carbon stocks to management is complex, varying depending on land use history and time since afforestation, therefore changes in soil carbon must also be included in monitoring (Paul et al., 2002; Poeplau et al., 2011). Inverse modelling of atmospheric CO_2 concentrations can help to explain the net ecosystem exchange of CO_2 (NEE) which includes

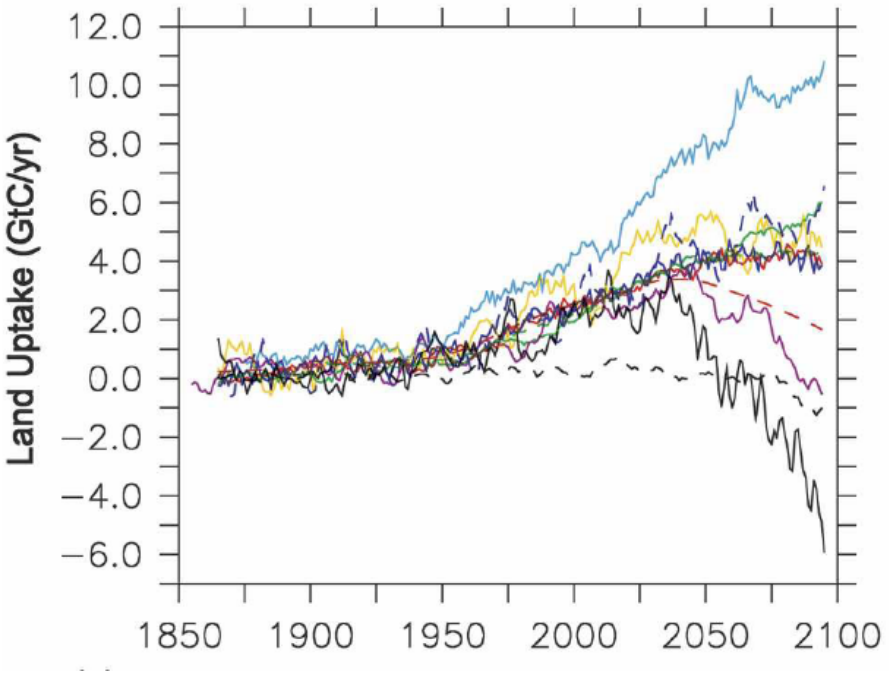

Figure 1.5: Global land carbon uptake (positive values represent a net sink) as simulated by 11 state-of-the-art models. Shows that uncertainty in projections increases the further in the future the simulation progresses as models diverge, due to differences in the representation of ecosystem processes within land surface models. Figure from Friedlingstein et al. (2006)

soil CO_2 exchange (Gerbig et al., 2009; Peters et al., 2010).

1.4 Investigation of surface CO_2 exchange with simulation models

Simulation models, such as Earth System Models (ESMs), are an important tool in furthering our understanding of ecosystem-atmosphere exchange. ESMs have their origin in early general circulation models (GCMs) which simulated atmospheric transport with a simple representation of ocean and terrestrial processes (Gates et al., 1999). Over time, model complexity has progressively increased, with the coupling of ocean models to simulate ocean circulation and exchange (Covey et al., 2003), and the addition of detailed land surface models (LSMs) which include climate-biogeochemical feedbacks (Cox et al., 2000). The current generation of ESMs contain state-of-the-art mathematical descriptions of processes such as atmospheric dynamics, ocean circulation, cryosphere, terrestrial and marine ecosystems (e.g. HadGEM2, Collins et al.,

2011).

Interactions between the terrestrial ecosystem and the atmosphere are simulated by LSMs. There are a broad range of LSMs, with varying levels of complexity, ranging from those which deal with exchange of water and energy only to mechanistic representations of biogeochemical (e.g. photosynthesis and respiration) and biogeophysical processes (e.g. reflectance due to albedo). The level of detail and complexity in LSMs varies depending on the model's purpose; most LSMs contain a representation of the vegetative canopy / leaf level processes, soil hydrology, soil thermal properties, and a mechanism to represent partitioning of the surface energy balance into latent, sensible and ground heat fluxes in response to meteorological drivers. Appropriate partitioning of the surface energy balance is critical to drive realistic near surface turbulent mixing and planetary boundary layer (PBL) development (Steeneveld et al., 2011; Xie et al., 2012). Each heat flux term plays an important role in coupling the surface and lower atmosphere, for example increases in latent heat results in a surface cooling effect, while sensible heat significantly impacts vertical mixing in the PBL and ground heat flux allows the soil to act as a heat store during the day which is released at night. A significant component of latent heat is transpiration which in turn is regulated through stomatal conductance (Avissar, 1998). Regulation of stomatal conductance is a key ecosystem function impacting the partitioning of net radiation, moreover stomatal conductance represents a coupling point between ecosystem hydrological and carbon cycles (Avissar, 1998; Tuzet et al., 2003).

Transpiration is dependent on both atmospheric demand for water and available water supply from the soil, regulated through stomatal conductance (Tuzet et al., 2003). Transpiration is commonly implemented into LSMs using the Penman-Monteith equation (Monteith, 1965; Jones, 1992), which attempts to mechanistically estimate leaf transpiration rate based on net radiation, atmospheric demand, boundary layer conductance and stomatal conductance. The simplest method for estimating stomatal conductance is through use of an equation describing the empirical relationship between field observations of stomatal conductance and atmospheric demand (e.g. Jarvis, 1976). Jarvis type empirical models are commonly used in offline LSMs or those which do not in-

clude a representation of the carbon cycle (e.g. NOAH, Chen and Dudhia, 2001). A common alternative to a Jarvis type empirical model is a semi-empirical representation of stomatal conductance which links transpiration to photosynthetic activity and atmospheric demand, such as Ball-Berry (Collatz et al., 1991). The Ball-Berry model of stomatal conductance, or its variants, have been implemented in many widely used LSMs (e.g. Sellers et al., 1996; Oleson et al., 2010; Best et al., 2011; Niu et al., 2011). In semi-empirical models of stomatal conductance, such as Ball-Berry, the impact of soil water stress on rates of transpiration and photosynthesis are included through an empirical coefficient dependant on soil moisture within the rooting zone relative to a prescribed wilting point (e.g. Jules, Clark et al., 2011). However, there are some LSMs which use mechanistic models of stomatal conductance that explicitly couple photosynthesis to atmospheric demand and available supply of water from the soil, creating a soil-plant-atmosphere continuum (Williams et al., 1996; Tuzet et al., 2003).

LSMs intended for use in ESMs for long term global simulations ($>$10 years) must, in addition to simulating ecosystem processes, be able to simulate successional processes such as the dynamic global vegetation model (DGVM) TRIFFID model used in HadCM3 (Cox et al., 2000; Cox, 2001). DGVMs include a representation of ecosystem carbon dynamics that describes seasonal variation in ecosystem phenology, representing distinct plant functional types (PFTs) such as forests or grassland. Moreover DGVMs often contain parameterisations of competition between PFTs, allowing the surface composition of PFTs to vary over time, representing successional processes (e.g. Woodward et al., 1995; Cox et al., 2000; Krinner et al., 2005). However, many LSMs contain simplified parameterisation of carbon dynamics which simulate seasonally varying ecosystem phenology, suitable for relatively short multi-annual simulations ($<$10 years), such as NOAH-MP (Niu et al., 2011).

As our understanding of ecosystem processes has improved and as computational resources have increased, LSMs have been upgraded to include additional ecosystem processes and improved parameterisation. The current generation of LSMs commonly represent both biogeophysical and biogeochemical processes, to allow realistic representation of complex atmosphere-ecosystem feedbacks (Figure 1.6) (Bonan, 2008).

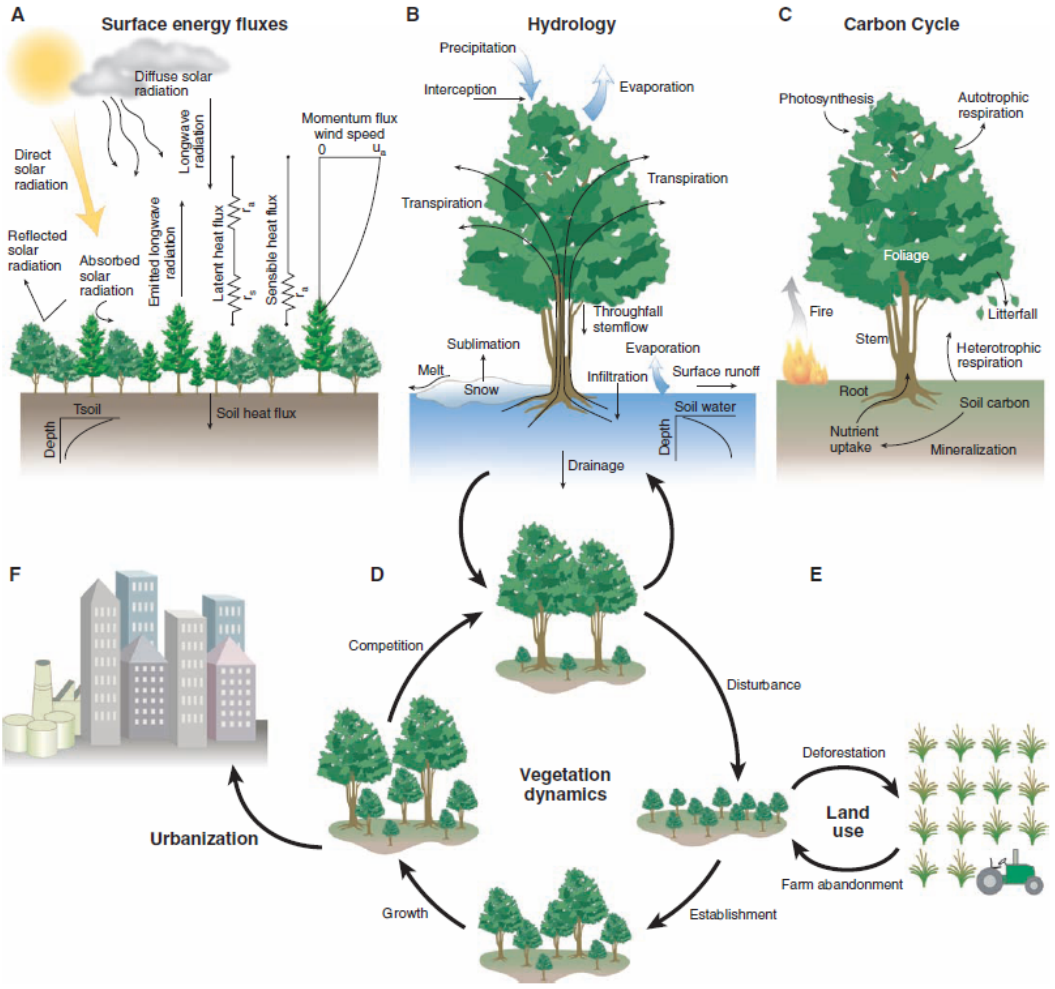

Fig. 2. The current generation of climate models treats the biosphere and atmosphere as a coupled system. Land surface parameterizations represent the biogeophysics, biogeochemistry, and biogeography of terrestrial ecosystems. **(A)** Surface energy fluxes and **(B)** the hydrologic cycle. These are the core biogeophysical processes. Many models also include **(C)** the carbon cycle and **(D)** vegetation dynamics so that plant ecosystems respond to climate change. Some models also include **(E)** land use and **(F)** urbanization to represent human alteration of the biosphere.

Figure 1.6: Shows many of the key processes and interactions between vegetation and the atmosphere which are now commonly included in land surface models. Figure from Bonan (2008)

State-of-the-art LSMs can now include parameterisations for multi-layer canopies accounting for radiative transfer through the canopy (Wang and Leuning, 1998) and turbulent processes above, within and below the canopy (e.g. Sellers et al., 1996; Niu et al., 2011).

Until recently crop modelling within LSMs has received little attention (Sus et al., 2010). Previously crops were often modelled as a natural grassland (Osborne et al., 2007). But, as our understanding of the importance of human management of the land surface has improved, such as the impact of arable agriculture on surface albedo (Betts et al., 2007; Van den Hoof et al., 2011), LSMs increasingly include parameter-

isation that include managed ecosystems and their impacts on atmosphere-ecosystem exchange (Lokupitiya et al., 2009; Sus et al., 2010; Van den Hoof et al., 2011; Levis et al., 2012).

Land-atmosphere exchanges and feedbacks are often distinct to each ecosystem type, particularly at longer time scales (e.g. seasonal and longer) (Stoy et al., 2009). These feedbacks, mediated through biogeochemical and biogeophysical processes, are linked to ecosystem phenology which can vary significantly between ecosystems, such as forest and cropland. Therefore heterogeneity in the land surface needs to be realistically modelled to accurately predict regional scale exchange (Avissar, 1998; Schomburg et al., 2012). However ecosystem heterogeneity occurs at fine spatial scales (e.g. kilometre scale or less) necessitating the use of coupled atmosphere-ecosystem models that are able to simulate the land surface at a high enough spatial resolution to accurately simulate the effects of ecosystem heterogeneity, but also dynamic ecosystem phenology.

Mesoscale meteorological models are useful for studying regional scale processes due to their ability to operate at high spatial resolutions. High spatial resolutions allow improved simulation, compared to global ESMs, of mesocale circulation that have a significant impact on regional transport e.g. coastal winds, katabatic winds (Nicholls et al., 2004; Riley et al., 2005; Ahmadov et al., 2009), and complex forcing of heterogeneous vegetation (Sarrat et al., 2007). Ahmadov et al. (2009) demonstrated a three fold improvement in correlation between simulated atmospheric CO_2 concentrations and observations made at a tall tower, when comparing between coarse (0.83°x1.25° or $\sim$92 km x $\sim$100 km) and fine (2 km x 2 km) horizontal model resolutions.

Mesoscale models provide a means to upscale land surface exchanges (i.e. net release and net uptake of CO_2) to observations made within the PBL (e.g. at a tall tower or aircraft observations) (Ahmadov et al., 2009; Tolk et al., 2009). Atmospheric tracers of CO_2 can be used to explore respiratory and photosynthetic exchange transported through the atmosphere, making it possible to gain information on how each ecosystem contributes to observations of atmospheric CO_2 (e.g. Tolk et al., 2009) and how these contributions vary at seasonal and interannual time scales. Mesoscale models are

also used to drive atmospheric inversions of atmospheric CO_2 observations made at a tall tower or by aircraft, to inform on regional scale carbon fluxes (e.g. Gurney et al., 2002; Nehrkorn et al., 2010; Peters et al., 2010; Lauvaux et al., 2012). In response to the requirement for more observations to be made at tall towers, several regional networks have been established, such as the European Union supported Integrated Carbon Observing System (ICOS, 2012).

Atmospheric inversion models of observations of atmospheric CO_2 concentrations are able to detect large scale, large magnitude interannual variations in CO_2 exchange, such as the Europe wide heat wave in 2003 which is estimated to have resulted in a large scale reduction in carbon sequestration across Europe (Ciais et al., 2005; Peters et al., 2010). However there remains uncertainty over the ability of regional scale inversions to detect small magnitude changes in surface exchange. Peters et al. (2010) suggested two contrasting hypotheses to explain increases in regional estimates of sequestration in the years following the European 2003 heat wave. First, increased sequestration may have been due to interannual variation in plant phenology, i.e. regrowth of leaf area lost due to water stress during the heat wave. Second, interannual variation of atmospheric transport may have significantly altered the footprint of tall tower observations. Changes to the footprint alters the area for which the observations convey information potentially significantly altering the spatial distribution and magnitude of sequestration estimates, similar to the effect of altering the number of tall towers used to provide observations of a given area (e.g. Lauvaux et al., 2012).

1.5 Investigation of CO_2 exchange with observations made in the PBL

Site scale observations such as those from eddy covariance provide high temporal resolution information on ecosystem NEE, evaporation and sensible heat flux ($\sim$100 m to 1 ha scale) (Moncrieff et al., 1997). The eddy covariance method results in a temporally and spatially averaged net ecosystem exchange between the atmosphere and the land surface. Long term eddy covariance measurements provide information on diur-

nal, seasonal and interannual exchange and variation (e.g. Clement et al., 2012). Such information is critical for LSM development and validation. However, eddy covariance observations have a relatively small spatial coverage compared to policy demands for national scale estimates of CO_2 exchange. This creates a requirement for networks of eddy covariance observations such as CARBOEUROPE (Dolman et al., 2006) but also observations which are representative of larger spatial scales to inform on the regional carbon balance (ICOS, 2012).

Measurements of atmospheric CO_2 concentrations (e.g. aircraft profiles and tall towers) provide information, when used in conjunction with models, on the spatial distribution and magnitude of sources and sinks of CO_2 at regional scales (Vermeulen et al., 2011; Lauvaux et al., 2012; Miles et al., 2012). Vertical profiles of atmospheric CO_2 observed from aircraft provide spatially integrated information on regional CO_2 exchange, where the surface areas over which integration occurs progressively increases as the height of observation increases several kilometres above the surface. Vertical profiles also provide information on atmospheric transport through the vertical structure of the observed CO_2 profile. Accurate simulation of vertical profiles requires modelling of realistic transport, and appropriate source sink distribution and magnitude of CO_2 exchange. Aircraft observations, however, provide relatively poor temporal resolution and are commonly biased to day time observations only, due to logistical issues for airborne campaigns.

Observations made at tall towers provide high temporal resolution information allowing investigation of ecosystem processes at sub-diurnal to inter-annual scales. However, the typical measurement height from a tall tower ($\sim$200 m) is far lower than observations from aircraft, with the result that the observations integrate over a smaller area. Moreover tall tower observations are dominated by CO_2 exchange originating within the local area of a tower ($\sim$100 km) (Gerbig et al., 2009; Vermeulen et al., 2011; Lauvaux et al., 2012; Miles et al., 2012) but observations made at tall towers can also be influenced by regional scale exchange. For example at the Cabauw tower in the Netherlands, an area of $\sim$500 x 700 km is expected to contribute up to $\sim$ 50 % of the observed signal (Vermeulen et al., 2011).

Despite the local bias in observations made at tall towers, inversion studies have shown that the regional level net carbon balance can be detected using a relatively sparse network of tall towers (Lauvaux et al., 2012). However the spatial distribution of regional sources and sinks is dependent on the density and location of tall towers within an observing network (Lauvaux et al., 2012). Therefore it remains uncertain whether tall tower observations are able to detect changes in surface CO_2 due to changes in ecosystem composition which occurs at sub-regional scales (e.g. policy relevant afforestation).

1.6 Context of the PhD

Scotland offers an ideal opportunity for the development and use of a high resolution mesoscale meteorological model. Scotland provides a highly complex topography and land use heterogeneity, with a longitudinal gradient from dominantly forested and peatland areas in the north west to pasture in the central and south west and arable cropland in the east. Critically, multi-annual and multi-scale observations are available for Scotland's dominant ecosystem types (evergreen forest, managed grassland and arable cropland).

Scotland is host to what is currently the UK's only tall tower equipped for near continuous measurements of greenhouse gases, including CO_2. The tall tower is a 222 m (observation height above the surface) communication transmitter located at Angus (TTA), near Dundee, Scotland (Figure 1.7) and has been operational since the end of 2005 offering a multi-annual dataset. In addition, the School of GeoSciences, University of Edinburgh, collected vertical profiles of atmospheric CO_2 mixing ratios by light aircraft between 2001 and 2007. Aircraft profiles were collected above Griffin forest, Perthshire, Scotland at roughly 6 week intervals at heights ranging between 800 m - 3000 m above sea level, providing both seasonal and inter-annual observations of regionally integrated atmospheric CO_2 concentrations. Furthermore multi-annual eddy covariance observations are available for Scotland's dominant ecosystems, through the CarboEurope network (`www.carboeurope.org/`).

Figure 1.7: Tall tower Angus (TTA), a 222 m high (observation height) tall tower located on the east coast of Scotland, near Dundee. TTA is currently the only tall tower in the UK operationally collecting atmospheric measurements of CO_2 and other trace gases.

In this PhD the mesoscale meteorological Weather Research & Forecasting (WRF) model and the mechanistic terrestrial ecosystem Soil Plant Atmosphere (SPA) model were coupled, forming WRF-SPA. The novel WRF-SPA atmosphere-ecosystem model has been used to investigate the available wealth of multi-annual, multi-scale observation available for Scotland. WRF-SPA was used to (i) determine the effect of coupling a mechanistic LSM into the WRF model framework, (ii) improve our understanding of ecosystem information contained within observations made at TTA, and (iii) assess the detectability of afforestation by current and potential observations of Scotland.

1.6.1 WRF-SPA coupled ecosystem-atmosphere model

The weather research and forecasting model (WRF, Skamarock et al., 2008) is a state-of-the-art mesoscale numerical weather model. WRF uses non-hydrostatic dynamical equations, i.e. explicit simulation of 3-dimensional atmospheric transport, allowing simulation of very high horizontal spatial resolutions ($<$ 1 km). The WRF model is a rapidly developing system, which has been designed to be highly adaptable, with a

portable code for use on massively parallel systems and a modular structure to allow for tailoring to specific uses. The WRF model has been extensively validated over a range of locations around the world (e.g. Ahmadov et al., 2007; Borge et al., 2008; Zhang, 2008; Ahmadov et al., 2009; Wang et al., 2009) and performs favourably in comparison to other commonly used mesoscale meteorological models, such as the Regional Atmospheric Modelling System (RAMS) (Sarrat et al., 2007; Steeneveld et al., 2011). However WRF does not simulate exchange and transport of CO_2 between the land and atmosphere. Furthermore the default WRF LSM NOAH, while methodologically advanced, does not include a carbon cycle or mechanistic parameterisations of ecosystem hydraulics (e.g. regulation of stomatal conductance). Due to WRF's modular structure and advanced representation of atmospheric dynamics, the model is ideal for coupling with a new LSM to address the deficiencies in its current representation of the land surface. The SPA terrestrial ecosystem model includes both a representation of the terrestrial carbon cycle and a mechanistic parameterisation of plant hydraulics (Williams et al., 1996, 2005).

The Soil Plant Atmosphere (SPA, Williams et al., 1996) model is a mechanistic terrestrial ecosystem model. SPA has a vertically distributed canopy model allowing variation of photosynthetic parameters through the canopy, based on field measurements, and a multi-layer radiative transfer scheme that models the distribution of direct and diffuse radiation, and sunlit and shaded leaf areas (Williams et al., 1998). SPA uses a mechanistic model of stomatal conductance linking atmospheric demand and available water supply from the soil through plant hydraulics, explicitly coupling plant carbon and hydrological cycles (Williams et al., 1996, 2001). Unlike the commonly used semi-empirical Ball-Berry model of stomatal conductance, SPA is parameterised directly from ecophysiological measurements such as rooting depth, plant hydraulic conductance and canopy structure (e.g. Wright et al., 2012). A crop development model has been included in SPA allowing for inclusion of this highly important ecosystem under human management (Sus et al., 2010).

SPA has been extensively validated against eddy covariance observations from several distinct ecosystems including temperate deciduous forests (Williams et al., 1996), Arc-

tic tundra (Williams et al., 2000), temperate evergreen forests (Williams et al., 2001) and, temperate crop systems (Sus et al., 2010). While not initially developed for use in coupled atmosphere-ecosystem models, SPA has previously been coupled to PBL models (Lee and Mahrt, 2004; Hill et al., 2008). Hill et al. (2008) successfully demonstrated that SPA could include feedbacks and drive PBL development that agreed with radiosonde observations.

WRF-SPA, the coupling between WRF and SPA, combines a state-of-the-art representation of atmospheric dynamics with a mechanistic terrestrial ecosystem model, capable of generating realistic feedbacks to drive PBL development. The addition of ecosystem specific CO_2 tracers representing net uptake and release of CO_2 make it possible to scale from observations made at the site scale (e.g. eddy covariance) to those impacted by regional scale exchange (e.g. at a tall tower and with aircraft profiles).

1.7 Research Questions

ESMs and mesoscale models have been successfully used to investigate the carbon cycle at both global and regional scales. However, there remains uncertainty in the predicted response of the terrestrial ecosystem, through net ecosystem exchange of CO_2 (NEE) and feedbacks mediated through the close coupling between the land surface and PBL processes (Friedlingstein et al., 2006; Bonan, 2008; Sitch et al., 2008; Friedlingstein and Prentice, 2010). Progress in this area requires further development of the representation of land surface processes in LSMs used within atmospheric models, and in this thesis the mechanistic SPA model was coupled to WRF, creating WRF-SPA. Chapter 2 describes the coupling of WRF-SPA (additional information on the WRF-SPA coupling is available in Appendix A), modifications to either model and an extensive validation using multi-scale, multi-annual observations. The impact on surface exchange due to the addition of SPA has been assessed through a comparison with the unmodified WRFv3.2 at hourly and seasonal time scales. In Chapter 2 we test two hypothesis "The addition of a mechanistic LSM will lead to improvements in the prediction of surface exchanges compared with the less mechanistic NOAH LSM" and

"The mechanistic representation of surface fluxes and feedbacks simulated by SPA will drive realistic atmospheric transport". To assess these hypotheses a number of specific questions were asked.

Q1 Can WRF-SPA realistically model surface meteorological variables and fluxes across a multi-annual period?

Q2 Does WRF-SPA scale realistically from surface measurements to regional scale observations, specifically aircraft profiles?

Q3 Does WRF-SPA lead to an improvement in surface fluxes compared to the unmodified WRFv3.2?

Observations of atmospheric CO_2 concentrations made at tall towers are used by both forward running models and atmospheric inversion models to help explain surface CO_2 exchange. Therefore models are dependent on the relevant ecosystem information contained within these observations. In chapter 3 ecosystem specific CO_2 tracers are used to investigate how Scotland's dominant ecosystems contribute to observations of atmospheric CO_2 concentrations from TTA, at seasonal and interannual time scales. Furthermore, model-data mismatches have been investigated to determine whether ecosystem process knowledge can be inferred. Chapter 3 asks a number of specific questions to address the following hypothesis "Observations of atmospheric CO_2 concentrations made at tall tower Angus contains information representative of seasonal and interannual variation of ecosystem activity at the national scale of Scotland".

Q4 Does WRF-SPA more accurately simulated observed atmospheric CO_2 concentrations compared to a coarse resolution global atmospheric inversion model?

Q5 Can ecosystem specific CO_2 tracers be used to inform on which ecosystem processes and land covers are responsible for observed variations in atmospheric CO_2 concentrations?

Q6 Can observations made at TTA detect variation in ecosystem carbon uptake, for ecosystems within the footprint of TTA, at seasonal and interannual time scales?

ESM have been used to simulate the global scale impacts of land use and land cover change, such as historical expansion of agriculture (Betts et al., 2007) and potential future afforestation (Arora and Montenegro, 2011). However, the ability of regional scale observations of atmospheric CO_2 concentrations, such as those made at tall towers, to detect changes in terrestrial carbon balance due to policy relevant land cover management remains uncertain. Furthermore, altering the surface ecosystem composition will change the surface net radiation and turbulent exchange, potentially resulting in changes to regional scale atmospheric transport.

In chapter 4, the detectability of a policy relevant afforestation experiment is assessed using WRF-SPA. Simulated afforestation is consistent with current policy of the Scottish Government, where an additional 650,000 ha of Scotland is planned to be afforested by 2050 as part of Scotland's commitment to reducing its net carbon emissions. Specific questions are asked to address the hypothesis "Afforestation will result in a reduction in atmospheric CO_2 concentration of a magnitude greater than observation detection limits".

Q7 Does afforestation result in a change in atmospheric CO_2 concentrations which is detectable by current observations made at a tall tower Angus?

Q8 Can detection of afforestation on forest carbon uptake be improved through use of an alternate tall tower or a network of tall towers?

Q9 Can detection of seasonal variation in ecosystem carbon uptake be improved through use of a tall tower network?

Q10 Does changing Scotland's ecosystem composition, i.e. afforestation, alter atmospheric transport?

Q11 Does afforestation result in changes to surface meteorological variables?

The overall objective of this thesis is the development of a new coupled mesoscale model, WRF-SPA, and to use WRF-SPA to improve our understanding of regional scale observations of atmospheric CO_2 concentrations and the information contained

within them relating observations to exchanges by the terrestrial ecosystem. The thesis is divided into three research papers (Chapters 2–4) which set out to answer the 11 questions asked above, with a view to addressing the overall thesis objective.

1.8 Declaration of other authors contributions

The research chapters in this thesis have been written as manuscripts for submission to scientific journals. I declare that all research and text are written by Luke Smallman. John B. Moncrieff and Mathew Williams, as the thesis supervisors and co-authors, provided comments and guidance relevant to their role as supervisors and as such was their contribution to the manuscripts for submission.

References

Ahmadov, R., C. Gerbig, R. Kretschmer, R. Koerner, B. Neininger, A. J. Dolman, and C. Sarrat, 2007: Mesoscale covariance of transport and CO_2 fluxes: Evidence from observations and simulations using the WRF-VPRM coupled atmosphere-biosphere model. *J. Geophys. Res.-Atmos.*, **112**, D11.

Ahmadov, R., C. Gerbig, R. Kretschmer, S. Koerner, C. Roedenbeck, P. Bousquet, and M. Ramonet, 2009: Comparing high resolution WRF-VPRM simulations and two global CO_2 transport models with coastal tower measurements of CO_2. *Biogeosciences*, **6**, 807–817.

Arora, V. K. and A. Montenegro, 2011: Small temperature benefits provided by realistic afforestation efforts. *Nat. Geosci.*, **4**, 514–518, doi:10.1038/NGEO1182.

Arrhenius, S., 1896: On the influence of carbonic acid in the air upon the temperature of the ground. *Journal of Science (Fifth Series)*, **41**, 237–276.

Avissar, R., 1998: Which type of soil vegetation atmosphere transfer scheme is needed for general circulation models: a proposal for a higher order scheme. *J. Hydrol.*, **212213**, 136 – 154, doi:10.1016/S0022-1694(98)00227-3.

Bala, G., K. Caldeira, M. Wickett, T. J. Phillips, D. B. Lobell, C. Delire, and A. Mirin, 2007: Combined climate and carbon-cycle effects of large-scale deforestation. *Proc. Natl. Acad. Sci. U. S. A.*, **104**, 6550–6555, doi:10.1073/pnas.0608998104.

Best, M. J., M. Pryor, D. B. Clark, G. G. Rooney, R. L. H. Essery, C. B. Menard, J. M. Edwards, M. A. Hendry, A. Porson, N. Gedney, L. M. Mercado, S. Sitch, E. Blyth, O. Boucher, P. M. Cox, C. S. B. Grimmond, and R. J. Harding, 2011: The Joint UK Land Environment Simulator (JULES), model description - Part 1: Energy and water fluxes. *Geosci. Model Dev.*, **4**, 677–699, doi:10.5194/gmd-4-677-2011.

Betts, R. A., P. D. Falloon, K. K. Goldewijk, and N. Ramankutty, 2007: Biogeophysical effects of land use on climate: Model simulations of radiative forcing and large-scale temperature change. *Agr. Forest Meteorol.*, **142**, 216–233.

Bonan, G. B., 2008: Forests and climate change: Forcings, feedbacks, and the climate benefits of forests. *Science*, **320**, 1444–1449.

Borge, R., V. Alexandrov, J. J. del Vas, J. Lumbreras, and E. Rodriguez, 2008: A comprehensive sensitivity analysis of the WRF model for air quality applications over the Iberian Peninsula. *Atmos. Environ.*, **42**, 8560–8574, doi:10.1016/j.atmosenv.2008.08.032.

Bradley, R., R. Milne, J. Bell, A. Lilly, C. Jordan, and A. Higgins, 2005: A soil carbon and land use database for the United Kingdom. *Soil Use Manage.*, **21**, 363–369, doi:10.1079/SUM2005351.

Brohan, P., J. J. Kennedy, I. Harris, S. F. B. Tett, and P. D. Jones, 2006: Uncertainty estimates in regional and global observed temperature changes: A new data set from 1850. *J. Geophys. Res.-Atmos.*, **111**, n/a–n/a, doi:10.1029/2005JD006548.

Canadell, J. G., C. Le Quere, M. R. Raupach, C. B. Field, E. T. Buitenhuis, P. Ciais, T. J. Conway, N. P. Gillett, R. A. Houghton, and G. Marland, 2007: Contributions to accelerating atmospheric CO_2 growth from economic activity, carbon intensity, and efficiency of natural sinks. *P. Natl. Acad. Sci. USA.*, **104**, 18866–18870, doi:10.1073/pnas.0702737104.

Charney, J. G., 1975: Dynamics of deserts and drought in the Sahel. *Q. J. Roy. Meteor. Soc.*, **101**, 193–202.

Chen, F. and J. Dudhia, 2001: Coupling an advanced land surface-hydrological model with the penn state - ncar modelling system. part i: Model implementation and sensitivity. *Monthly Weather Review*, **129**, 569 – 585.

Ciais, P., M. Reichstein, N. Viovy, A. Granier, J. Ogee, V. Allard, M. Aubinet, N. Buchmann, C. Bernhofer, A. Carrara, F. Chevallier, N. De Noblet, A. Friend, P. Friedlingstein, T. Grunwald, B. Heinesch, P. Keronen, A. Knohl, G. Krinner, D. Loustau, G. Manca, G. Matteucci, F. Miglietta, J. Ourcival, D. Papale, K. Pilegaard, S. Rambal, G. Seufert, J. Soussana, M. Sanz, E. Schulze, T. Vesala, and R. Valentini, 2005: Europe-wide reduction in primary productivity caused by the heat and drought in 2003. *Nature*, **437**, 529–533, doi:10.1038/nature03972.

Clark, D. B., L. M. Mercado, S. Sitch, C. D. Jones, N. Gedney, M. J. Best, M. Pryor, G. G. Rooney, R. L. H. Essery, E. Blyth, O. Boucher, R. J. Harding, C. Huntingford, and P. M. Cox, 2011: The Joint UK Land Environment Simulator (JULES), model description - Part 2: Carbon fluxes and vegetation dynamics. *Geosci. Model Dev.*, **4**, 701–722, doi:10.5194/gmd-4-701-2011.

Clement, R. J., P. G. Jarvis, and J. B. Moncrieff, 2012: Carbon dioxide exchange of a Sitka spruce plantation in Scotland over five years. *Agr. Forest Meteorol.*, **153**, 106–123.

Collatz, G., J. Ball, C. Grivet, and J. Berry, 1991: Physiological and environmental-regulation of stomatal conductance, photosynthesis and transpiration - A model that includes laminar boundary-layer. *Agr. Forest Meteorol.*, **54**, 107–136, doi:10.1016/0168-1923(91)90002-8.

Collins, W. J., N. Bellouin, M. Doutriaux-Boucher, N. Gedney, P. Halloran, T. Hinton, J. Hughes, C. D. Jones, M. Joshi, S. Liddicoat, G. Martin, F. O'Connor, J. Rae, C. Senior, S. Sitch, I. Totterdell, A. Wiltshire, and S. Woodward, 2011: Development and evaluation of an Earth-System model-HadGEM2. *Geosci. Model Dev.*, **4**, 1051–1075, doi:10.5194/gmd-4-1051-2011.

Cook, E. R., J. Esper, and R. D. DArrigo, 2004: Extra-tropical northern hemisphere land temperature variability over the past 1000 years. *Quaternary Science Reviews*, **23**, 2063 – 2074, doi:10.1016/j.quascirev.2004.08.013.

Covey, C., K. AchutaRao, U. Cubasch, P. Jones, S. Lambert, M. Mann, T. Phillips, and K. Taylor, 2003: An overview of results from the Coupled Model Intercomparison Project. *Glob. Planet. Change*, **37**, 103–133, doi:10.1016/S0921-8181(02)00193-5.

Cox, P. M., 2001: Description of the triffid dynamic global vegetation model. Hadley Centre technical note 24, Hadley Centre, Met Office, FitzRoy Road, Exeter, Devon, EX1 3PB, UK.

Cox, P. M., C. D. Jones, S. A. Spall, and I. J. Totterdell, 2000: Acceleeration of global warming due to carbon - cycle feedbacks in a coupled climate model. *Nature*, **408**, 184–187.

Davin, E. L. and N. de Noblet-Ducoudre, 2010: Climatic Impact of Global-Scale Deforestation: Radiative versus Nonradiative Processes. *J. Clim.*, **23**, 97–112, doi:10.1175/2009JCLI3102.1.

Dolman, A. J., J. Noilhan, P. Durand, C. Sarrat, A. Brut, B. Piguet, A. Butet, N. Jarosz, Y. Brunet, D. Loustau, E. Lamaud, L. Tolk, R. Ronda, F. Miglietta, B. Gioli, V. Magliulo, M. Esposito, C. Gerbig, S. Korner, R. Glademard, M. Ramonet, P. Ciais, B. Neininger, R. W. A. Hutjes, J. A. Elbers, R. Macatangay, O. Schrems, G. Perez-Landa, M. J. Sanz, Y. Scholz, G. Facon, E. Ceschia, and P. Beziat, 2006: The CarboEurope regional experiment strategy. *Bull. Amer. Meteorol. Soc.*, **87**, 1367+, doi:10.1175/BAMS-87-10-1367.

ESA, 2012: Report for Mission Selection: Biomass, ESA SP-1324/1 (3 volume series). European Space Agency, Noordwijk, The Netherlands.

Forestry Commission Scotland, 2009: The Scottish Government's Rational for Woodland Expansion. The scottish government strategy document, Forestry Commission, Edinburgh, EH12 7AT, Scotland.

Friedlingstein, P., P. Cox, R. Betts, L. Bopp, W. Von Bloh, V. Brovkin, P. Cadule, S. Doney, M. Eby, I. Fung, G. Bala, J. John, C. Jones, F. Joos, T. Kato, M. Kawamiya, W. Knorr, K. Lindsay, H. D. Matthews, T. Raddatz, P. Rayner, C. Reick, E. Roeckner, K. G. Schnitzler, R. Schnur, K. Strassmann, A. J. Weaver, C. Yoshikawa, and N. Zeng, 2006: Climate-carbon cycle feedback analysis: Results from the C_4MIP model intercomparison. *J. Climate*, **19**, 3337–3353, doi:10.1175/JCLI3800.1.

Friedlingstein, P. and I. C. Prentice, 2010: Carbon-climate feedbacks: a review of model and observation based estimates. *Curr. Opin. Environ. Sustainability*, **2**, 251–257.

Gates, W., J. Boyle, C. Covey, C. Dease, C. Doutriaux, R. Drach, M. Fiorino, P. Gleckler, J. Hnilo, S. Marlais, T. Phillips, G. Potter, B. Santer, K. Sperber, K. Taylor, and D. Williams, 1999: An overview of the results of the Atmospheric Model Intercomparison Project (AMIP I). *Bull. Amer. Meteorol. Soc.*, **80**, 29–55, doi:10.1175/1520-0477(1999)080¡0029:AOOTRO¿2.0.CO;2.

Gerbig, C., A. J. Dolman, and M. Heimann, 2009: On observational and modelling strategies targeted at regional carbon exchange over continents. *Biogeosciences*, **6**, 1949–1559.

Gurney, K., R. Law, A. Denning, P. Rayner, D. Baker, P. Bousquet, L. Bruhwiler, Y. Chen, P. Ciais, S. Fan, I. Fung, M. Gloor, M. Heimann, K. Higuchi, J. John, T. Maki, S. Maksyutov, K. Masarie, P. Peylin, M. Prather, B. Pak, J. Randerson, J. Sarmiento, S. Taguchi, T. Takahashi, and C. Yuen, 2002: Towards robust regional estimates of CO2 sources and sinks using atmospheric transport models. *Nature*, **415**, 626–630, doi:10.1038/415626a.

Hays, J. D., J. Imbrie, and N. J. Shackleton, 1976: Variations in earths orbit - pacemaker of the ice ages. *Science*, **194**, 1121–1132, doi:10.1126/science.194.4270.1121.

Hill, T. C., M. Williams, and J. B. Moncrieff, 2008: Modeling feedbacks between a boreal forest and the planetary boundary layer. *J. Geophys. Res.-Atmos.*, **113**, doi:10.1029/2007JD009412.

ICOS, 2012: Integrated Carbon Observing System: Stakeholders Handbook. A European Infrastructure - European Union, LSCE-Orme, CEA-Orme des Merisiers, F-91191 GIF-SUR-YVETTE CEDEX.

IPCC, 2007: Climate Change 2007: Synthesis Report. Contribution of Working Groups I, II and III to the Fourth Assessment Report of the Intergovernmental Panel on Climate Change. Core Writing Team, Pachauri, R.K. and Reisinger, A. (Eds.)., IPCC, Geneva, Switzerland. pp 104.

Janssens, I., A. Freibauer, B. Schlamadinger, R. Ceulemans, P. Ciais, A. Dolman, M. Heimann, G. Nabuurs, P. Smith, R. Valentini, and E. Schulze, 2005: The carbon budget of terrestrial ecosystems at country-scale - a European case study. *Biogeosciences*, **2**, 15–26.

Jarvis, P., 1976: Interpretation of variations in leaf water potentual and stomatal conductance found in canopies in the field. *Philos. Trans. R. Soc. Lond. Ser. B-Biol. Sci.*, **273**, 593–610, doi:10.1098/rstb.1976.0035.

Jones, H. G., 1992: Plants and microclimate. Cambridge University Press, Cambridge.

Jouzel, J., V. Masson-Delmotte, O. Cattani, G. Dreyfus, S. Falourd, G. Hoffmann, B. Minster, J. Nouet, J. M. Barnola, J. Chappellaz, H. Fischer, J. C. Gallet, S. Johnsen, M. Leuenberger, L. Loulergue, D. Luethi, H. Oerter, F. Parrenin, G. Raisbeck, D. Raynaud, A. Schilt, J. Schwander, E. Selmo, R. Souchez, R. Spahni, B. Stauffer, J. P. Steffensen, B. Stenni, T. F. Stocker, J. L. Tison, M. Werner, and E. W. Wolff, 2007: Orbital and millennial Antarctic climate variability over the past 800,000 years. *Science*, **317**, 793–796, doi:10.1126/science.1141038.

— 2007: Epica dome c ice core 800kyr deuterium data and temperature estimates. IGBP PAGES/World Data Center for Paleoclimatology Data Contribution Series 2007-091, NOAA/NCDC Paleoclimatology Program, Boulder CO, USA.

Junge, C. and G. Czeplak, 1968: Some aspects of seasonal variation of carbon dioxide and ozone. *Tellus*, **20**, 422–&.

Kaplan, J. O., K. M. Krumhardt, and N. E. Zimmermann, 2012: The effects of land use and climate change on the carbon cycle of Europe over the past 500 years. *Glob. Change Biol.*, **18**, 902–914, doi:10.1111/j.1365-2486.2011.02580.x.

Kawamura, K., F. Parrenin, L. Lisiecki, R. Uemura, F. Vimeux, J. P. Severinghaus, M. A. Hutterli, T. Nakazawa, S. Aoki, J. Jouzel, M. E. Raymo, K. Matsumoto, H. Nakata, H. Motoyama, S. Fujita, K. Goto-Azuma, Y. Fujii, and O. Watanabe, 2007: Northern Hemisphere forcing of climatic cycles in Antarctica over the past 360,000 years. *Nature*, **448**, 912–U4, doi:10.1038/nature06015.

Keeling, C., 1960: The concentration and isotopic abundances of carbon dioxide in the atmosphere. *Tellus*, **12**, 200–203.

Keeling, C., R. Bacastow, A. Bainbridge, C. Ekdahl, P. Guenther, L. Waterman, and J. Chin, 1976: Atmospheric carbon-dioxide variations at Mauna-Loa Observatory, Hawaii. *Tellus*, **28**, 538–551.

Keeling, C. and T. Whorf, 2005: *Atmospheric CO_2 records from sites in the SiO air sampling network. In: Trends: A Compendium of Data on Global Change.*. Carbon Dioxide Information Analysis Center, Oak Ridge National Laboratory, U.S. Department of Energy, Oak Ridge, TN.

Keeling, C. D., S. C. Piper, T. P. Whorf, and R. F. Keeling, 2011: Evolution of natural and anthropogenic fluxes of atmospheric CO_2 from 1957 to 2003. *Tellus Ser. B-Chem. Phys. Meteorol.*, **63**, 1–22, doi:10.1111/j.1600-0889.2010.00507.x.

Koppen, W., 1936: Das geographisca System der Klimate, in: Handbuch der Klimatologie. Core Writing Team, Pachauri, R.K. and Reisinger, A. (Eds.)., edited by: Koppen, W. and Geiger, G., 1. C. Gebr, Borntraeger, pp 144.

Krinner, G., N. Viovy, N. de Noblet-Ducoudre, J. Ogee, J. Polcher, P. Friedlingstein, P. Ciais, S. Sitch, and I. Prentice, 2005: A dynamic global vegetation model for studies of the coupled atmosphere-biosphere system. *Glob. Biogeochem. Cycle*, **19**, doi:10.1029/2003GB002199.

Lauvaux, T., A. E. Schuh, M. Bocquet, L. Wu, S. Richardson, N. Miles, and K. J. Davis, 2012: Network design for mesoscale inversions of CO_2 sources and sinks. *Tellus Ser. B-Chem. Phys. Meteorol.*, **64**, doi:10.3402/tellusb.v64i0.17980.

Le Toan, T., S. Quegan, M. W. J. Davidson, H. Balzter, P. Paillou, K. Papathanassiou, S. Plummer, F. Rocca, S. Saatchi, H. Shugart, and L. Ulander, 2011: The BIOMASS mission: Mapping global forest biomass to better understand the terrestrial carbon cycle. *Remote Sens. Environ.*, **115**, 2850–2860, doi:10.1016/j.rse.2011.03.020.

Lee, Y. and L. Mahrt, 2004: Comparison of heat and moisture fluxes from a modified soil-plant-atmosphere model with observations from BOREAS. *J. Geophys. Res.-Atmos.*, **109**, doi:10.1029/2003JD003949.

Levis, S., G. B. Bonan, E. Kluzek, P. E. Thornton, A. Jones, W. J. Sacks, and C. J. Kucharik, 2012: Interactive crop management in the Community Earth System Model (CESM1): Seasonal influences on land-atmosphere fluxes. *J. Clim.*, **25**, 4839–4859.

Lokupitiya, E., S. Denning, K. Paustian, I. Baker, K. Schaefer, S. Verma, T. Meyers, C. J. Bernacchi, A. Suyker, and M. Fischer, 2009: Incorporation of crop phenology in Simple Biosphere Model (SiBcrop) to improve land-atmosphere carbon exchanges from croplands. *Biogeosciences*, **6**, 969–986.

Luthi, D., M. L. Floch, B. Bereiter, T. Blunier, J.-M. Barnola, U. Siegenthaler, D. Raynaud, J. Jouzel, H. Fischer, K. Kawamura, and T. Stocker, 2008: Epica dome c ice core 800kyr carbon dioxide data. IGBP PAGES/World Data Center for Paleoclimatology Data Contribution Series 2008-055, NOAA/NCDC Paleoclimatology Program, Boulder CO, USA.

Miles, N. L., S. J. Richardson, K. J. Davis, T. Lauvaux, A. E. Andrews, T. O. West, V. Bandaru, and E. R. Crosson, 2012: Large amplitude spatial and temporal gradients in atmospheric boundary layer CO2 mole fractions detected with a tower-based network in the U.S. upper Midwest. *J. Geophys. Res.-Biogeosci.*, **117**, doi:10.1029/2011JG001781.

Moncrieff, J., J. Massheder, H. deBruin, J. Elbers, T. Friborg, B. Heusinkveld, P. Kabat, S. Scott, H. Soegaard, and A. Verhoef, 1997: A system to measure surface fluxes of momentum, sensible heat, water vapour and carbon dioxide. *J. Hydrol.*, **189**, 589–611.

Monteith, J. L., 1965: Evaporation and environment. *Symposia of the Society for Experimental Biology*, **19**, 205–234.

Nehrkorn, T., J. Eluszkiewicz, S. C. Wofsy, J. C. Lin, C. Gerbig, M. Longo, and S. Freitas, 2010: Coupled weather research and forecasting-stochastic time-inverted lagrangian transport (WRF-STILT) model. *Meteorol. Atmos. Phys.*, **107**, 51–64, doi:10.1007/s00703-010-0068-x.

Nicholls, M., A. Denning, L. Prihodko, P. Vidale, I. Baker, K. Davis, and P. Bakwin, 2004: A multiple-scale simulation of variations in atmospheric carbon dioxide using a coupled biosphere-atmospheric model. *J. Geophys. Res.-Atmos.*, **109**, doi:10.1029/2003JD004482.

Niu, G.-Y., Z.-L. Yang, K. E. Mitchell, F. Chen, M. B. Ek, M. Barlage, A. Kumar, K. Manning, D. Niyogi, E. Rosero, M. Tewari, and Y. Xia, 2011: The community Noah land surface model with multiparameterization options (Noah-MP): 1. Model description and evaluation with local-scale measurements. *J. Geophys. Res.-Atmos.*, **116**, doi:10.1029/2010JD015139.

Oleson, K. W., D. M. Lawrence, G. B. Bonan, M. G. Flanner, E. K. Kluzek, P. J. Lawrence, S. Levis, S. C. Swenson, and P. E. Thornton, 2010: Technical description of version 4.0 of the community land model (clm).

Osborne, T. M., D. M. Lawrence, A. J. Challinor, J. M. Slingo, and T. R. Wheeler, 2007: Development and assessment of a coupled crop-climate model. *Glob. Change Biol.*, **13**, 169–183.

Paul, K., P. Polglase, J. Nyakuengama, and P. Khanna, 2002: Change in soil carbon following afforestation. *Forest Ecol. Manag.*, **168**, 241–257, doi:10.1016/S0378-1127(01)00740-X.

Peters, W., M. C. Krol, G. R. van der Werf, S. Houweling, C. D. Jones, J. Hughes, K. Schaefer, K. A. Masarie, A. R. Jacobson, J. B. Miller, C. H. Cho, M. Ramonet, M. Schmidt, L. Ciattaglia, F. Apadula, D. Helta, F. Meinhardt, A. G. di Sarra, S. Piacentino, D. Sferlazzo, T. Aalto, J. Hatakka, J. Strom, L. Haszpra, H. A. J. Meijer, S. van der Laan, R. E. M. Neubert, A. Jordan, X. Rodo, J. A. Morgui, A. T. Vermeulen, E. Popa, K. Rozanski, M. Zimnoch, A. C. Manning, M. Leuenberger, C. Uglietti, A. J. Dolman, P. Ciais, M. Heimann, and P. P. Tans, 2010: Seven years of recent European net terrestrial carbon dioxide exchange constrained by atmospheric observations. *Glob. Change Biol.*, **16**, 1317–1337, doi:10.1111/j.1365-2486.2009.02078.x.

Petit, J. R., J. Jouzel, D. Raynaud, N. I. Barkov, J. Barnola, I. Basile, M. Bender, J. Chappellaz, M. Davis, G. Delaygue, M. Delmotte, V. M. Kotlyakov, M. Legrand, V. Y. Lipenkov, C. Lorius, L. Pépin, C. Ritz, E. Saltzman, and M. Stievenard, 1999: Climate and atmospheric history of the past 420,000 years from the Vostok ice core, Antarctica. *Nature*, **399**, 429–436, doi:10.1038/20859.

Poeplau, C., A. Don, L. Vesterdal, J. Leifeld, B. Van Wesemael, J. Schumacher, and A. Gensior, 2011: Temporal dynamics of soil organic carbon after land-use change in the temperate zone - carbon response functions as a model approach. *Glob. Change Biol.*, **17**, 2415–2427, doi:10.1111/j.1365-2486.2011.02408.x.

Qian, H., R. Joseph, and N. Zeng, 2010: Enhanced terrestrial carbon uptake in the Northern High Latitudes in the 21st century from the Coupled Carbon Cycle Climate Model Intercomparison Project model projections. *Glob. Change Biol.*, **16**, 641–656, doi:10.1111/j.1365-2486.2009.01989.x.

Riley, W. J., J. T. Randerson, P. N. Foster, and T. J. Lueker, 2005: Influence of terrestrial ecosystems and topography on coastal CO_2 measurements: A case study at Trinidad Head, California. *J. Geophys. Res.-Biogeosci.*, **110**, doi:10.1029/2004JG000007.

Sarrat, C., J. Noilhan, A. J. Dolman, C. Gerbig, R. Ahmadov, L. F. Tolk, A. G. C. A. Meesters, R. W. A. Hutjes, H. W. Ter Maat, G. Perez-Landa, and S. Donier, 2007:

Atmospheric CO_2 modeling at the regional scale: an intercomparison of 5 mesoscale atmospheric models. *Biogeosciences*, **4**, 1115–1126.

Schomburg, A., V. Venema, F. Ament, and C. Simmer, 2012: Disaggregation of screen-level variables in a numerical weather prediction model with an explicit simulation of subgrid-scale land-surface heterogeneity. *Meteorol. Atmos. Phys.*, **116**, 81–94, doi:0.1007/s00703-012-0183-y.

Sellers, P., D. Randall, G. Collatz, J. Berry, C. Field, D. Dazlich, C. Zhang, G. Collelo, and L. Bounoua, 1996: A revised land surface parameterization (SiB2) for atmospheric GCMs .1. Model formulation. *J. Climate*, **9**, 676–705, doi:10.1175/1520-0442(1996)009¡0676:ARLSPF¿2.0.CO;2.

Sitch, S., C. Huntingford, N. Gedney, P. E. Levy, M. Lomas, S. L. Piao, R. Betts, P. Ciais, P. Cox, P. Friedlingstein, C. D. Jones, I. C. Prentice, and F. I. Woodward, 2008: Evaluation of the terrestrial carbon cycle, future plant geography and climate-carbon cycle feedbacks using five Dynamic Global Vegetation Models (DGVMs). *Glob. Change Biol.*, **14**, 2015–2039.

Skamarock, W. C., J. B. Klemp, J. Dudhia, D. O. Gill, D. M. Barker, M. G. Duda, X.-Y. Huang, W. Wang, and J. G. Powers, 2008: A description of the advanced research wrf version 3.

Steeneveld, G. J., L. F. Tolk, A. F. Moene, O. K. Hartogensis, W. Peters, and A. A. M. Holtslag, 2011: Confronting the WRF and RAMS mesoscale models with innovative observations in the Netherlands: Evaluating the boundary layer heat budget. *J. Geophys. Res.-Atmos.*, **116**, doi:10.1029/2011JD016303.

Stoy, P. C., M. Williams, M. Disney, A. Prieto-Blanco, B. Huntley, R. Baxter, and P. Lewis, 2009: Upscaling as ecological information transfer: a simple framework with application to Arctic ecosystem carbon exchange. *Landscape Ecology*, **24**, 971–986.

Sus, O., M. Williams, C. Bernhofer, P. Beziat, N. Buchmann, E. Ceschia, R. Doherty, W. Eugster, T. Gruenwald, W. Kutsch, P. Smith, and M. Wattenbach, 2010: A linked

carbon cycle and crop developmental model: Description and evaluation against measurements of carbon fluxes and carbon stocks at several European agricultural sites. *Agr. Ecosyst. Environ.*, **139**, 402–418.

Thomson, A. M. and M. van Oijen, 2007: UK Emissions by Sources and Removals by Sinks due to Land Use, Land Use Change and Forestry Activities. *Annual Report for Defra Contract GA01088*.

Tolk, L. F., W. Peters, A. G. C. A. Meesters, M. Groenendijk, A. T. Vermeulen, G. J. Steeneveld, and A. J. Dolman, 2009: Modelling regional scale surface fluxes, meteorology and CO_2 mixing ratios for the Cabauw tower in the Netherlands. *Biogeosciences*, **6**, 2265–2280.

Tuzet, A., A. Perrier, and R. Leuning, 2003: A coupled model of stomatal conductance, photosynthesis and transpiration. *Plant Cell Environ.*, **26**, 1097–1116, doi:10.1046/j.1365-3040.2003.01035.x.

Van den Hoof, C., E. Hanert, and P. L. Vidale, 2011: Simulating dynamic crop growth with an adapted land surface model - JULES-SUCROS: Model development and validation. *Agr. Forest Meteorol.*, **151**, 137–153.

Vermeulen, A. T., A. Hensen, M. E. Popa, W. C. M. van den Bulk, and P. A. C. Jongejan, 2011: Greenhouse gas observations from Cabauw Tall Tower (1992-2010). *Atmos. Meas. Tech.*, **4**, 617–644, doi:10.5194/amt-4-617-2011.

Wang, Y., C. N. Long, L. R. Leung, J. Dudhia, S. A. McFarlane, J. H. Mather, S. J. Ghan, and X. Liu, 2009: Evaluating regional cloud-permitting simulations of the WRF model for the Tropical Warm Pool International Cloud Experiment (TWP-ICE), Darwin, 2006. *J. Geophys. Res.-Atmos.*, **114**, 1–21, doi:10.1029/2009JD012729.

Wang, Y. P. and R. Leuning, 1998: A two-leaf model for canopy conductance, photosynthesis and partitioning of available energy I: Model description and comparison with a multi-layered model. *Agr. Forest Meteorol.*, **91**, 89–111.

Williams, M., W. Eugster, E. Rastetter, J. McFadden, and F. Chapin, 2000: The controls on net ecosystem productivity along an Arctic transect: a model comparison with flux measurements. *Glob. Change Biol.*, **6**, 116–126.

Williams, M., B. Law, P. Anthoni, and M. Unsworth, 2001: Use of a simulation model and ecosystem flux data to examine carbon-water interactions in ponderosa pine. *Tree Physiol.*, **21**, 287–298.

Williams, M., Y. Malhi, A. Nobre, E. Rastetter, J. Grace, and M. Pereira, 1998: Seasonal variation in net carbon exchange and evapotranspiration in a Brazilian rain forest: a modelling analysis. *Plant Cell Environ.*, **21**, 953–968, doi:10.1046/j.1365-3040.1998.00339.x.

Williams, M., E. B. Rastetter, D. N. Fernandes, M. L. Goulden, S. C. Wofsy, G. R. Shaver, J. M. Melillo, J. W. Munger, S. M. Fan, and K. J. Nadelhoffer, 1996: Modelling the soil-plant-atmosphere continuum in a Quercus-Acer stand at Harvard Forest: the regulation of stomatal conductance by light, nitrogen and soil/plant hydraulic properties. *Plant Cell Environ.*, **19**, 911–927.

Williams, M., P. A. Schwarz, B. E. Law, J. Irvine, and M. Kurpius, 2005: An improved analysis of forest carbon dynamics using data assimilation. *Glob. Change Biol.*, **11**, 89–105.

Woodward, F., T. Smith, and W. Emanuel, 1995: A global land primary productivity and phytogeography model. *Glob. Biogeochem. Cycle*, **9**, 471–490, doi:10.1029/95GB02432.

Wright, J. K., M. Williams, G. Starr, J. McGee, and R. J. Mitchell, 2012: Measured and modelled leaf and stand-scale productivity across a soil moisture gradient and a severe drought. *Plant Cell Environ.*, doi:10.1111/j.1365-3040.2012.02590.x.

Xie, B., J. C. H. Fung, A. Chan, and A. Lau, 2012: Evaluation of nonlocal and local planetary boundary layer schemes in the WRF model. *J. Geophys. Res.-Atmos.*, **117**, doi:10.1029/2011JD017080.

Zhang, Y., 2008: Online-coupled meteorology and chemistry models: history, current status, and outlook. *Atmos. Chem. Phys.*, **8**, 2895–2932.

Chapter 2

WRFv3.2-SPAv2: Development and validation of a coupled ecosystem-atmosphere model, scaling from surface fluxes of CO_2 and energy to atmospheric profiles

T.L. Smallman, J. B. Moncrieff and M. Williams

School of GeoSciences, University of Edinburgh, Edinburgh, EH9 3JN

Geosci. Model Dev., 6, 1079–1093, 2013
www.geosci-model-dev.net/6/1079/2013/
doi:10.5194/gmd-6-1079-2013

Geoscientific Model Development
Open Access

WRFv3.2-SPAv2: development and validation of a coupled ecosystem–atmosphere model, scaling from surface fluxes of CO_2 and energy to atmospheric profiles

T. L. Smallman[1,2], **J. B. Moncrieff**[1], **and M. Williams**[1,2]

[1]School of GeoSciences, University of Edinburgh, Edinburgh, EH9 3JN, UK
[2]National Centre for Earth Observation, University of Edinburgh, Edinburgh, EH9 3JN, UK

Correspondence to: T. L. Smallman (t.l.smallman@.ed.ac.uk)

Received: 15 January 2013 – Published in Geosci. Model Dev. Discuss.: 4 March 2013
Revised: 11 June 2013 – Accepted: 26 June 2013 – Published: 29 July 2013

Abstract. The Weather Research and Forecasting meteorological (WRF) model has been coupled to the Soil–Plant–Atmosphere (SPA) terrestrial ecosystem model, to produce WRF-SPA. SPA generates realistic land–atmosphere exchanges through fully coupled hydrological, carbon and energy cycles. The addition of a land surface model (SPA) capable of modelling biospheric CO_2 exchange allows WRF-SPA to be used for investigating the feedbacks between biosphere carbon balance, meteorology, and land use and land cover change. We have extensively validated WRF-SPA using multi-annual observations of air temperature, turbulent fluxes, net radiation and net ecosystem exchange of CO_2 at three sites, representing the dominant vegetation types in Scotland (forest, managed grassland and arable agriculture). For example air temperature is well simulated across all sites (forest $R^2 = 0.92$, RMSE $= 1.7\,^{\circ}$C, bias $= 0.88\,^{\circ}$C; managed grassland $R^2 = 0.73$, RMSE $= 2.7\,^{\circ}$C, bias $= -0.30\,^{\circ}$C; arable agriculture $R^2 = 0.82$, RMSE $= 2.2\,^{\circ}$C, bias $= 0.46\,^{\circ}$C; RMSE, root mean square error). WRF-SPA generates more realistic seasonal behaviour at the site level compared to an unmodified version of WRF, such as improved simulation of seasonal transitions in latent heat flux in arable systems. WRF-SPA also generates realistic seasonal CO_2 exchanges across all sites. WRF-SPA is also able to realistically model atmospheric profiles of CO_2 over Scotland, spanning a 3 yr period (2004–2006), capturing both profile structure, indicating realistic transport, and magnitude (model–data residual $<\pm 4$ ppm) indicating appropriate source sink distribution and CO_2 exchange. WRF-SPA makes use of CO_2 tracer pools and can therefore identify and quantify land surface contributions to the modelled atmospheric CO_2 signal at a specified location.

1 Introduction

The land surface is a key driver of climate and biogeochemical cycles at regional and global scales (Pielke et al., 1997; Cox et al., 2000; Esau and Lyons, 2002). Understanding land–atmosphere interactions for matter and energy is essential, as changes in global climate have likely led to significant but poorly understood changes in the global carbon balance (Forster et al., 2007). The direction and magnitude of future changes to the Earth system will depend on feedbacks between biogeochemistry and climate, linked to human modification of the land surface related to land use and land cover change. However, the importance of the land surface has been relatively poorly explored in terms of the climate–biogeochemical coupling (Betts et al., 2007).

Simulation models provide the only effective means to investigate the dynamics of land–atmosphere interactions. However, models typically have a genesis in either the atmospheric or in the terrestrial biogeochemistry/ecological communities. To overcome deficiencies arising from these alternate perspectives has required coupling the most advanced descriptions of atmospheric dynamics with ecosystem processes. Coupled land–atmosphere models are now used to investigate global- and regional-scale exchange between the land and atmosphere, and have highlighted the complex

Published by Copernicus Publications on behalf of the European Geosciences Union.

feedbacks that result (e.g. Ciais et al., 2005; Friedlingstein et al., 2006; Betts et al., 2007; Friedlingstein and Prentice, 2010).

Mesoscale models in particular are useful for studying regional-scale processes due to their ability to operate at high spatial resolutions, allowing accurate prediction of mesoscale circulation phenomena that have a significant impact on regional transport e.g. coastal winds, katabatic winds (Nicholls et al., 2004; Riley et al., 2005; Ahmadov et al., 2009), and complex forcing of heterogeneous vegetation (Sarrat et al., 2007). Mesoscale models also provide a means to upscale land surface exchanges to observations within the planetary boundary layer (PBL), of regionally integrated exchange (e.g. tall towers or aircraft observations) (Ahmadov et al., 2009; Tolk et al., 2009). Atmospheric tracers of CO_2 for respiratory and photosynthetic exchange can be transported through the atmosphere making it possible to gain information on how variations in land use and ecosystem coverage contribute to observations of regional exchange of CO_2 (Tolk et al., 2009).

Over time land surface models (LSMs), used in coupled land–atmosphere models, have been upgraded to include more processes and improved parameterisation. The current generation of LSMs commonly represent both biogeophysical and biogeochemical processes (Bonan, 2008). For example the widely used mesoscale model Weather Research and Forecasting (WRF, Skamarock et al., 2008) uses the advanced Noah-MP LSM (Niu et al., 2011). Noah-MP includes detailed parameterisation for radiative transfer of sunlit and shaded leaf area for a big leaf canopy, a semi-empirical model of stomatal conductance and a carbon model allowing dynamic ecosystem phenology. However there remains uncertainty in the predicted response of the terrestrial ecosystem, net ecosystem exchange (NEE) of CO_2 and feedbacks mediated through the close coupling between the land surface and PBL processes (Friedlingstein et al., 2006; Bonan, 2008; Sitch et al., 2008; Friedlingstein and Prentice, 2010).

Feedbacks between the land and atmosphere are highly complex and non-linear, requiring an increasingly mechanistic approach to provide realistic responses of key ecosystem processes (i.e. photosynthesis, respiration and evapotranspiration) (Tuzet et al., 2003; Bonan, 2008; Sprintsin et al., 2012). Significant improvements in the prediction of photosynthesis and stomatal conductance are made by using a multi-layer canopy in radiative transfer, where direct and diffuse radiation, and sunlit and shaded leaf areas are modelled (Wang and Leuning, 1998; Dai et al., 2003; Sprintsin et al., 2012). Moreover, stomatal conductance is a key determinant of land surface hydrological and carbon cycles, and energy balance (Avissar, 1998). Semi-empirical representations which link photosynthesis to atmospheric demand for water, such as Ball-Berry (Collatz et al., 1991) or its variants is widely used in LSMs (e.g. Sellers et al., 1996; Oleson et al., 2010; Best et al., 2011; Niu et al., 2011). Models such as Ball–Berry do not couple atmospheric demand for water to available water supply from the soil, thus lacking important ecophysiological processes (Tuzet et al., 2003).

Furthermore, land–atmosphere feedbacks are often distinct to each land cover type, particularly at longer timescales (Stoy et al., 2009). Therefore heterogeneity in the land surface needs to be realistically modelled to accurately predict regional-scale exchange (Avissar, 1998; Schomburg et al., 2012). These feedbacks are mediated through biogeochemical and biogeophysical processes (Bonan, 2008) that are related to plant phenology (e.g. canopy height and leaf area index). Realistic modelling of phenology is particularly important as most land surface systems have a distinct annual cycle. Human intervention adds further complexity to annual cycles, for example in agricultural systems. Crop modelling in LSMs has received little attention until recently (Sus et al., 2010) and crops are often modelled as a natural grassland (Osborne et al., 2007). Croplands play a significant role in global biogeochemical and biogeophysical cycles (Bondeau et al., 2007; Denman et al., 2007), significantly impacting both turbulent fluxes (Van den Hoof et al., 2011) and surface albedo (Betts et al., 2007). Due to the importance of cropland a number of LSMs have been modified to include developmental crop models to improve the presentation of crop phenology and management (Lokupitiya et al., 2009; Sus et al., 2010; Van den Hoof et al., 2011; Levis et al., 2012).

The Soil–Plant–Atmosphere (SPA, Williams et al., 1996) model is a mechanistic ecosystem model. SPA uses a vertically distributed canopy model allowing variation of photosynthetic parameters through the canopy, based on field measurements, and a multi-layer radiative transfer scheme that models the distribution of direct and diffuse radiation, and sunlit and shaded leaf areas (Williams et al., 1998). SPA also uses a mechanistic model of stomatal conductance linking atmospheric demand and water availability from the soil through the plant, explicitly coupling plant carbon and hydrological cycles (Williams et al., 1996, 2001). Unlike a Ball–Berry model, SPA is parameterised directly from ecophysiological measurements such as rooting depth, plant hydraulic conductance and canopy structure (e.g. Wright et al., 2012). A developmental crop model has also been included in SPA allowing for inclusion of this highly important ecosystem under human management (Sus et al., 2010).

In this paper we describe a novel coupling between the WRF and SPA, forming WRF-SPA. An overview of both models, their strengths, any modifications made to either code or their forcing data is described. WRF is a state-of-the-art non-hydrostatic mesoscale meteorological model (Skamarock et al., 2008), it is considered to be one of the best models of its type available (Sarrat et al., 2007; Steeneveld et al., 2011). WRF-SPA uses a number of CO_2 tracer pools to upscale land surface processes, photosynthesis and respiration, specific to each land surface type.

Here WRF-SPA is validated at both local and regional scales, using observations from Scotland over multiple years, to evaluate the model against a range of meteorological

conditions. At the local-scale surface observations of meteorological conditions and fluxes of CO_2, heat and water have been used for validation. Regional-scale validation used aircraft profile measurements of atmospheric CO_2 concentrations. The unmodified WRFv3.2 and WRF-SPA have been compared, at the local scale, to investigate the impacts of the addition of a new LSM. We aim to answer a number of specific questions:

i. Can WRF-SPA realistically model surface meteorological variables and fluxes across a multi-annual period?

ii. Does WRF-SPA scale realistically from surface measurements to regional-scale observations, specifically aircraft profiles?

iii. Does WRF-SPA lead to an improvement in surface fluxes compared to the unmodified WRFv3.2?

2 Model description: WRF

The Weather Research and Forecasting (v3.2) (http://www.mmm.ucar.edu/wrf/users/, accessed 19 October 2009) model is a well supported and rapidly developing high resolution non-hydrostatic meteorological model (Skamarock et al., 2008). WRF is designed to be highly adaptable, with a portable code for use on massively parallel systems and a modular structure to allow for tailoring to specific uses. The model has been extensively validated over a range of locations around the world (Ahamdov et al., 2007; Ahmadov et al., 2009; Borge et al., 2008; Zhang, 2008; Wang et al., 2009) and performs favourably in comparison to other commonly used regional meteorological models (Sarrat et al., 2007; Steeneveld et al., 2011). Here we use the Advanced Research WRF (ARW) dynamical solver which uses non-hydrostatic equations, allowing horizontal resolutions of < 1 km.

2.1 Atmospheric CO_2 tracers

WRF-SPA has been modified with the addition of several CO_2 tracer pools (Table 1). CO_2 transport is simulated within the model domain concurrently with meteorological variables (feedback on atmospheric radiative transfer due to variable CO_2 is neglected). The CO_2 tracer scheme is a modified version of the scheme used in WRF-VPRM (Vegetation Photosynthesis and Respiration Model) (Ahamdov et al., 2007).

Atmospheric CO_2 fields were provided by Carbon Tracker Europe (CTE, Peters et al., 2010) TM5 providing $1^\circ \times 1^\circ$ resolution fields at 3 h intervals. CTE CO_2 fields were used to provide WRF-SPA CO_2 initial conditions (IC) and lateral boundary conditions (LBC) were linearly interpolated to the WRF-SPA domain. LBC for the outer domain have been set with zero inflow and zero-gradient outflow for all CO_2 fields, except total atmospheric CO_2 and "forcings only" CO_2 (Table 1), to allow for tracers to easily leave the domain and prevent artificial influx from outside the domain.

Table 1. Tracer pools and definitions used by WRF-SPA.

Tracer ID	Description
1_CO_2	Total CO_2 concentration, includes all sources and sinks of CO_2, for comparison to observations
2_CO_2	Forest assimilation
3_CO_2	Anthropogenic emissions
4_CO_2	Anthropogenic emissions, ocean sequestration, initial and lateral boundary conditions only
5_CO_2	Crop assimilation
6_CO_2	Ocean sequestration
7_CO_2	Forest respiration
8_CO_2	Crop respiration
9_CO_2	Managed grassland respiration
10_CO_2	Other vegetation respiration
11_CO_2	Managed grassland assimilation
12_CO_2	Other vegetation assimilation

Global flux maps of anthropogenic emissions and ocean absorption, also from CTE, at $1^\circ \times 1^\circ$ resolution with 3 h updates were used to provide non-biospheric surface exchange. The fluxes were interpolated using 4 point weighted means based on latitude and longitude co-ordinates. Biospheric fluxes of CO_2 are simulated by the LSM (SPA, described in Sect. 3). All surface CO_2 fluxes were calculated as rates which were added to the lowest model atmospheric layer of the WRF grid at each time step.

3 Model description: SPA

The Soil–Plant–Atmosphere model is a high vertical resolution mechanistic point model (up to 10 canopy layers and 20 soil layers). SPA uses coupled energy, hydrological and carbon cycles to provide surface fluxes of heat, water and CO_2 to WRF. SPA provides realistic responses to meteorological drivers by coupling its hydrological and carbon cycles through ecophysiological principles (Williams et al., 1996).

SPA has been extensively validated against eddy covariance observations over several ecosystems including temperate deciduous forests (Williams et al., 1996), Arctic tundra (Williams et al., 2000), temperate evergreen forests (Williams et al., 2001) and, with the addition of a crop development model, temperate crop systems (Sus et al., 2010). SPA has been coupled to PBL models (Lee and Mahrt, 2004; Hill et al., 2008). Hill et al. (2008) successfully demonstrated that SPA could include feedbacks and drive PBL development that agreed with radiosonde observations.

A brief description of the SPA model will be given here, followed by a detailed description of the modifications made to the SPA for use with the WRF; a detailed description of major SPA developments can be found in Williams et al.

(1996, 1998, 2001, 2005) and Sus et al. (2010). A complete parameter list is available in the Supplement.

WRF provides SPA with meteorological drivers from the lowest atmospheric model level including air temperature, precipitation, vapour pressure deficit (VPD), wind speed, friction velocity, atmospheric CO_2, air pressure, short and long-wave incoming radiation. SPA currently has parameters for 8 vegetation types (evergreen forest, deciduous forest, mixed forest, crops, managed grassland, grassland, upland and urban) suitable for UK application and 13 soil types. Vegetation and soil classifications are from the WRF default land cover maps (Mesoscale and Microscale Meteorology Division, 2011).

Plant phenology and carbon dynamics are described by a box carbon model (the Data Assimilation Linked Ecosystem Carbon (DALEC) model), which is fully integrated into SPA, to simulate the main ecosystem C pools (Williams et al., 2005). C pools (foliage, structural/wood carbon, fine roots, labile, soil organic matter (SOM) and surface litter) were "spun-up", in an offline SPA simulation (except for crops) using 3 yr of meteorology (1998–2000) from Griffin Forest. These observations are broadly representative of the Scottish average and are from a period not simulated here. The observations were obtained from the CarboEurope network (www.carboeurope.org/) and looped for a 30 yr period. A 30 yr period was found to be sufficient for carbon pools to reach steady state when SOM was initialised with realistic values for Scotland based on the soil carbon stocks from Bradley et al. (2005). No spin up of the above ground vegetation in crops was needed as arable crop systems are annual with complete clearing of the biosphere at harvest and addition of labile carbon in the form of seed. DALEC (Data Assimilation Linked Ecosystem Carbon) provides a direct coupling between the carbon cycle and plant phenology, specifically foliar and fine root C, where foliar C determines leaf area index (LAI) and root C impacts water uptake potential. Crops have two additional C pools; storage organ C (i.e. harvestable C) and dead foliar C (still standing) (Sus et al., 2010). Urban cover is assumed to be a low density evergreen forest with a reduced emissivity to be consistent with urban construction materials, all other surface properties remain unchanged; WRF-SPA used the same emissivity value for urban cover as used in the default WRF LSM, Noah. However, we expect this parameterisation to have little impact as urban cover represents < 1 % of the modelled land surface.

The Farquhar model of photosynthesis (Farquhar and von Caemmerer, 1982), the Penman–Monteith model of leaf transpiration (Jones, 1992) and the leaf energy balance are coupled via a mechanistic model of stomatal conductance. SPA maximises carbon assimilation per unit nitrogen but within a minimum leaf water potential to prevent cavitation via a series of bisection procedures. Leaf water potential links atmospheric demand for water and soil water supply, by including the effects of soil and stem hydraulic resistance on water transport to the leaves (Williams et al., 1996).

The soil surface energy balance is solved following the approach by Hinzman et al. (1998) and the soil temperature profile is updated by an implicit method of Crank–Nicolson (Farlow, 1993). Soil hydrology is calculated through determining soil surface evaporative flux and water movement within the soil profile due to gravity, root uptake and thermal distribution through the profile. Soil hydraulic parameters are calculated using equations from Saxton et al. (1986).

SPA uses a detailed radiative transfer scheme which models the absorption, transmittance and reflectance of near infra-red (NIR), direct and diffuse photosynthetically active radiation (PAR) and long-wave radiation for both sunlit and shaded fractions of each canopy level (Williams et al., 1998). Albedo is calculated from the overall reflectance and absorption of NIR and PAR from the canopy and soil surfaces.

The biological components of SPA remain unchanged in WRF-SPA. Modifications to the physical processes include updates to the canopy interception of precipitation, water storage and drainage calculations; a new aerodynamic scheme for momentum decay above and within the canopy; leaf level conductance calculating both free and forced convective exchange; an integrative procedure for calculating turbulent exchange of soil surface through the canopy; inclusion of dew formation and wet surface canopy evaporation within the canopy energy balance and addition of dead foliage LAI and post harvest litter within the radiative transfer scheme. Modifications are described in turn, below.

3.1 Canopy hydrological parameters

Canopy interception, water storage and drainage have a significant impact on potential wet canopy evaporation, dew formation (and therefore on the canopy energy balance), and soil surface water. Canopy interception of precipitation (I; fraction) and maximum canopy water storage ($C_{\max}$; mm) are related to LAI by coefficients α (0.5) and μ (0.2), respectively. α has been selected to generate canopy interception fractions which are consistent with Rutter et al. (1975). Canopy storage coefficient μ is intended to calculate values which are consistent with canopy storage values used in a previous SPA study (Williams et al., 2001).

$$I = \alpha \mathrm{LAI} \tag{1}$$

and

$$C_{\max} = \mu \mathrm{LAI} \tag{2}$$

Canopy drainage rate is calculated using an empirical relationship derived by Rutter et al. (1975), with an LAI adjustment factor.

$$D = \exp(a + bC_{\mathrm{stor}}), \tag{3}$$

where D is drainage rate (mm min^{-1}), b is an empirical coefficient ($b = 3.7$), C_{stor} is the current canopy storage of water

(mm) and a accounts for the canopy water content relative to $C_{\max}$.

$$a = \ln(D_c) - bC_{\max} \quad (4)$$

D_c is the rate of drainage on a canopy where $C_{stor} = C_{\max}$. D_c is adjusted via a proportional relationship to $C_{\max}$ (Rutter et al., 1975).

$$D_c = 0.002(C_{\max}/1.05) \quad (5)$$

3.2 Aerodynamic scheme: canopy exchange

SPA models both the above and within canopy momentum decay. Wind speeds are used in determining leaf level and soil surface conductance (described later). Above canopy momentum decay follows the standard log law decay with the Monin–Obukov similarity theory stability correction (Garratt, 1992).

$$\frac{dU}{dz} = \frac{u_*}{\kappa(z+d)}\Phi_m, \quad (6)$$

where dU/dz is the gradient of wind speed decay above the canopy at height z (m), κ is Von Karman constant (0.41), d is the canopy zero plane displacement height (m), u_* is the friction velocity ($m\,s^{-1}$) and Φ_m is the Monin–Obukov stability correction coefficient. The gradient of wind speed decay is integrated over the vertical distance between the wind speed at the reference height to the canopy top. It is important to note that currently the roughness sub-layer is not included in decay calculations.

The displacement height and roughness length (z_o) are calculated based on canopy structure (height z_h and LAI) as described in Raupach (1994).

$$d = z_h\left[1 - \frac{1-\exp(-(C_{d1}\mathrm{LAI})^{0.5})}{(C_{d1}\mathrm{LAI})^{0.5}}\right] \quad (7)$$

and

$$z_o = \left(1 - \frac{d}{z_h}\right)\exp\left(-\kappa\frac{u_h}{u_*} - \Psi_h\right)z_h\,, \quad (8)$$

where z_h is the canopy height (m), C_{d1} is an empirically fitted parameter (7.5) and Ψ_h parameterises the effect of the roughness sub-layer on roughness length (0.193) (Raupach, 1994).

Within canopy momentum, decay is carried out using the method described in Harman and Finnigan (2007). Decay within the canopy is assumed to be exponential, where $U_{(z)}$ is the wind speed ($m\,s^{-1}$) at height z within the canopy. Decay is dependent on the canopy mixing length (l_m) and ratio of $\frac{u_*}{u_h} = u_r$ (where u_h is the wind speed at canopy top).

$$U_{(z)} = u_h\exp((u_r(z - z_h))/l_m) \quad (9)$$

The canopy mixing length is described by u_r and the canopy length scale L_c (m),

$$l_m = 2u_r^3 L_c\,, \quad (10)$$

where the length scale is calculated assuming a uniform canopy.

$$L_c = \frac{4z_h}{\mathrm{LAI}} \quad (11)$$

The resulting within-canopy wind speed profile is used in the calculation of canopy layer specific boundary layer conductance ($m\,s^{-1}$) of heat and water vapour. Boundary layer conductance at each canopy layer is assumed to be the maximum conductance between free and forced convection at that layer. A detailed description of the leaf level conductance is given in Nikolov et al. (1995):

$$g_h = \frac{D_h S_h}{d_o}\,, \quad (12)$$

where g_h is the leaf level conductance for heat ($m\,s^{-1}$), D_h is the molecular diffusivity of heat ($m^2\,s^{-1}$), S_h the Sherwood number and d_o is the leaf or needle (cone if free convection) diameter. For calculation of water vapour conductance, g_{wv}, the molecular diffusivity of water, D_{wv}, is used.

3.3 Aerodynamic scheme: soil exchange

The bare soil surface conductance (g_{soil}; $m\,s^{-1}$) for heat and water vapour are assumed to be equal.

$$g_{soil} = U_{soil}\frac{\kappa^2}{\ln\left(\frac{z_{ref}}{z_{soil}}\right)^2}, \quad (13)$$

where U_{soil} is the wind speed near the soil surface, and z_{ref} is the reference height of the lowest model level to which the soil is exchanging. The soil surface roughness length (z_{soil}; m), is assumed to be equal to 0.01 m both when under a canopy and as bare ground.

When the soil is under a canopy, the soil conductance is first calculated as a resistance. Soil resistance is integrated through the canopy based on the turbulent eddy diffusivity following Niu and Yang (2004).

$$r_{soil} = \int_{z_{soil}}^{d+z_o} dz/K_h(z), \quad (14)$$

where dz is the vertical step size (m) through the canopy and K_h is the eddy diffusivity at z position (m) within the canopy. Eddy diffusivity (K_h; $m^2\,s^{-1}$) is assumed to have an exponential decay through the canopy (as with momentum). Eddy diffusivity at the canopy top is estimated as specified in Kaimal and Finnigan (1994).

$$K_h(z_h) = \kappa u_*(z_h - d) \quad (15)$$

K_h is decayed through the canopy as described below.

$$K_h(z) = K_h(z_h)\exp(-f\,(1 - z/z_h)) \quad (16)$$

$$f = (c_d z_h \mathrm{LAI}/l_m)^{0.5}\,(\Phi_m)^{0.5} \quad (17)$$

The coefficient of momentum decay f is dependant on c_d the coefficient of drag for foliage (0.2), LAI, l_m and soil surface Φ_m. Φ_m was calculated as described in Garratt (1992). When $\zeta > 0$,

$$\Phi_m(\zeta) = (1 - \gamma\zeta)^{0.25}; \quad (18)$$

when $\zeta < 0$,

$$\Phi_m(\zeta) = (1 + \beta_1\zeta), \quad (19)$$

where $\zeta > 0$ conditions are unstable, while $\zeta < 0$ are stable conditions, with coefficients $\gamma = 16$ and $\beta_1 = 5$. $\zeta = z/L$ is described in Qin et al. (2002).

$$z/L = \frac{\kappa z g H_{soil}}{\rho c p_{air} u_*^3}, \quad (20)$$

where L is the Obukov length, g is acceleration due to gravity ($9.81\,m\,s^{-2}$), cp_{air} is the specific heat capacity of dry air ($1004.6\,J\,kg^{-1}\,K^{-1}$), ρ is the density of the air ($kg\,m^{-3}$). H_{soil} is the sensible heat flux from the soil in the previous time step.

3.4 Leaf energy balance

SPA uses an iterative procedure to solve stomatal conductance, and as part of this procedure, the leaf energy balance is solved. Net radiation is partitioned between latent and sensible heat fluxes ($W\,m^{-2}$); the metabolic storage term is assumed to be small and is neglected. Evaporation is calculated from the Penman–Monteith equation; sensible heat is based on the temperature difference between the leaf surface and surrounding air. The radiative transfer scheme initially distributes long-wave radiation assuming that the canopy and surrounding air are in isothermal net radiation balance (Rni; $W\,m^{-2}$). Rni is updated to the net radiation (Rn; $W\,m^{-2}$) in the first iteration.

$$Rn \simeq Rni + 4\epsilon\sigma T_a^3(\Delta T) \quad (21)$$

The Rn correction is based on the temperature difference (ΔT) between the input leaf temperature T_{leaf}, in the first iteration, and the absolute air temperature (T_a; K). T_{leaf} is solved by balancing the canopy energy balance Eq. (22).

$$Rn = E_{leaf}\lambda + H_{leaf} + E_{wet}\lambda \quad (22)$$

$$E_{leaf} = \frac{[\epsilon Rn/\lambda] + g_{wv}\delta c_w}{\epsilon + 1 + (g_{wv}/g_s)} \quad (23)$$

E_{leaf} is transpiration ($kg\,m^{-2}\,s^{-1}$), δc_w is the absolute humidity deficit ($kg\,m^{-3}$) and $\epsilon = s/\gamma$. s ($Pa\,K^{-1}$) is the slope of curve that relates saturation vapour pressure with air temperature and γ is the psychrometer constant ($Pa\,K^{-1}$). g_s is stomatal conductance ($m\,s^{-1}$), and λ is the latent heat of vaporisation ($J\,kg^{-1}$).

$$H_{leaf} = 2g_h cp_{air}\rho(\Theta_{leaf} - \Theta_{air}) \quad (24)$$

H_{leaf} is sensible heat ($W\,m^{-2}$), Θ_{leaf} and Θ_{air} are potential leaf and air temperatures respectively. The factor 2 is to account for the two different sides of the leaf.

Wet canopy evaporation is calculated via a multi-stage process. The Penman–Monteith equation is used to calculate the potential evaporation or dew formation (E_{pot}; $kg\,m^{-2}\,s^{-1}$), i.e. with aerodynamic conductance only.

$$E_{pot} = \frac{s Rn + cp_{air}\rho g_{wv}\delta e}{\lambda(s + \gamma)} \quad (25)$$

δe is the vapour pressure deficit (Pa). If dew is forming this is restricted to no larger than C_{max}. Dew mass is added to the canopy in the following time step, while the energy exchange is added to Rn for the next iteration of the canopy. Wet evaporation (E_{wet}, $kg\,m^{-2}\,s^{-1}$) is restricted by the amount of water stored on the canopy (C_{stor}, Eq. 26) and E_{leaf} that has occurred Eq. (26).

$$E_{wet}\lambda = \frac{C_{stor}}{C_{max}} E_{pot} - E_{leaf}\lambda \quad (26)$$

An iterative solution is used to model both wet canopy evaporation, (or) dew formation and update the canopy distribution of long-wave radiation. (i) Leaf temperature is calculated solving the canopy energy balance; (ii) long-wave radiation distribution is updated based on current leaf temperature values; (iii) leaf temperature is re-solved; (iv) canopy net radiation is used to calculate wet evaporation or dew; (v) the available net radiation for the canopy energy balance is adjusted based on wet evaporation or dew. The procedure is iterated up to 10 times; steady state of the canopy balance typically occurs by the 4th iteration.

3.5 Modifications to the crop model in SPA

The crop development model developed for SPA is described and validated in Sus et al. (2010). This allows SPA to model the growth of both winter wheat and winter barley. While only modelling winter cereals will introduce a bias, it is a reasonable assumption as winter wheat and barley are the dominant arable crops in the UK. The model represents crop development from sowing through vegetative growth, flowering and maturity through to harvest.

Sowing is assumed to occur once the daily mean temperature has dropped below 10 °C for winter crops. Van den Hoof et al. (2011) demonstrated that this assumption produces realistic sowing times. Harvest is assumed to occur once the developmental crop model reaches the mature development stage, which typically coincides with the storage organ (the crop yield) reaching its peak value and complete foliage senescence.

The albedo of crops changes as it matures, this change leads to a significantly greater albedo in mature crops compared to during vegetative growth. Seasonal shifts in albedo significantly alter the surface energy balance, changing both surface temperature and turbulent fluxes (Betts et al., 2007).

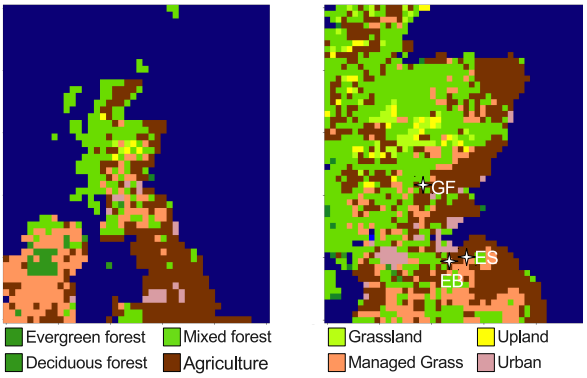

Fig. 1. Land classification map covering the spatial extent of the model domain, the left panel is the parent domain at 18 km × 18 km, right panel is nested domain at 6 km × 6 km resolution. The field sites are marked with a star Griffin Forest (GF), East Saltoun (ES) and Easter Bush (EB). The maps used in WRF is a modified MODIS land cover map provided with the WRF model.

To account for this, foliage which has senescenced is retained within the canopy as a non-photosynthetically active (non-transpiring) dead LAI. In addition to decoupling dead foliage from the plant hydrological cycle, dead LAI is assigned its own NIR and PAR reflectance values (Nagler et al., 2003). Assigning dead LAI reflectance allows for inclusion of their effect on the surface energy balance, impacting both leaf level processes and radiative transfer.

Post harvest, litter also plays an important role in the surface energy balance by increasing surface albedo relative to the underlying soil. As with dead foliage, post harvest surface litter is prescribed a separate albedo which is weighted with that of the underlying soil, based on fractional area cover. Litter fractional cover is estimated based on the mass of surface litter (C_{sflit}) present. Surface litter from both wheat and barley are assumed to have the same mass–area relationship as wheat from Nagler et al. (2003).

$$\%\mathrm{cover} = -0.0007C_{\mathrm{sflit}}^2 + 0.5053C_{\mathrm{sflit}} + 7.4017 \quad (27)$$

4 Model domain and validation datasets

4.1 Model domain

WRF-SPA was run over two domains with two-way nesting; the outer domain has a resolution of 18 km × 18 km and the inner 6 km × 6 km (Fig. 1). Model output from the inner domain only was used in the validation. Scotland provides a highly complex topography and land use heterogeneity, with a longitudinal gradient from dominantly forested areas in the northwest to pasture in the central and southwest and arable cropland in the east.

A 5 yr period (2002–2006) was simulated for use in a multi-annual validation of the model at different spatial scales, from surface measurements to vertical aircraft profiles of CO_2 atmospheric concentrations. The first 2 yr were considered to be a spin up period to allow for differentiation of the vegetation phenology. The main features of the model set-up are presented in Table 2.

All meteorological data required for the ICs and LBCs are from the Global Forecasting System (GFS) reanalysis product (http://www.emc.ncep.noaa.gov/) with 1° × 1° longitude/latitude resolution at 6 h time steps (available from http://rda.ucar.edu/datasets/ds083.2/).

4.2 Validation data

The surface validation used surface observations of net radiation, turbulent fluxes (latent and sensible), net ecosystem exchange of CO_2 (NEE) and air temperature from three sites in Scotland. The sign convention used for NEE is negative fluxes represent net sequestration of carbon and positive fluxes represent a net source. Observations used were averaged to an hourly time step. The three sites are important as they are representative of the dominant land cover types in Scotland outside of the central northern mountain ranges (Fig. 1).

The sites are (i) Griffin Forest, an intensively managed Sitka spruce plantation (LAI $\sim 6\,\mathrm{m^2\,m^{-2}}$) in central Scotland (56.61° N, 3.80° W, 340 m a.s.l.). Established in 1982, the site has an mean annual air temperature of ∼ 6.6 °C and precipitation of $\sim 1126\,\mathrm{mm\,yr^{-1}}$ (Clement et al., 2012). (ii) East Saltoun, has mixed use with a spring barley crop and grassland (for silage) (55.91° N, 2.85° W, 73 m a.s.l). A mean annual air temperature of ∼ 8.5 °C and precipitation of $\sim 700\,\mathrm{mm\,yr^{-1}}$. (iii) Easter Bush, a managed grassland (55.86° N, 3.21° W, 190 m a.s.l). Management varies each year including both grazing and cutting. The site has a mean annual air temperature of ∼ 7.8 °C and precipitation of $\sim 978\,\mathrm{mm\,yr^{-1}}$. All three sites are part of the CarboEurope network (www.carboeurope.org/).

An aircraft collected vertical profiles of atmospheric CO_2 concentrations over Griffin Forest between 2004 and 2006. Air samples were collected at a range of altitudes above sea level (m a.s.l.), 800, 1100, 1600, 2100, 2600 and 3100. Sampling (all daytime) occurred throughout each year covering the whole seasonal cycle. This provides information at all development stages of the vegetation and includes a range of meteorological conditions. The profiles provide integrated regional-scale information allowing for validation at the regional-scale of WRF-SPA's carbon balance.

5 Results

5.1 Surface validation

Statistical validation (analysed in R v2.15.2; R Core Team, 2012) against hourly observations are presented for WRF-SPA and WRF (Table 3). Seasonal behaviour is explored

Table 2. Parameter and model options used in both WRF-SPA and WRF.

Basic equations	Non-hydrostatic, compressible Advanced Research WRF (ARW)
Radiative transfer scheme	Rapid Radiative Transfer Model for GCMs (RRTMG) for both long wave and short wave
Planetary boundary layer scheme	Yonsei University
Surface scheme	Monin–Obukov
Land surface scheme	Noah (WRFv3.2 only)
Microphysics scheme	WSM 3-class simple ice
Cumulus parameterisation	Grell 3D ensemble scheme (coarse domain only)
Nesting	Two-way nesting
Domain, resolution	44×47, 18 km 48×54, 6 km 35 vertical levels
Domain centre	56.63° N, 3.35° W

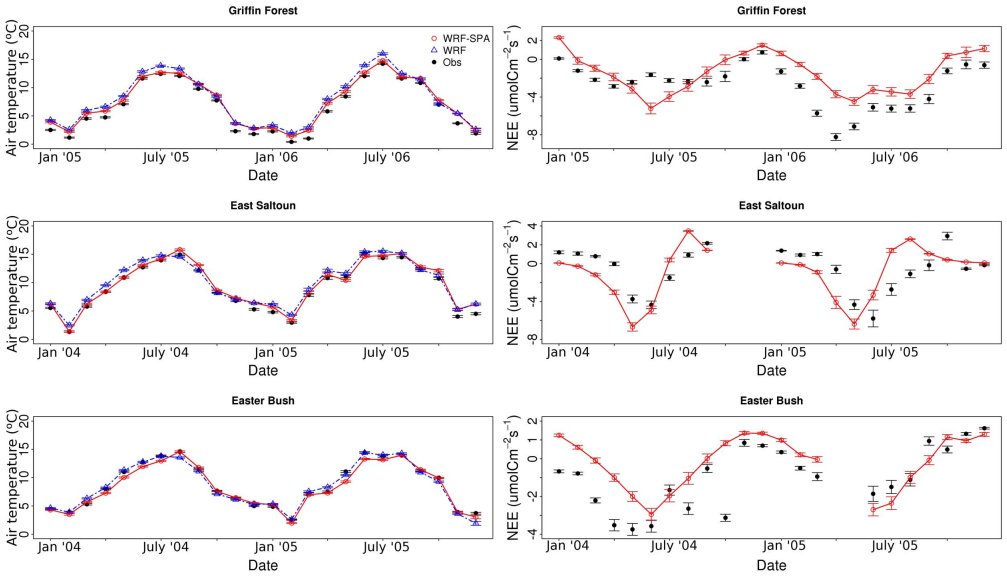

Fig. 2. Monthly mean values for air temperature and net ecosystem exchange by observations, WRF-SPA and WRF. Error bars are ± 1 standard error, accounting for temporal averaging only.

by comparing monthly mean (and standard error) values for observations and the models. To ensure comparability, the model means are calculated using only values where a corresponding observation is available.

Both models demonstrate good skill in predicting surface observations, particularly air temperature. R^2 and biases are similar (Table 3); on average the differences between the modelled biases are 0.16 °C and 4.2 W m^{-2} for temperature and turbulent fluxes, respectively. There is a tendency for latent and sensible fluxes to be positively biased, except at Griffin Forest where WRF underestimates latent heat. The overestimation of turbulent fluxes is in part due to overestimation of net radiation, typically 10–15 W m^{-2} for both models (Table 3). However errors in partitioning to ground heat flux are also likely to play a significant role. In WRF-SPA, ground heat flux is relatively insensitive seasonally; underestimating the magnitude of ground heat flux may lead to a bias in energy partitioning to turbulent fluxes during summer (data not shown). WRF-SPA tends to have larger RMSEs for latent (5–20 %) and sensible heat fluxes (5–92 %) than WRF, while for temperature RMSEs are similar with a maximum difference of 0.2 °C. The largest RMSEs are for East Saltoun and are discussed later.

Air temperature is well predicted by both models with a typical annual absolute bias of < 1 °C and RMSE of ~ 2 °C. This is broadly consistent across all sites at the annual timescale, representing skill in modelling a range of highly distinct vegetative systems. At seasonal scales, more

Table 3. Summary of WRF-SPA and WRF multi-annual statistics for surface validation sites during 2004–2005 (East Saltoun and Easter Bush) and 2005–2006 (Griffin Forest). Statistics are for hourly observations of the surface air temperature, net ecosystem exchange (NEE) (WRF-SPA only), latent (LH) and sensible heat (SH) fluxes. Statistics are mean annual bias, root mean square error and R^2 values.

	WRF-SPA			WRFv3.2		
	Bias	RMSE	R^2	Bias	RMSE	R^2
Easter Bush						
Air temperature (°C)	−0.30	2.7	0.73	-3.7×10^{-6}	2.6	0.74
LH ($W\,m^{-2}$)	10.3	43.1	0.41	7.9	37.6	0.43
SH ($W\,m^{-2}$)	7.4	55.5	0.49	8.2	38.4	0.43
Net Radiation ($W\,m^{-2}$)	11.3	86.4	0.61	16.0	85.2	0.63
NEE ($\mu mol\,C\,m^{-2}\,s^{-1}$)	0.81	4.6	0.54	–	–	–
East Saltoun						
Air temperature (°C)	0.46	2.2	0.82	0.73	2.3	0.81
LH ($W\,m^{-2}$)	5.8	42.7	0.36	11.2	40.2	0.41
SH ($W\,m^{-2}$)	25.7	90.9	0.43	14.6	47.3	0.53
Net Radiation ($W\,m^{-2}$)	11.4	113.7	0.55	3.1	102.8	0.58
NEE ($\mu mol\,C\,m^{-2}\,s^{-1}$)	−0.25	6.9	0.32	–	–	–
Griffin Forest						
Air temperature (°C)	0.88	1.7	0.92	1.4	1.9	0.93
LH ($W\,m^{-2}$)	8.8	65.0	0.54	−22.9	54.9	0.54
SH ($W\,m^{-2}$)	5.4	68.3	0.51	24.2	65.3	0.57
Net Radiation ($W\,m^{-2}$)	8.8	86.5	0.70	13.6	89.8	0.69
NEE ($\mu mol\,C\,m^{-2}\,s^{-1}$)	1.1	6.2	0.51	–	–	–

significant differences are apparent between the two models. WRF produces a consistent overestimation of monthly mean temperatures at Griffin and East Saltoun, while during winter both models overestimate air temperature by a similar amount (Fig. 2). WRF-SPA more closely predicts monthly mean temperatures during the majority of the year, except at Easter Bush during the spring and summer months where WRF-SPA underestimates temperature. At Griffin Forest both models realistically predict seasonal behaviour, while at East Saltoun and Easter Bush WRF-SPA more accurately predicts the observed seasonality than WRF. Including accurate prediction of peak summer monthly mean temperature in August for both East Saltoun and Easter Bush during 2004.

NEE is reasonably well predicted by WRF-SPA at each site, particularly at the seasonal timescales (Fig. 2). However hourly RMSEs are high, typically $\sim 6\,\mu mol\,CO_2\,m^{-2}\,s^{-1}$ while biases remain relatively small, usually $< 1\,\mu mol\,CO_2\,m^{-2}\,s^{-1}$ (Table 3). Seasonally, each of the sites show different biases throughout the year from each other. WRF-SPA underestimates net carbon sequestration at both Griffin Forest and Easter Bush over the observation period, including during winter indicating an overestimation of respiration in the model. The WRF-SPA model–observation mismatch at Griffin Forest varies between years. WRF-SPA overestimates peak sequestration (NEE is more negative) during 2005 and fails to capture a peak summer reduction in carbon sequestration shown in the observations (Fig. 2), whereas in 2006 WRF-SPA captures the seasonal behaviour of the forest but there is some underestimation in fluxes (Fig. 2).

At East Saltoun, NEE appears to be poorly modelled at the hourly level with an R^2 of 0.32. While at seasonal timescales we can see that WRF-SPA models NEE reasonably well, however the phenology is out of phase (Fig. 2). Despite this the growing-season peak sink strength and post-harvest respiration peaks are of appropriate magnitude. In both years WRF-SPA predicts peak sequestration two months early and overestimates early season sequestration. The model observation mismatch is consistent with WRF-SPA modelling winter barley at East Saltoun, while the crop planted during 2004 and 2005 is spring barley.

WRF-SPA overestimates latent heat fluxes at all three sites, particularly during the summer when more energy is available. WRF overestimates at both East Saltoun and Easter Bush, and underestimates latent heat at Griffin Forest (Fig. 3). Seasonally we can see that WRF-SPA performs better, particularly in modelling the transitions into and out of summer. This is most evident during 2004 at East Saltoun where, while the peak latent heat flux is too high, the peak period timing and duration is considerably better represented than by WRF.

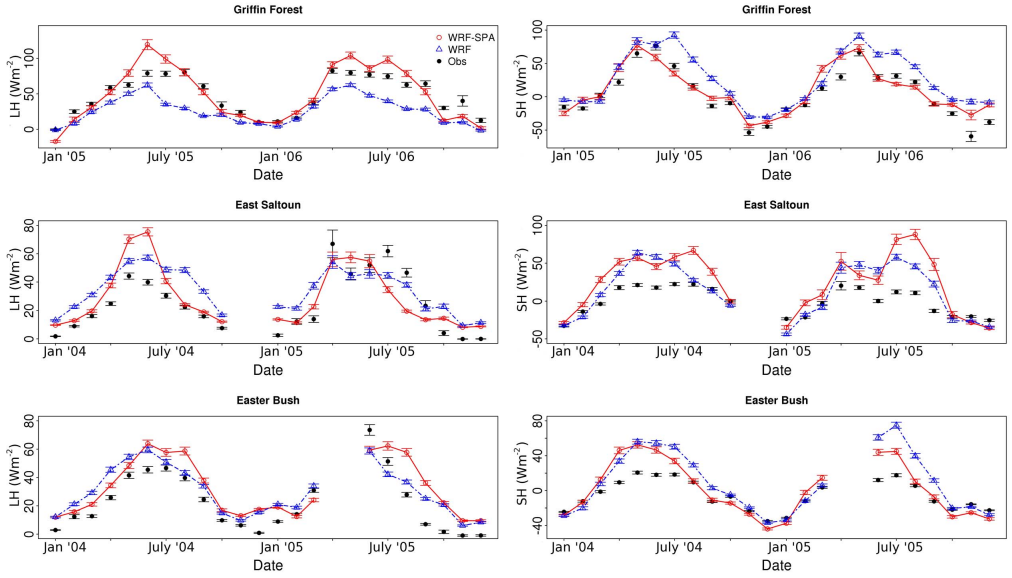

Fig. 3. Monthly mean values for LH and SH fluxes by observations, WRF-SPA and WRF. Error bars are ±1 standard error, accounting for temporal averaging only.

A similar situation is observed for sensible heat (Fig. 3) with particularly good agreement at Griffin Forest by WRF-SPA while less so by WRF. Seasonal transition periods are well captured (Fig. 3), which is expected due to the coupling between latent and sensible heat fluxes. WRF-SPA captures the bimodal peaks during both years, which is at least partly driven by harvest. When the crop is harvested this removes much of the high albedo mature vegetation and exposes the low albedo soil, resulting in a higher net radiation. Removal of crop vegetation also restricts evaporation to water available in the upper soil layers. This has a significant impact on partitioning of net radiation into sensible and ground heat fluxes.

5.2 Scaling to aircraft profiles

Aircraft profiles were compared to WRF-SPA modelled profiles of CO_2 to provide validation of regionally integrated measurement of CO_2 exchange (Fig. 4). Profiles include both summer and winter flights throughout the simulation period, to investigate model performance both seasonally and multi-annually. Figures show two modelled profiles, (i) total atmospheric concentration and (ii) "forcings only" profiles. The "forcings only" pool, contains CO_2 which originates from external forcings only, including LBC nudging, oceanic fluxes and anthropogenic emissions (i.e. total CO_2 minus the modelled biospheric fluxes). This allows us to visually show the impact of the "simulated biosphere" on atmospheric CO_2 concentrations within the domain.

The modelled profiles of total CO_2 compare well with observations. All predicted profiles are typically within

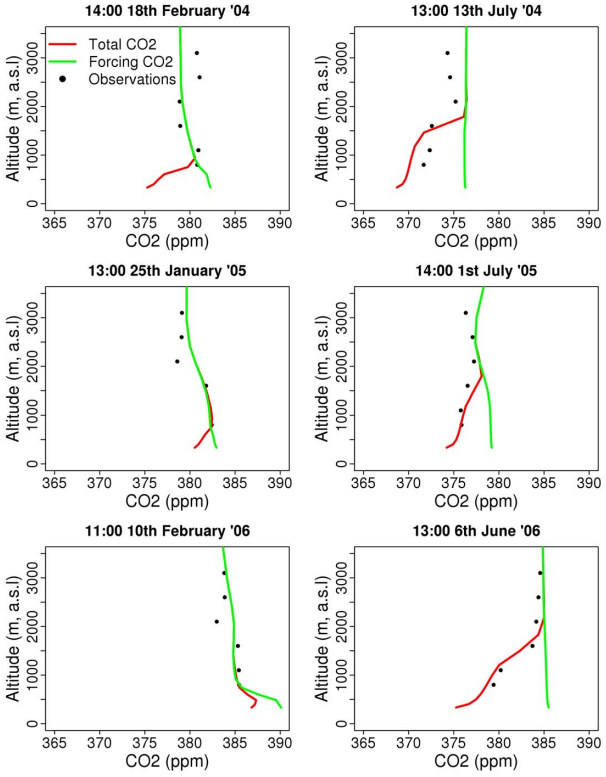

Fig. 4. Observed and WRF-SPA modelled profiles of CO_2 above Griffin Forest. Modelled profiles include the total atmosphere profile CO_2 and "forcings only" CO_2 to show the impact of the modelled biosphere.

2–4 ppm of observations, a selection of which are shown in Fig. 4. The profile structure and PBL heights of modelled total CO_2 profiles compare well with observations indicating that regional transport and distribution of biospheric sources and sinks is broadly realistic. "Forcing only" CO_2 profiles show distinctly different structures and CO_2 concentrations within the PBL, indicating that the good agreement we find in the total CO_2 pool is due to the modelling of the biosphere by WRF-SPA.

There are differences in model performance across seasonal scales. During peak growing season, WRF-SPA overestimates regional biosphere sequestration, leading to up to 4 ppm underestimation in the modelled profile (e.g. July 2004 and June 2006; Fig. 4). This is different to the observed underestimation of carbon sink strength at Griffin Forest (Table 3). The likely reason for this is that forest cover is overrepresented within the model domain. At the resolution used in WRF-SPA, the MODIS land cover map used in WRF-SPA estimates that forest-type land covers make up 43 % of the total land cover. The MODIS forest cover estimate is significantly greater than the Scottish estimate of ~ 17.8 % forest cover (National Forest Inventory, 2011). This issue could be rectified through replacement of the MODIS map with a more realistic representation of UK land cover (e.g. LCM 2007, http://www.ceh.ac.uk/LandCoverMap2007.html).

6 Discussion and conclusions

The purpose of this study is to present and validate the novel coupled model WRF-SPA. Validation of WRF-SPA was conducted at both local (site level) and regional (aircraft profiles) scales, against a range of observations relevant to CO_2 exchange and validation of the meteorological capability of the WRF-SPA.

WRF-SPA demonstrated that it can produce comparable statistics to those of WRF (Table 3) at the site level against hourly observations. WRF-SPA tends to have lower annual bias, however WRF-SPA has higher RMSEs. Higher RMSEs are not unexpected due to the greater level of complexity of SPA compared to the default WRF LSM, Noah. WRF is often considered to be one of the best mesoscale models available in terms of simulating vertical profiles of temperature (Steeneveld et al., 2011) and surface meteorological variables (Sarrat et al., 2007). Therefore, we can infer that WRF-SPA is also comparable to many other models that are currently used in regional-scale research.

At seasonal timescales WRF-SPA shows realistic behaviour across each of the land cover types presented here. Air temperature was consistently better modelled by WRF-SPA at both Griffin Forest and East Saltoun, while summer peak temperatures were better captured at Easter Bush by WRF-SPA. NEE is well modelled by WRF-SPA, particularly seasonality (Fig. 2). There remain, however, several issues including an overestimation in winter respiration at Griffin Forest and Easter Bush, which may be linked to an overestimation of soil carbon stocks or an overestimation of soil organic matter turnover. Given Scotland's high soil organic matter content it is likely that WRF-SPA's modelling of soil processes as inorganic is a significant component of this error.

There remain several model–observation mismatches at Griffin Forest during the growing season (Fig. 2). Where WRF-SPA overestimates carbon sequestration in 2005 but underestimates sequestration in 2006. Further, there is presence of a lag in simulated NEE, particularly evident in 2006. Underestimating sequestration in 2006 is consistent with WRF-SPA underestimation of LAI at Griffin Forest (modelled $\sim 4\,m^2\,m^{-2}$, observed $\sim 6\,m^2\,m^{-2}$). Griffin Forest underwent selective logging in 2004 (~ 37 % reduction in above ground biomass), therefore during 2005 the forest was likely in the process of recovery before returning to pre-harvest sequestration levels in 2006. The early season lag is a known issue with the evergreen carbon model in SPA, were the evergreen model lacks a labile carbon pool. As a result needle growth is limited in springtime to carbon available from photosynthesis at that time, rather than rapid release of carbon stored from the previous year (Williams et al., 2005).

WRF-SPA overestimates latent heat at all three sites compared to observations (Fig. 3). However the model–data mismatch may be due to an underestimate of turbulent fluxes in observations due to non-closure of the surface energy balance (Stoy et al., 2013). Stoy et al. (2013) also found evidence that non-closure of the energy balance is greater in crop systems, which is consistent with the greatest model–data mismatch seen as East Saltoun.

Seasonal changes in latent and sensible heat fluxes are well predicted by WRF-SPA compared to WRF. Transition periods in particular from winter to spring and summer to autumn are well captured by WRF-SPA compared to WRF, e.g. latent heat fluxes observed at East Saltoun during 2004 (Fig. 3). As the bimodal peak in sensible heat flux at East Saltoun appears to be driven by human intervention on the ecosystem, demonstrating it is important to include the impacts of human management of ecosystems. This is consistent with other studies which have previously highlighted agricultural land as a significant component of the European and global energy and carbon balance (Betts et al., 2007; Denman et al., 2007). WRF also displays a bimodal peak during 2006, the cause of this is unclear but appears to be linked to a larger amount of incoming short-wave radiation in WRF than WRF-SPA during the mid- to late-summer. The differences in incoming radiation between the models is likely as a result of combination of feedbacks where in WRF-SPA the higher evaporation rate and sensible heat flux lead to increased cloud cover and atmospheric albedo.

Comparison with aircraft profiles show that WRF-SPA is capable of upscaling to regional measurements of atmospheric CO_2. Indicating that the modelled CO_2 sources/sink

distribution is well modelled as is transport within the atmosphere. The absolute errors of the modelled profiles are comparable to other studies (e.g. Ahamdov et al., 2007; Ter Maat et al., 2010). What is unique about our study is that we carried out this analysis over a several year period showing multi-annual consistency. WRF-SPA successfully predicts PBL height for the observed profiles which is critical to achieve realistic regional-scale mixing and meteorological variables (Steeneveld et al., 2011; Xie et al., 2012). Steeneveld et al. (2011) showed in a comparison between different PBL parameterisations, using WRF and RAMS, that correct modelling of PBL structure and temperature profiles was only achieved with significant overestimation of sensible heat fluxes of up to 50 %, which is consistent with the overestimate of sensible heat fluxes predicted by WRF-SPA.

WRF-SPA has demonstrated that it is capable of realistically predicting exchange of CO_2 at the regional scale. Further work will look at using CO_2 tracers to de-construct observations of regional exchange to investigate how each vegetative ecosystem contributes to the regional signal. In particular a currently unexplored multi-annual dataset of continuous measurement of CO_2 from the tall tower Angus site, Scotland.

In conclusion, three specific questions were asked of this validation. (i) Can WRF-SPA realistically model surface meteorological variables and fluxes across a multi-annual period? We have shown that WRF-SPA can realistically model surface observations at hourly timescales which are comparable to WRF. (ii) Does WRF-SPA scale realistically from the surface measurements to regional-scale observations, specifically aircraft profiles? We have shown across multiple years and across seasons that WRF-SPA upscales to observed atmospheric CO_2 concentration profiles. (iii) Does WRF-SPA lead to an improvement in surface fluxes compared to the unmodified WRFv3.2? We have demonstrated that at monthly means WRF-SPA predicts more realistic seasonal behaviour than WRF.

Supplementary material related to this article is available online at: http://www.geosci-model-dev.net/6/1079/2013/gmd-6-1079-2013-supplement.pdf.

Acknowledgements. The authors would like to thank the PhD project funding body, the National Centre for Earth Observation, a UK Natural Environment Research Council research centre. Christoph Gerbig of the Max Plank Institute is thanked for providing the original CO_2 tracer modifications for WRF. John Finnigan of CSIRO is thanked for help in implementing a new canopy momentum decay parameterisation within SPA. The aircraft observations were funded by the AEROCARB project of the EU Framework Programme 5.

Edited by: R. Sander

References

Ahamdov, R., Gerbig, C., Kretschmer, R., Koerner, R., Neininger, B., Dolman, A. J., and Sarrat, C.: Mesoscale covariance of transport and CO_2 fluxes: evidence from observations and simulations using the WRF-VPRM coupled atmosphere-biosphere model, J. Geophys. Res.-Atmos., 112, D22107, doi:10.1029/2007JD008552, 2007.

Ahmadov, R., Gerbig, C., Kretschmer, R., Körner, S., Rödenbeck, C., Bousquet, P., and Ramonet, M.: Comparing high resolution WRF-VPRM simulations and two global CO_2 transport models with coastal tower measurements of CO_2, Biogeosciences, 6, 807–817, doi:10.5194/bg-6-807-2009, 2009.

Avissar, R.: Which type of soil vegetation atmosphere transfer scheme is needed for general circulation models: a proposal for a higher order scheme, J. Hydrol., 212–213, 136–154, doi:10.1016/S0022-1694(98)00227-3, 1998.

Best, M. J., Pryor, M., Clark, D. B., Rooney, G. G., Essery, R. L. H., Ménard, C. B., Edwards, J. M., Hendry, M. A., Porson, A., Gedney, N., Mercado, L. M., Sitch, S., Blyth, E., Boucher, O., Cox, P. M., Grimmond, C. S. B., and Harding, R. J.: The Joint UK Land Environment Simulator (JULES), model description – Part 1: Energy and water fluxes, Geosci. Model Dev., 4, 677–699, doi:10.5194/gmd-4-677-2011, 2011.

Betts, R. A., Falloon, P. D., Goldewijk, K. K., and Ramankutty, N.: Biogeophysical effects of land use on climate: model simulations of radiative forcing and large-scale temperature change, Agr. Forest Meteorol., 142, 216–233, 2007.

Bonan, G. B.: Forests and climate change: forcings, feedbacks, and the climate benefits of forests, Science, 320, 1444–1449, 2008.

Bondeau, A., Smith, P. C., Zaehle, S., Schaphoff, S., Lucht, W., Cramer, W., Gerten, D., Lotze-Campen, H., Mueller, C., Reichstein, M., and Smith, B.: Modelling the role of agriculture for the 20th century global terrestrial carbon balance, Glob. Change Biol., 13, 679–706, doi:10.1111/j.1365-2486.2006.01305.x, 2007.

Borge, R., Alexandrov, V., del Vas, J. J., Lumbreras, J., and Rodriguez, E.: A comprehensive sensitivity analysis of the WRF model for air quality applications over the Iberian Peninsula, Atmos. Environ., 42, 8560–8574, doi:10.1016/j.atmosenv.2008.08.032, 2008.

Bradley, R., Milne, R., Bell, J., Lilly, A., Jordan, C., and Higgins, A.: A soil carbon and land use database for the United Kingdom, Soil Use Manage., 21, 363–369, doi:10.1079/SUM2005351, 2005.

Ciais, P., Reichstein, M., Viovy, N., Granier, A., Ogee, J., Allard, V., Aubinet, M., Buchmann, N., Bernhofer, C., Carrara, A., Chevallier, F., De Noblet, N., Friend, A., Friedlingstein, P., Grunwald, T., Heinesch, B., Keronen, P., Knohl, A., Krinner, G., Loustau, D., Manca, G., Matteucci, G., Miglietta, F., Ourcival, J., Papale, D., Pilegaard, K., Rambal, S., Seufert, G., Soussana, J., Sanz, M., Schulze, E., Vesala, T., and Valentini, R.: Europe-wide reduction in primary productivity caused by the heat and drought in 2003, Nature, 437, 529–533, doi:10.1038/nature03972, 2005.

Clement, R. J., Jarvis, P. G., and Moncrieff, J. B.: Carbon dioxide exchange of a Sitka spruce plantation in Scotland over five years, Agr. Forest Meteorol., 153, 106–123, 2012.

Collatz, G., Ball, J., Grivet, C., and Berry, J.: Physiological and environmental-regulation of stomatal conductance, photosynthesis and transpiration – a model that includes laminar boundary-

layer, Agr. Forest Meteorol., 54, 107–136, doi:10.1016/0168-1923(91)90002-8, 1991.

Cox, P. M., Jones, C. D., Spall, S. A., and Totterdell, I. J.: Acceleration of global warming due to carbon – cycle feedbacks in a coupled climate model, Nature, 408, 184–187, 2000.

Dai, Y., Dickenson, R. E., and Wang, Y. P.: A two-big-leaf model for canopy temperature, photosynthesis and stomatal conductance, Am. Meteorol. Soc., 17, 2281–2299, 2003.

Denman, K., Brasseur, G., Chidthaisong, A., Ciai, P., Cox, P., Dickinson, R., Hauglustaine, D., Heinze, C., Holland, E., Jacob, D., Lohmann, U., Ramachandran, S., da Silva Dias, P., Wofsy, S., and Zhang, X.: Couplings between changes in the climate system and biogeochemistry, in: Climate Change 2007: The Physical Science Basis. Contribution of Working Group I to the Fourth Assessment Report of the Intergovernmental Panel on Climate Change, edited by: Solomon, S., Qin, D., Manning, M., Chen, Z., Marquis, M., Averyt, K. B., Tignor, M., and Miller, H. L., Cambridge University Press, Cambridge, UK and New York, NY, USA, 2007.

Esau, I. N. and Lyons, T. J.: Effect of sharp vegetation boundary on the convective atmosphere boundary layer, Agr. Forest Meteorol., 114, 3–13, 2002.

Farlow, S. J.: Partial Differential Equations for Scientists and Engineers, Dover, New York, 1993.

Farquhar, G. D. and von Caemmerer, S.: Modelling of photosynthetic response to the environment, in: Physiological Plant Ecology II, Encyclopedia of Plant Physiology, Springer-Verlag, Berlin, 1982.

Forster, P., Ramaswamy, V., Artaxo, P., Bernsten, T., Betts, R., Fahey, D. W., Haywood, J., Lean, J., Lowe, D. C., Myhre, G., Nganga, J., Prinn, R., Raga, G. M. S., and Dorland, R. V.: Changes in atmospheric constituents and in radiative forcing, in: Climate Change 2007: The Physical Science Basis. Contribution of Working Group I to the Fourth Assessment Report of the Intergovernmental Panel on Climate Change, edited by: Solomon, S., Qin, D., Manning, M., Chen, Z., Marquis, M., Averyt, K. B., Tignor, M., and Miller, H. L., Cambridge University Press, Cambridge, UK, New York, NY, USA, 2007.

Friedlingstein, P. and Prentice, I. C.: Carbon-climate feedbacks: a review of model and observation based estimates, Curr. Opin. Environ. Sustainability, 2, 251–257, 2010.

Friedlingstein, P., Cox, P., Betts, R., Bopp, L., Von Bloh, W., Brovkin, V., Cadule, P., Doney, S., Eby, M., Fung, I., Bala, G., John, J., Jones, C., Joos, F., Kato, T., Kawamiya, M., Knorr, W., Lindsay, K., Matthews, H. D., Raddatz, T., Rayner, P., Reick, C., Roeckner, E., Schnitzler, K. G., Schnur, R., Strassmann, K., Weaver, A. J., Yoshikawa, C., and Zeng, N.: Climate-carbon cycle feedback analysis: results from the C(4)MIP model intercomparison, J. Climate, 19, 3337–3353, doi:10.1175/JCLI3800.1, 2006.

Garratt, J. R.: The Atmospheric Boundary Layer, Cambridge University Press, Cambridge, UK, 1992.

Harman, I. N. and Finnigan, J. J.: A simple unified theory for flow in the canopy and roughness sublayer, Bound. Lay. Meteorol., 123, 339–363, 2007.

Hill, T. C., Williams, M., and Moncrieff, J. B.: Modeling feedbacks between a boreal forest and the planetary boundary layer, J. Geophys. Res.-Atmos., 113, D15122, doi:10.1029/2007JD009412, 2008.

Hinzman, L. D., Goering, D. J., and Kane, D. L.: A distributed thermal model for calculating soil temperature profiles and depth of thaw in permafrost regions, J. Geophys. Res., 103, 28975–28991, 1998.

Jones, H. G.: Plants and Microclimate, Cambridge University Press, Cambridge, 1992.

Kaimal, J. C. and Finnigan, J. J.: Atmospheric Boundary Layer Flows: Their Structure and Measurement, Oxford University Press, 200 Madison Avenue, NY 10016, USA and Oxford University, Oxford UK, 1994.

Lee, Y. and Mahrt, L.: Comparison of heat and moisture fluxes from a modified soil-plant-atmosphere model with observations from BOREAS, J. Geophys. Res.-Atmos., 109, D08103, doi:10.1029/2003JD003949, 2004.

Levis, S., Bonan, G. B., Kluzek, E., Thornton, P. E., Jones, A., Sacks, W. J., and Kucharik, C. J.: Interactive crop management in the Community Earth System Model (CESM1): seasonal influences on land-atmosphere fluxes, J. Climate, 25, 4839–4859, 2012.

Lokupitiya, E., Denning, S., Paustian, K., Baker, I., Schaefer, K., Verma, S., Meyers, T., Bernacchi, C. J., Suyker, A., and Fischer, M.: Incorporation of crop phenology in Simple Biosphere Model (SiBcrop) to improve land-atmosphere carbon exchanges from croplands, Biogeosciences, 6, 969–986, doi:10.5194/bg-6-969-2009, 2009.

Mesoscale and Microscale Meteorology Division: Weather Research and Forecasting ARW Version 3 Modelling System User's Guide, User's guide, National Center for Atmospheric Research, Colorado, USA, 2011.

Nagler, P., Inoue, Y., Glenn, E., Russ, A., and Daughtry, C.: Cellulose absorption index (CAI) to quantify mixed soil-plant litter scenes, Remote Sens. Environ., 87, 310–325, doi:10.1016/j.rse.2003.06.001, 2003.

National Forest Inventory: National Forest Inventory Woodland Area Statistics: Scotland, Forestry commission statistical release, Forestry Commission, Edinburgh, EH12 7AT, Scotland, 2011.

Nicholls, M., Denning, A., Prihodko, L., Vidale, P., Baker, I., Davis, K., and Bakwin, P.: A multiple-scale simulation of variations in atmospheric carbon dioxide using a coupled biosphere-atmospheric model, J. Geophys. Res.-Atmos., 109, D18117, doi:10.1029/2003JD004482, 2004.

Nikolov, N., Massman, W., and Schoettle, A.: Coupling biochemical and biophysical processes at the leaf level – an equilibrium photosynthesis model for leaves of C-3 plants, Ecol. Model., 80, 205–235, 1995.

Niu, G. Y. and Yang, Z. L.: Effects of vegetation canopy processes on snow surface energy and mass, J. Geophys. Res., 109, D23111, doi:10.1029/2004JD004884, 2004.

Niu, G.-Y., Yang, Z.-L., Mitchell, K. E., Chen, F., Ek, M. B., Barlage, M., Kumar, A., Manning, K., Niyogi, D., Rosero, E., Tewari, M., and Xia, Y.: The community Noah land surface model with multiparameterization options (Noah-MP): 1. Model description and evaluation with local-scale measurements, J. Geophys. Res.-Atmos., 116, D12109, doi:10.1029/2010JD015139, 2011.

Oleson, K. W., Lawrence, D. M., Bonan, G. B., Flanner, M. G., Kluzek, E. K., Lawrence, P. J., Levis, S., Swenson, S. C., and Thornton, P. E.: Technical Description of version 4.0 of the Community Land Model (CLM), NCAR/TN-478+STR, Climate and

Global Dynamics Division, National Center for Atmospheric Research, Boulder, Colorado, 2010.

Osborne, T. M., Lawrence, D. M., Challinor, A. J., Slingo, J. M., and Wheeler, T. R.: Development and assessment of a coupled crop-climate model, Glob. Change Biol., 13, 169–183, 2007.

Peters, W., Krol, M. C., van der Werf, G. R., Houweling, S., Jones, C. D., Hughes, J., Schaefer, K., Masarie, K. A., Jacobson, A. R., Miller, J. B., Cho, C. H., Ramonet, M., Schmidt, M., Ciattaglia, L., Apadula, F., Helta, D., Meinhardt, F., di Sarra, A. G., Piacentino, S., Sferlazzo, D., Aalto, T., Hatakka, J., Strom, J., Haszpra, L., Meijer, H. A. J., van der Laan, S., Neubert, R. E. M., Jordan, A., Rodo, X., Morgui, J. A., Vermeulen, A. T., Popa, E., Rozanski, K., Zimnoch, M., Manning, A. C., Leuenberger, M., Uglietti, C., Dolman, A. J., Ciais, P., Heimann, M., and Tans, P. P.: Seven years of recent European net terrestrial carbon dioxide exchange constrained by atmospheric observations, Glob. Change Biol., 16, 1317–1337, doi:10.1111/j.1365-2486.2009.02078.x, 2010.

Pielke, R. A., Lee, T. J., Copeland, J. H., Eastman, J. L., Ziegler, C. L., and Finley, C. A.: Use of USGS – provided data to improve weather and climate simulations, Ecol. Appl., 7, 3–21, 1997.

Qin, Z., Berliner, P., and Karnieli, A.: Numerical solution of a complete surface energy balance model for simulation of heat fluxes and surface temperature under bare soil environment, Appl. Math. Comput., 130, 171–200, 2002.

R Core Team: R: A Language and Environment for Statistical Computing, R Foundation for Statistical Computing, Vienna, Austria, available at: http://www.R-project.org/ (last access: 14 January 2013), ISBN 3-900051-07-0, 2012.

Raupach, M. R.: Simplified expressions for vegetation roughness length and zero-plane displacement as functions of canopy height and area index, Bound. Lay. Meteorol., 71, 211–216, 1994.

Riley, W. J., Randerson, J. T., Foster, P. N., and Lueker, T. J.: Influence of terrestrial ecosystems and topography on coastal CO_2 measurements: a case study at Trinidad Head, California, J. Geophys. Res.-Biogeo., 110, G01005, doi:10.1029/2004JG000007, 2005.

Rutter, A. J., Morton, A. J., and Robins, P. C.: A predictive model of rainfall interception in forests. II. Generalization of the model and comparison with observations in some coniferous and hardwood stands, J. Appl. Ecol., 12, 367–380, 1975.

Sarrat, C., Noilhan, J., Dolman, A. J., Gerbig, C., Ahmadov, R., Tolk, L. F., Meesters, A. G. C. A., Hutjes, R. W. A., Ter Maat, H. W., Pérez-Landa, G., and Donier, S.: Atmospheric CO_2 modeling at the regional scale: an intercomparison of 5 meso-scale atmospheric models, Biogeosciences, 4, 1115–1126, doi:10.5194/bg-4-1115-2007, 2007.

Saxton, K. E., Rawls, W. J., Romberger, J. S., and Papendick, R. I.: Estimating generalized soil-water characteristics from texture, Soil Sci. Soc. Am. J., 90, 1031–1036, 1986.

Schomburg, A., Venema, V., Ament, F., and Simmer, C.: Disaggregation of screen-level variables in a numerical weather prediction model with an explicit simulation of subgrid-scale land-surface heterogeneity, Meteorol. Atmos. Phys., 116, 81–94, doi:0.1007/s00703-012-0183-y, 2012.

Sellers, P., Randall, D., Collatz, G., Berry, J., Field, C., Dazlich, D., Zhang, C., Collelo, G., and Bounoua, L.: A revised land surface parameterization (SiB2) for atmospheric GCMs. 1. Model formulation, J. Climate, 9, 676–705, 1996.

Sitch, S., Huntingford, C., Gedney, N., Levy, P. E., Lomas, M., Piao, S. L., Betts, R., Ciais, P., Cox, P., Friedlingstein, P., Jones, C. D., Prentice, I. C., and Woodward, F. I.: Evaluation of the terrestrial carbon cycle, future plant geography and climate-carbon cycle feedbacks using five Dynamic Global Vegetation Models (DGVMs), Glob. Change Biol., 14, 2015–2039, 2008.

Skamarock, W. C., Klemp, J. B., Dudhia, J., Gill, D. O., Barker, D. M., Duda, M. G., Huang, X.-Y., Wang, W., and Powers, J. G.: A Description of the Advanced research WRF Version 3, NCAR/TN-475+STR, Mesoscale and Microscale Meteorology Division, National Center for Atmospheric Research, Boulder, Colorado, 2008.

Sprintsin, M., Chen, J. M., Desai, A., and Gough, C. M.: Evaluation of leaf-to-canopy upscaling methodologies against carbon flux data in North America, J. Geophys. Res.-Biogeo., 117, G01023, doi:10.1029/2010JG001407, 2012.

Steeneveld, G. J., Tolk, L. F., Moene, A. F., Hartogensis, O. K., Peters, W., and Holtslag, A. A. M.: Confronting the WRF and RAMS mesoscale models with innovative observations in the Netherlands: evaluating the boundary layer heat budget, J. Geophys. Res.-Atmos., 116, D23114, doi:10.1029/2011JD016303, 2011.

Stoy, P. C., Williams, M., Disney, M., Prieto-Blanco, A., Huntley, B., Baxter, R., and Lewis, P.: Upscaling as ecological information transfer: a simple framework with application to Arctic ecosystem carbon exchange, Landscape Ecol., 24, 971–986, 2009.

Stoy, P. C., Mauder, M., Foken, T., Marcolla, B., Boegh, E., Ibrom, A., Arain, M. A., Arneth, A., Aurela, M., Bernhofer, C., Cescatti, A., Dellwik, E., Duce, P., Gianelle, D., van Gorsel, E., Kiely, G., Knohl, A., Margolis, H., McCaughey, H., Merbold, L., Montagnani, L., Papale, D., Reichstein, M., Saunders, M., Serrano-Ortiz, P., Sottocornola, M., Spano, D., Vaccari, F., and Varlagin, A.: A data-driven analysis of energy balance closure across FLUXNET research sites: The role of landscape scale heterogeneity, Agr. Forest Meteorol., 171, 137–152, 2013.

Sus, O., Williams, M., Bernhofer, C., Beziat, P., Buchmann, N., Ceschia, E., Doherty, R., Eugster, W., Gruenwald, T., Kutsch, W., Smith, P., and Wattenbach, M.: A linked carbon cycle and crop developmental model: description and evaluation against measurements of carbon fluxes and carbon stocks at several European agricultural sites, Agr. Ecosyst. Environ., 139, 402–418, 2010.

Ter Maat, H. W., Hutjes, R. W. A., Miglietta, F., Gioli, B., Bosveld, F. C., Vermeulen, A. T., and Fritsch, H.: Simulating carbon exchange using a regional atmospheric model coupled to an advanced land-surface model, Biogeosciences, 7, 2397–2417, doi:10.5194/bg-7-2397-2010, 2010.

Tolk, L. F., Peters, W., Meesters, A. G. C. A., Groenendijk, M., Vermeulen, A. T., Steeneveld, G. J., and Dolman, A. J.: Modelling regional scale surface fluxes, meteorology and CO_2 mixing ratios for the Cabauw tower in the Netherlands, Biogeosciences, 6, 2265–2280, doi:10.5194/bg-6-2265-2009, 2009.

Tuzet, A., Perrier, A., and Leuning, R.: A coupled model of stomatal conductance, photosynthesis and transpiration, Plant Cell Environ., 26, 1097–1116, doi:10.1046/j.1365-3040.2003.01035.x, 2003.

Van den Hoof, C., Hanert, E., and Vidale, P. L.: Simulating dynamic crop growth with an adapted land surface model – JULES-

SUCROS: model development and validation, Agr. Forest Meteorol., 151, 137–153, 2011.

Wang, Y. P. and Leuning, R.: A two-leaf model for canopy conductance, photosynthesis and partitioning of available energy I: model description and comparison with a multi-layered model, Agr. Forest Meteorol., 91, 89–111, 1998.

Wang, Y. P., Long, C. N., Leung, L. R., Dudhia, J., McFarlane, S. A., Mather, J. H., Ghan, S. J., and Liu, X.: Evaluating regional cloud-permitting simulations of the WRF model for the Tropical Warm Pool International Cloud Experiment (TWP-ICE), Darwin, 2006, J. Geophys. Res.-Atmos., 114, 1–21, doi:10.1029/2009JD012729, 2009.

Williams, M., Rastetter, E. B., Fernandes, D. N., Goulden, M. L., Wofsy, S. C., Shaver, G. R., Melillo, J. M., Munger, J. W., Fan, S. M., and Nadelhoffer, K. J.: Modelling the soil-plant-atmosphere continuum in a Quercus-Acer stand at Harvard Forest: the regulation of stomatal conductance by light, nitrogen and soil/plant hydraulic properties, Plant Cell Environ., 19, 911–927, 1996.

Williams, M., Malhi, Y., Nobre, A., Rastetter, E., Grace, J., and Pereira, M.: Seasonal variation in net carbon exchange and evapotranspiration in a Brazilian rain forest: a modelling analysis, Plant Cell Environ., 21, 953–968, doi:10.1046/j.1365-3040.1998.00339.x, 1998.

Williams, M., Eugster, W., Rastetter, E., McFadden, J., and Chapin, F.: The controls on net ecosystem productivity along an Arctic transect: a model comparison with flux measurements, Glob. Change Biol., 6, 116–126, 2000.

Williams, M., Law, B., Anthoni, P., and Unsworth, M.: Use of a simulation model and ecosystem flux data to examine carbon-water interactions in ponderosa pine, Tree Physiol., 21, 287–298, 2001.

Williams, M., Schwarz, P. A., Law, B. E., Irvine, J., and Kurpius, M.: An improved analysis of forest carbon dynamics using data assimilation, Glob. Change Biol., 11, 89–105, 2005.

Wright, J. K., Williams, M., Starr, G., McGee, J., and Mitchell, R. J.: Measured and modelled leaf and stand-scale productivity across a soil moisture gradient and a severe drought, Plant Cell Environ., 467–483, doi:10.1111/j.1365-3040.2012.02590.x, 2012.

Xie, B., Fung, J. C. H., Chan, A., and Lau, A.: Evaluation of nonlocal and local planetary boundary layer schemes in the WRF model, J. Geophys. Res.-Atmos., 117, D12103, doi:10.1029/2011JD017080, 2012.

Zhang, Y.: Online-coupled meteorology and chemistry models: history, current status, and outlook, Atmos. Chem. Phys., 8, 2895–2932, doi:10.5194/acp-8-2895-2008, 2008.

Chapter 3

Can seasonal and interannual variation in landscape CO_2 fluxes be detected by atmospheric observations of CO_2 concentrations made at a tall tower?

Manuscript prepared for Biogeosciences
with version 4.2 of the LaTeX class copernicus.cls.
Date: 6 January 2014

Can seasonal and interannual variation in landscape CO_2 fluxes be detected by atmospheric observations of CO_2 concentrations made at a tall tower?

T. L. Smallman[1,2], **M. Williams**[1,2], **and J. B. Moncrieff**[1]

[1]School of GeoSciences, University of Edinburgh, Edinburgh, EH9 3JN
[2]National Centre for Earth Observation, University of Edinburgh, Edinburgh, EH9 3JN

Abstract. The coupled numerical weather model WRF-SPA has been used to investigate a 3 year time series of observed atmospheric CO_2 concentrations from a tall tower in Scotland. Ecosystem specific tracers of net CO_2 uptake and net CO_2 release were used to investigate the contributions to the tower signal of key land covers within its footprint, and how contributions varied at seasonal and interannual time scales. In addition, WRF-SPA simulated atmospheric CO_2 concentrations were compared with two coarse global inversion models, Carbon Tracker Europe and Carbon Tracker (CTE-CT). WRF-SPA realistically modelled both seasonal (except post harvest) and daily cycles seen in observed atmospheric CO_2 at the tall tower (R^2 = 0.67, rmse = 3.5 ppm, bias = 0.58 ppm). Atmospheric CO_2 concentrations from the tall tower were well simulated by CTE-CT, but the inverse model showed a poorer representation of diurnal variation and simulated a larger bias from observations (up to 1.9 ppm) at seasonal time scales, compared to the forward modelling of WRF-SPA. However, we have highlighted a consistent post harvest increase in the seasonal bias between WRF-SPA and observations. Ecosystem specific tracers of CO_2 exchange indicate that the increased bias is potentially due to the representation of agricultural processes within SPA, and/or biases in land cover maps. The ecosystem specific tracers also indicate that the majority of seasonal variation in CO_2 uptake for Scotland's dominant ecosystems (forests, cropland and managed grassland) is detectable in observations within the footprint of the tall tower, however the amount of variation explained varies between years. Interannual variation in tower CO_2 concentrations was not well captured, potentially due to seasonal and interannual variation in the simulated prevailing wind direction. This result highlights the importance of accurately representing atmospheric transport used within atmospheric inversion models used to estimate terrestrial source / sink distribution and magnitude.

Correspondence to: T. L. Smallman
(t.l.smallman@.ed.ac.uk)

1 Introduction

The global climate is changing and these changes are driven by human activities, in particular by anthropogenic emissions of CO_2 (IPCC, 2007). The terrestrial biosphere currently absorbs a significant fraction of anthropogenic emissions of CO_2 (Canadell et al., 2007). However, terrestrial ecosystems are highly complex and dynamic, creating a net land-atmosphere surface exchange that can be either a source or sink of CO_2. Furthermore, the magnitude of sources and sinks vary both spatially and temporally resulting in significant seasonal, interannual and spatial variation. The magnitude of net ecosystem exchange of CO_2 (NEE) is significantly impacted by changes in weather, climate and human management adding further complexity to ecosystem processes (IPCC, 2007). Higher spatial and temporal resolution observations over multi-annual periods are required to detect fine scale ecosystem heterogeneity and ecosystem response to drivers. A critical objective is an improved understanding of the information contained within observations of atmospheric greenhouse gas concentrations.

Both forward running and atmospheric inversion models have been used in conjunction with observations of atmospheric CO_2 concentrations to investigate regional scale exchange of CO_2. Forward running models, such as WRF or RAMS, have been used to investigate a wide range of topics including the impact of surface processes on atmospheric transport (e.g., Steeneveld et al., 2011) and how ecosystems contribute to observations made at the regional scale (e.g., Tolk et al., 2009). Inverse atmospheric models which infer surface fluxes from measurements of atmospheric CO_2 concentrations (e.g., made at a tall tower), have been used to constrain the terrestrial carbon balance at global, continental and regional scales (Gurney et al., 2002; Peters et al.,

2010; Lauvaux et al., 2012). Inverse models are able to detect large scale, large magnitude interannual variations in CO_2 exchange. For example the Europe wide heat wave in 2003 has been linked to a large scale reduction in carbon sequestration across Europe (Ciais et al., 2005; Peters et al., 2010). However, there remains uncertainty over the ability of regional scale inversions to successfully quantify small magnitude changes in surface fluxes. Peters et al. (2010) suggested two contrasting hypotheses to explain increases in regional estimates of sequestration in the years following the European 2003 heat wave. First, increased sequestration may have been due to interannual variation in plant phenology. Second, changes to atmospheric transport due to interannual variation in weather (e.g. due to turbulent exchange) may have significantly altered the footprint of tall tower observations.

Observations of atmospheric CO_2 concentrations made at tall towers contain seasonal and interannual phenological information about ecosystems near the tower (Miles et al., 2012). However the correlation between surface NEE and observed profiles of atmospheric CO_2 concentration declines with increasing distance from the observing tower (Gerbig et al., 2009; Miles et al., 2012). A reduction in correlation between tall tower observations and ecosystem activity is consistent with signal dilution due to atmospheric transport (Gerbig et al., 2009; Miles et al., 2012). The dominant influence on observations of atmospheric CO_2 concentrations are from the near field, although the total footprint can cover a large area. For example, an area of $\sim$ 500 km x 700 km has been simulated to contribute up to $\sim$ 50 % of the observed signal at the Cabauw tall tower in the Netherlands, while the land surface at the edge of this area contributes $\sim$10 time less than the land surface directly beneath the Cabauw tower (Vermeulen et al., 2011). Similarly Gerbig et al. (2009) investigated the Harvard forest tower, USA, estimating that the land surface fluxes within 20-60 km of the tower contributed a similar amount to observations as all other areas within their simulated domain combined (5000 km x 5000 km). Furthermore, atmospheric inversions are unable to attribute variation and / or anomalies in atmospheric CO_2 concentrations to a specific ecosystem process (e.g. respiration or photosynthesis). A forward model has the advantage that processes and source area contributing to the atmospheric CO_2 signal can be directly investigated.

We used a mesoscale model, WRF-SPA, operating in forward mode to simulate a 3 year period between 2006 and 2008 over northern Britain (Fig. 1). Simulated atmospheric CO_2 concentrations from WRF-SPA, and a global atmospheric inversion model, were compared to observations made at tall tower Angus (TTA) on the east coast of Scotland. TTA is currently Scotland's only tall tower equipped for measurement of atmospheric CO_2 concentrations. WRF-SPA provides a means to upscale land surface exchanges such as photosynthesis and respiration, using atmospheric CO_2 tracers, to observations made mostly within the planetary boundary layer (PBL) of regionally integrated CO_2 concentrations i.e. those made at TTA.

The overall aim of this paper is to use ecosystem specific CO_2 tracers of net uptake and net release of CO_2 to improve our understanding of how different ecosystems contribute to observations of atmospheric CO_2 concentrations and relate these contributions to surface processes (Tolk et al., 2009). A unique aspect of this study is the 3 yr observation dataset used to consider the detection of both seasonal and interannual variation.

Here we address the following questions:

i. Does WRF-SPA more accurately simulated observed atmospheric CO_2 concentrations compared to a coarse resolution global atmospheric inversion model?

ii. Can ecosystem specific CO_2 tracers be used to inform on which ecosystem processes and land covers are responsible for observed variations in atmospheric CO_2 concentrations?

iii. Can observations made at TTA detect variation in ecosystem carbon uptake, for ecosystems within the footprint of TTA, at seasonal and interannual time scales?

2 Model description: WRF-SPA

WRF-SPA (Smallman et al., 2013) is a coupling between the high resolution non-hydrostatic mesoscale model Weather Research and Forecasting (WRF) and the mechanistic land surface model (LSM) Soil Plant Atmosphere (SPA). SPA is fully integrated into the WRF model framework where WRF simulates meteorological fields and atmospheric transport of the CO_2 fields. SPA in return provides WRF with surface temperature, roughness length, albedo, and exchanges of energy, heat, water and CO_2. A brief description of the WRF and SPA models are given below.

2.1 WRF

The Weather Research & Forecasting model (WRFv3.2) (http://www.mmm.ucar.edu/wrf/users/, accessed 19/10/2009 15:00) is a state of the art non-hydrostatic mesoscale meteorological community model (Skamarock et al., 2008). WRF provides a highly adaptable model framework into which SPA has been integrated. In addition to simulating meteorology WRF is responsible for simulating atmospheric transport of CO_2 tracers released by SPA and originating from the anthropogenic and oceanic flux maps as well as lateral boundary and initial conditions. WRFv3.2 includes a number of land surface maps including vegetation type and soil classification used by SPA, but also orography which impacts simulation of air flow within the model (Mesoscale and Microscale Meteorology Division, 2011).

2.2 SPA

The SPA model is a high vertical resolution mechanistic terrestrial ecosystem model (up to 10 canopy layers and 20 soil layers). SPA provides WRF with surface fluxes of heat, water and CO_2 exchange in response to meteorological drivers through a close coupling of its hydrological and carbon cycles, based on ecophysiological principles (Williams et al., 1996). Detailed descriptions of the major SPA developments can be found in Williams et al. (1996, 1998, 2001, 2005); Sus et al. (2010); Smallman et al. (2013).

WRF provides SPA with meteorological drivers including air temperature, precipitation, vapour pressure deficit (VPD), wind speed, friction velocity, atmospheric CO_2 mixing ratios, air pressure & short and long wave incoming radiation. SPA currently has parameters for 8 vegetation types (evergreen forest, deciduous forest, mixed forest, arable cropland, managed grassland, grassland, upland and urban) suitable for UK application and 13 soil types impacting soil hydrology. Vegetation cover is specified by the MODIS land cover map provided with WRFv3.2, while soil classifications are from the default WRF soil cover maps (Mesoscale and Microscale Meteorology Division, 2011).

The Farquhar model of photosynthesis (Farquhar and von Caemmerer, 1982), the Penman-Monteith model of leaf transpiration (Jones, 1992) and the leaf energy balance are coupled via a mechanistic model of stomatal conductance. Stomatal conductance is modelled by linking atmospheric demand for water and available water supply from the soil through plant hydraulics (Williams et al., 1996, 2001). SPA maximises carbon assimilation per unit nitrogen within a minimum leaf water potential constraint to prevent cavitation (Williams et al., 1996). SPA uses detailed multi-layer parameterisations of canopy processes including radiative transfer (Williams et al., 1998), above and within canopy momentum decay and leaf level boundary layer conductance (Smallman et al., 2013).

Plant phenology is described by a box carbon model to simulate the main ecosystem carbon (C) pools (Williams et al., 2005; Sus et al., 2010). C pools are foliage, structural wood carbon, fine roots, labile, soil organic matter (SOM) and surface litter. Crops have two additional C pools; storage organ C (i.e. harvestable C) and dead foliar C (still standing). The C pools within WRF-SPA are 'spun-up' as described in Smallman et al. (2013), using meteorology which is broadly representative of the median meteorological conditions in Scotland. The carbon model provides a direct coupling between the plant carbon cycle and plant phenology, specifically foliar and fine root C. Foliar C determines the leaf area index (LAI) while fine root C impacts water uptake potential.

2.3 Initial and lateral boundary conditions for CO_2

Initial conditions (IC) and lateral boundary conditions (LBC) for atmospheric CO_2 (except 2008) are from Carbon Tracker Europe (CTE, Peters et al., 2010) providing 1°x 1° resolution fields at 3 hourly intervals. Optimised CO_2 fields were not available for 2008 from CTE; instead CO_2 fields for 2008 are from Carbon Tracker (Peters et al., 2007). These are also available at 3 hourly intervals, but at a coarse 3°x 2° resolution. IC and LBC for atmospheric CO_2 were linearly interpolated to the WRF-SPA domain.

Global flux maps of anthropogenic CO_2 emissions and ocean absorption were used to provide non-biospheric surface CO_2 exchange. The global flux maps were also from CTE at 1° x 1° resolution with 3 hourly update interval. Fluxes were interpolated using 4 point weighted mean based on latitude and longitude coordinates. Biospheric fluxes of CO_2 are simulated by SPA. All surface CO_2 fluxes were calculated as rates which were added to the lowest model atmospheric layer in each time step.

2.4 Atmospheric CO_2 tracers

WRF-SPA has been modified with the addition of several atmospheric CO_2 tracer pools (Table 1). CO_2 tracer transport is simulated within the model domain concurrently with meteorological variables (feedback on atmospheric radiative transfer due to variable CO_2 is neglected as its impact is expected to be small at $\sim$3 %).

We compared simulated atmospheric CO_2 with an active biosphere versus simulated without a biosphere ("forcings only"). "Forcings only" CO_2 tracer contains IC, LBC, anthropogenic emissions and ocean sequestration of CO_2 (i.e. CO_2 exchange not calculated by WRF-SPA) but no exchange with the SPA simulated biosphere. Comparison between the total atmospheric CO_2 concentration and "forcings only" CO_2 concentration allow for isolations of the impact due to inclusion of the simulated biosphere. Furthermore, CTE (2006-2007) and CT (2008) atmospheric CO_2 concentrations are compared to TTA observations to assess how well CTE-CT simulates atmospheric CO_2 at a tower not included in the inversion model.

2.4.1 Ecosystem specific tracers

The ecosystem specific tracers of net uptake and net release of CO_2 are used to investigate the information content on these processes contained within the total atmospheric CO_2 concentrations simulated at TTA. We investigate how representative observations at TTA are of the underlying surface fluxes of CO_2. Note that LBCs for the outer domain have been set with zero inflow and zero-gradient outflow for ecosystem specific net uptake and net release CO_2 tracers. Zero gradient inflow / outflow allow tracers to easily leave the domain and prevent artificial influx to the CO_2 tracer fields.

The land surface can be either a net source or net sink of atmospheric CO_2, varying both spatially and temporally. Whether the land surface is a net sink or source of CO_2 is determined by the net result of photosynthetic and respiratory processes. Atmospheric CO_2 concentrations represent a spatial and temporal integration of the net flux of CO_2 between the land surface and the lower atmosphere. Therefore, when the simulated surface flux of CO_2 represents a net removal of CO_2 from the atmosphere, an ecosystem specific 'net uptake CO_2 tracer' is released into the simulated atmosphere at the same rate as the 'surface net CO_2 uptake flux' (i.e. rate of NEE). Correspondingly, when the surface net CO_2 uptake flux represents a net addition of CO_2 to the atmosphere an ecosystem specific 'net release CO_2 tracer' is released.

The net uptake CO_2 tracers are considered to be non-interacting / non-interactive, while the net release CO_2 tracers are interacting / interactive. The net uptake CO_2 tracers are non-interacting as they represent a removal of atmospheric CO_2 and as such cannot interact with the land surface. After their emission from the surface the net uptake CO_2 tracers are transported through the model atmosphere. Conversely, net release CO_2 tracers represent an addition of a physical mass of CO_2 to the atmosphere via respiration, which can therefore be subsequently removed from the atmosphere by photosynthesis after its initial release. Allowing the removal of a net release CO_2 tracer prevents a respiratory signal from being simulated at TTA which in reality does not reach TTA due to being consumed en route in a physically consistent manor.

Net release CO_2 tracers are removed from the atmosphere if they are present in the lowest model atmospheric level and the land surface below represents a net removal of CO_2. If there are multiple ecosystem specific net release CO_2 tracers present in the same model atmosphere grid box, then removal is determined by the relative fraction of each ecosystem specific tracer. For example, to determine the removal of crop net release CO_2 tracer

$$\gamma \uparrow t_{crop}rm = \frac{\uparrow t_{crop}}{\uparrow t_{crop} + \uparrow t_{forest} + \uparrow t_{grass} + \uparrow t_{other}} \quad (1)$$

where $\gamma \uparrow t_{crop}rm$ is the fraction of surface CO_2 flux (i.e. NEE) to be applied to the crop net release CO_2 tracer. $\uparrow t_{crop}$ is the crop net release (as indicated by the direction of the arrow and t indicates it being a tracer) CO_2 tracer concentration, similarly for forest, managed grassland and 'other' land cover types.

2.4.2 Investigating representivity and detection of seasonal and interannual variation using CO_2 tracers

Ecosystem specific CO_2 tracers are used to infer representativeness of the simulated atmospheric CO_2 concentrations at TTA of surface CO_2 flux and to investigate how much seasonal and interannual information is contained within these atmospheric CO_2 concentrations. We assumed that the simulated atmospheric CO_2 tracers are driven by the simulated surface CO_2 fluxes (from which they originate) and that atmospheric transport determines how much information on surface fluxes is represented within atmospheric CO_2 concentrations at any given location within the simulated atmosphere. To minimise the effects of short term transport and to focus only on large seasonal variations, we conducted these analyses using monthly mean values.

We investigated the representativeness of atmospheric CO_2 concentrations simulated at TTA of surface CO_2 flux. We compared the fraction of each ecosystem specific net uptake CO_2 tracer (e.g. for crop $\downarrow t_{crop}$) simulated at TTA to the fraction of ecosystem specific surface net CO_2 uptake flux (e.g. for crop $\downarrow f_{crop}$, where f indicates this is a flux). Each flux is the integral over the land surface included within the land surface mask detailed in section 3.1.

$$\gamma \downarrow t_{crop} = \frac{\downarrow t_{crop}}{\downarrow t_{crop} + \downarrow t_{forest} + \downarrow t_{grass} + \downarrow t_{other}} \quad (2)$$

$$\gamma \downarrow f_{crop} = \frac{\downarrow f_{crop}}{\downarrow f_{crop} + \downarrow f_{forest} + \downarrow f_{grass} + \downarrow f_{other}} \quad (3)$$

Representativeness for any given ecosystem type is assumed to be when

$$\gamma \downarrow t_{crop} \approx \gamma \downarrow f_{crop} \quad (4)$$

Moreover, this comparison provides an indication of whether the activity of a given ecosystem is over-represented (i.e. $\gamma \downarrow t_{crop} > \gamma \downarrow f_{crop}$) or under-represented (i.e. $\gamma \downarrow t_{crop} < \gamma \downarrow f_{crop}$) in simulated atmospheric CO_2 concentrations. Such information can help the interpretation of results from comparing ecosystem specific CO_2 tracers and the simulated atmospheric CO_2 concentrations.

Investigation of seasonal variation is achieved through linear regression analysis between the surface net CO_2 uptake flux and net uptake CO_2 tracer concentration, for a given land cover type. As net uptake CO_2 tracers originate from the simulated surface net CO_2 uptake flux, differences between seasonal variation of tracer concentrations and surface fluxes are due to how atmospheric transport relays variations in flux to TTA. To investigate interannual variation simulated to be detected at TTA, we assume that a change in surface net CO_2 uptake flux for a given ecosystem should be reflected in the net uptake CO_2 tracers simulated at TTA.

2.5 Model domain

The WRF-SPA simulation is comprised of two grids in two-way nesting mode; the outer domain has a resolution of 18 km x 18 km and inner domain 6 km x 6 km (Fig. 1). Scotland provides a highly complex topography and land use heterogeneity, with a longitudinal gradient from dominantly forested and peatland areas in the north west to pasture in the central and south west and arable cropland in the east.

All meteorological data required e.g., sea surface temperature (SST), soil initialisation, initial conditions and lateral boundary conditions were taken from the Global Forecasting System (GFS) reanalysis product (http://www.emc.ncep.noaa.gov/). GFS data are available at 1°x 1° longitude / latitude resolution with 6 hourly time steps (available from http://rda.ucar.edu/datasets/ds083.2/). The main features of the WRF model set up are presented in Table 2.

3 Tall tower observations

Observations of atmospheric CO_2 concentration are from TTA, a 222 m tower (observation height) near Dundee, Scotland (56.56 N, 2.99 W). TTA is equipped for continuous measurement of atmospheric CO_2 concentrations producing half hourly observations which have been averaged to hourly time scales for comparison with WRF-SPA. TTA has been operational since the end of 2005 to the current date. Observations made at TTA have an accuracy limit of 0.1 ppm. TTA was part of the CHIOTTO network during the period of analysis reported here (EVK2-CT-2002-00163) and as such was fully integrated into the calibration and validation methodologies of that project. The data continues to be quality controlled under the InGOS project (http://www.ingos-infrastructure.eu/, accessed 09/12/2013, 16:30 UTC).

3.1 TTA footprint

Currently there are no published assessment of TTA's observation footprint, however the footprint of Mace Head, located on the west coast of Ireland has been assessed in multiple studies (e.g. Henne et al., 2010; Rigby et al., 2011; Brunner et al., 2012). Mace Head is exposed to similar meteorological conditions in north west Europe, and therefore we expect a similar footprint. Henne et al. (2010) calculated a 12 hour inversion, estimating the footprint of Mace Head to be the land surface within ∼195 km of the tower. Therefore, if a similar footprint is assumed for TTA ∼98 % of the inner domain's land surface is within the footprint of TTA. We use this estimate of footprint to mask the area of the land surface which is presented throughout this study.

4 Results

4.1 CO_2 time series at TTA

We compared hourly observations of atmospheric CO_2 concentrations from TTA (2006-2008) with both the WRF-SPA simulated total atmospheric CO_2 (R^2 = 0.67, rmse = 3.5 ppm, bias = 0.58 ppm, linear regression) and "forcings only" CO_2 (R^2 = 0.71, rmse = 3.3 ppm, bias = 0.82 ppm). These results suggest a slightly negative impact of including the modelled biosphere. However the annual bias for total atmospheric CO_2 from WRF-SPA is lower than "forcings only" CO_2, highlighting the impact of Scotland's biosphere sink (Fig. 2a). Furthermore the addition of biospheric fluxes captures diurnal variation in hourly observations which is otherwise absent in "forcings only" CO_2 (Fig. 2ab). However, inclusion of biospheric fluxes results in an overestimation of night time atmospheric CO_2 concentrations simulated at the tall tower (Fig. 2b). A comparison between atmospheric CO_2 concentrations observed at TTA and CTE (2006-2007) and CT (2008) atmospheric inversion model (R^2 = 0.69, rmse = 3.5 ppm, bias = 0.92 ppm) suggesting comparable skill to WRF-SPA. However CTE-CT does not simulate daily cycles in observed atmospheric CO_2 concentrations as well as WRF-SPA (Fig. 2b). As CTE-CT are available at 3 hourly intervals the analysis was conducted against TTA observations averaged to a 3 hourly time step.

The impact of the biosphere is more clearly seen at seasonal time scales using monthly means (Fig. 3). Total atmospheric CO_2 (R^2 = 0.96, rmse = 1.2 ppm, bias = 0.54 ppm), which includes biospheric exchange, shows improved statistical agreement with observations compared to "forcings only" CO_2 (R^2 = 0.91, rmse = 1.6 ppm, bias = 0.71 ppm) and CTE-CT atmospheric CO_2 concentrations (R^2 = 0.94, rmse = 1.5 ppm, bias = 0.94 ppm). The monthly mean bias between total atmospheric CO_2 and observations is reduced for the majority of the comparison period relative to "forcings only" CO_2 and CTE-CT. The seasonal bias is reduced in total atmospheric CO_2 by up to 2.8 ppm and 1.9 ppm between March and June of each year compared to "forcings only" CO_2 and CTE-CT respectively (Fig. 3). However, the modelled biosphere does not capture the observed seasonal minimum in atmospheric CO_2 concentrations which occurs in July - August of each year (Figs. 2,3). During July - September total atmospheric CO_2 has a larger bias than both "forcings only" CO_2 and CTE-CT, compared to observations. A larger positive bias in total atmospheric CO_2 than "forcings only" CO_2 indicates that modelled ecosystems within the footprint of the tall tower have become a net source of CO_2 at a time when they should remain a net sink (Fig. 3).

4.2 Ecosystem contributions to atmospheric CO_2 concentrations at TTA

The dominant ecosystems simulated within the footprint are forest, crop and managed grassland (Fig. 1). Over the validation period WRF-SPA simulated forest (-2.56$\pm$0.05 tC ha^{-1} yr^{-1}, $\pm$ standard error accounting for spatial and temporal uncertainty only) and managed grassland (-0.48$\pm$0.02 tC ha^{-1} yr^{-1}) ecosystems to be mean annual sinks of carbon. Crop ecosystems (0.89$\pm$0.01 tC ha^{-1} yr^{-1}) were simulated to be a mean annual source of carbon. WRF-SPA estimates Scotland to be on average a carbon sink of -0.99$\pm$0.04 tC ha^{-1} yr^{-1}. CTE-CT estimate Scotland to be a carbon source of +0.65 tC ha^{-1} yr^{-1}.

Net uptake and net release CO_2 tracers simulated at TTA suggest that cropland ecosystems have a distinct seasonal cycle from that of forests, managed grassland and 'other' land cover types (Fig. 4). Managed grassland and 'other' land covers are not included in the figure due to their contribution to atmospheric CO_2 concentrations being small, never exceeding 0.7 ppm. Peak net uptake CO_2 tracer simulated at TTA occurs 1 month earlier in crops than forest (except in 2006), while net release CO_2 tracer simulated at TTA for cropland shows a similar seasonality to all other ecosystems. Peak crop respiration coincides with crop harvest, a point in time when plant biomass has undergone senescence and has subsequently either been removed as part of harvest processes or remains after harvest as residue added to the litter pool (mean simulated harvest day of year: 2006 is $225^{+}_{-}17.9$, 2007 is $229^{+}_{-}21.4$, 2008 is $229^{+}_{-}21.5$, standard deviation accounting for spatial variability only). While crops contribute a similar amount of net release CO_2 tracer as forest during the growing season, during winter crop net release CO_2 tracer is less than half that of forest (Fig. 4). Anthropogenic CO_2 simulated at TTA is comparable in magnitude to that of CO_2 released by the biosphere. Also, anthropogenic CO_2 does not display a strong seasonal trend (Fig. 4).

Forest and crops dominate the net uptake CO_2 tracer simulated at TTA (65 - 93 % of TTA tracer concentration and 72 - 91 % of surface flux) (Fig. 5). On average crop and managed grassland are over-represented in net uptake CO_2 tracers simulated at TTA by 3 % and 3.4 % respectively. Managed grassland represents on average just ∼13 % of surface net CO_2 uptake flux compared to ∼40 % for crops. Forest and 'other' ecosystems are under-represented by 5 % and 1.2 % respectively. However the over / under-representation varies at seasonal time scales, e.g. the largest under-representation of forests at TTA occurs between August 2006 and January 2007 (21 %) while at other times atmospheric CO_2 simulated at TTA is more representative. The bias towards crops is consistent with the spatial distribution of crops and forest cover in relation to TTA's location (Fig. 1). Crops is the dominant ecosystem, both in terms of net uptake CO_2 tracer and surface net CO_2 uptake flux during the growing season (Fig. 5). After harvest (July of each year) forest becomes the dominant land cover for driving CO_2 exchange, as crop surface net CO_2 uptake flux declines due to senescence and removal of plants.

4.3 Seasonal and interannual variation

Net uptake CO_2 tracers simulated at TTA are able to explain the majority of seasonal variation in surface net CO_2 uptake for crops, forest, managed grassland and 'other' land covers (Table 3). The seasonal cycles in net uptake CO_2 tracers are more variable during the growing season (i.e. May - August), such that there is a mismatch between peak net uptake CO_2 tracers and surface net CO_2 uptake flux by $^{+}_{-}$ one month (Fig. 6). Moreover the amount of variation in surface net CO_2 flux explained by net uptake CO_2 tracers simulated at TTA varied between years (e.g. forest 2006 R^2 = 0.79 and 2008 R^2 = 0.58). The rank order of net uptake CO_2 tracers simulated at TTA from each year does not correspond with the rank order of surface net CO_2 uptake flux for any ecosystem (Fig. 6). Interannual variation in mean annual surface net CO_2 uptake flux was ∼9 % while interannual variation for mean annual net uptake CO_2 tracer at TTA was ∼19 %.

The annual prevailing wind direction over Scotland varied between years; in 2006 and 2008 the prevailing wind direction was broadly south / south west, while in 2007 the prevailing wind direction was westerly. Moreover, the prevailing wind direction varied at seasonal time scales. During the peak growing season (May to August) there was considerable variation (Fig. 7). In 2006 prevailing wind direction during the growing season varied between southerly and westerly. While in 2007 and 2008 there were periods of northerly and easterly winds, particularly during June; returning to more south westerly directions by August in each year. This interannual and seasonal variation in wind direction will have impacted the detected footprint by TTA.

5 Discussion

5.1 CO_2 time series

WRF-SPA demonstrated that it can recreate observations of atmospheric CO_2 concentrations (Fig. 2ab). The dominant seasonal cycle reproduced by WRF-SPA is largely driven by forcings external to the modelled domain, i.e. the global signal from lateral boundary conditions (Fig. 2a) as indicated by the "forcings only" CO_2 tracer. Atmospheric CO_2 concentrations are underestimated during the winter, however the bias is of a smaller magnitude in total atmospheric CO_2 than in "forcings only" CO_2 (Fig. 3). The underestimation during winter likely indicates that SPA underestimates net release of CO_2 flux (i.e. respiration) from the land surface. WRF-SPA has previously been validated against eddy covariance observations of NEE at forest, managed grassland and cropland sites, where forest and managed grassland NEE was overestimated during winter while cropland was underestimated (Smallman et al., 2013). Given that net release CO_2 tracers simulated at TTA for crops is half the magnitude for forests, crops are a plausible candidate to explain the winter time underestimate in simulated atmospheric CO_2 concentrations (Fig. 4). Smallman et al. (2013) hypothesised that the underestimate in crop could be related to an underestimation of soil organic matter or the rate of soil organic matter turnover within the carbon model, however there remain several possibilities to be explored (e.g. ploughing).

In contrast CTE-CT continues to overestimate atmospheric CO_2 until late in the year (November / December) indicating that the inversion analysis continues to underestimate Scotland's carbon sink / overestimate carbon source

during this period (Fig. 3). The WRF-SPA modelled biosphere generates diurnal cycles of realistic magnitude in the modelled CO_2 time series (Fig. 2b) and reduces the seasonal bias seen in "forcing only" CO_2 (Fig. 3), however nocturnal atmospheric CO_2 concentrations are overestimated. The nocturnal overestimation of atmospheric CO_2 concentrations is likely due to an error in the YSU PBL scheme used in WRF-SPA. The error results in an overestimation of atmospheric eddy diffusivity under stable conditions, ultimately leading to a higher PBL (Hu et al., 2013). However, given that day time CO_2 concentrations remain well simulated it is unlikely that the nocturnal error persists into the well mixed boundary layer due to rapid turnover of the atmosphere through nudging by LBCs. Moreover, WRF-SPA has been previously assessed against surface fluxes of heat, water and CO_2, and daytime vertical profiles of atmospheric CO_2 concentrations where profile structure was well simulated, from which we can infer appropriate atmospheric transport (Smallman et al., 2013). Furthermore WRF-SPA's performance is comparable with several studies which have compared observations of atmospheric CO_2 concentrations made at tall towers to high resolution mesoscale model simulations (e.g., Ahmadov et al., 2009; Tolk et al., 2009; Pillai et al., 2011).

Atmospheric CO_2 concentrations from CTE-CT were also compared to observation made at TTA, at both 3 hourly averaged (Fig. 2b) and monthly mean time scales (Fig. 3). The statistical comparison suggests little impact of high resolution simulation using WRF-SPA, which contrasts with similar comparisons between high and coarse horizontal resolution models (e.g. Ahmadov et al., 2009). However, CTE-CT do not capture the observed diurnal cycle seen in TTA observation as well as WRF-SPA (Fig. 2b). The mean bias between observations of atmospheric CO_2 concentrations from TTA (which are not included in the CTE-CT atmospheric inversion) and CTE-CT is comparable to towers which were included in the inverse model (Peters et al., 2010). At seasonal time scales CTE-CT tends to show a reduced bias compared with "forcings only" CO_2, however the growing season bias remains larger than in total atmospheric CO_2 concentrations simulated by WRF-SPA (Fig. 3).

The prevailing wind direction over the UK is south westerly allowing the tower at Mace Head, Ireland to provide an estimate of the background CO_2 concentration and to act as a boundary condition upwind of the air which passes over Scotland. Mace Head is used to provide a boundary condition in the CTE-CT atmospheric inversion (Peters et al., 2010). Importantly the bias between observations made at Mace Head and CTE-CT is small at +0.05 ppm (Peters et al., 2010). Therefore, it can be inferred that the errors between modelled estimates of atmospheric CO_2 concentrations and observations is largely due to the simulation of surface exchanges within the model domain presented here.

5.2 Scotland's carbon balance

WRF-SPA's estimate of carbon sink magnitude is $\sim$5 fold greater than the official estimate of Scotland's carbon sink by the UK National Atmospheric Emissions Inventory (NAEI), which estimates Scotland's carbon balance to be -0.20 tC ha^{-1} yr^{-1} (Thomson et al., 2012). WRF-SPA does not account for a number of management impacts such as biomass burning and land cover change. Excluding these fluxes the NAEI estimate for Scotland's carbon sink is -0.44 tC ha^{-1} yr^{-1}. While WRF-SPA agrees with the NAEI that Scotland is a net sink of carbon, there appears to be a large discrepancy in the magnitude of the sink strength, the causes of which remain to be identified. However as we currently lack an error analysis of atmospheric CO_2 concentrations simulated by WRF-SPA it remains unknown whether the discrepancy shown here is within errors.

WRF-SPA simulated mean forest sequestration (-2.56 tC ha^{-1} yr^{-1}) is approximately double estimates for UK wide (Cannell et al., 1999) and average European forest sequestration (Janssens et al., 2005; Luyssaert et al., 2010). Scotland specific estimates of forest sequestration are more similar to the simulations; Scotland specific estimates range between $\sim$1.8 tC ha^{-1} yr^{-1} (Thomson et al., 2012) and $\sim$2.0 tC ha^{-1} yr^{-1} (Forestry Commission Scotland, 2009). Forest activity is under-represented in atmospheric CO_2 concentrations simulated at TTA as indicated by the lower fraction of net uptake CO_2 tracer simulated at TTA compared to the fraction of surface net CO_2 uptake flux originating from forest land cover. This under-representation of forest cover may explain why there is no apparent overestimation of Scotland's net carbon sink in the comparison between simulated CO_2 at TTA and observations. Grasslands were simulated to be a net carbon sink (-0.48 tC ha^{-1} yr^{-1}) while croplands were simulated to be a net carbon source (0.89 tC ha^{-1} yr^{-1}). Estimates of grassland carbon sink are more comparable with other estimates, which range between -0.69 tC ha yr^{-1} (UK average, Janssens et al., 2005) and -0.15 tC ha yr^{-1} (Scotland specific, Thomson et al., 2012). The WRF-SPA estimate of cropland source magnitude is also comparable with other UK wide (0.53 tC ha^{-1} yr^{-1}, Janssens et al., 2005) and Scotland specific estimates (0.88 tC ha^{-1} yr^{-1}, Thomson et al., 2012).

The simulated representation of arable cropland within WRF-SPA is likely to be responsible for the increase in the monthly mean bias between July - September in total atmospheric CO_2 (Fig. 3). Cropland net uptake CO_2 tracer simulated at TTA declines in magnitude concurrently with the increase in total atmospheric CO_2 bias in July (Figs. 3,4). In addition, the total atmospheric CO_2 bias exceeds the "forcings only" CO_2 bias in August as cropland respiration increases due to the input of litter from harvest. Above ground carbon is removed as part of the harvest, leaving a fraction of above ground carbon as surface residue and root carbon within the soil. Both the surface residue and root carbon are

added to the litter carbon pool, which begin to decompose significantly increasing respiration from cropland.

In Scotland on average ∼36 % of agricultural land is uncultivated, including woodland patches, hedgerows and fallow land (The Scottish Government, 2012). However, WRF-SPA does not simulate uncultivated land associated with agriculture. These unmodelled vegetative components are likely to be perennial systems, lacking intensive management and as a result have a longer growing season. For example, forest and managed grassland ecosystems continue to have a significant level of surface CO_2 uptake flux for several months after cropland harvest (Fig. 6). Therefore, uncultivated systems represent a significant contribution to the agricultural carbon balance at regional scales (Smith, 2004). Further development in the representation of agricultural land within LSMs is needed. For example, modelling at high spatial resolutions may allow land cover maps to resolve some of this heterogeneity, alternatively a tiling system could be used to represent this sub-grid heterogeneity.

5.3 Representativeness and seasonal variation of TTA observations

Cropland is most often the dominant ecosystem specific net uptake CO_2 tracer simulated at TTA and the dominant surface net CO_2 uptake flux (Fig. 6). Cropland is also fractionally over-represented at TTA compared to its surface net CO_2 uptake flux (Fig. 5). Over-representation of crops is expected given the spatial distribution of the land cover types in relation to TTA (Fig. 1). Our results are consistent with other findings of both modelling and observational studies in this regard (Gerbig et al., 2009; Vermeulen et al., 2011; Lauvaux et al., 2012; Miles et al., 2012). Forests dominate the fractional activity after cropland harvest due to their continuing biological activity in the late summer (Figs. 5, 6).

Atmospheric CO_2 concentrations simulated at TTA contains significant seasonal information on ecosystems that are not adjacent to the tower (i.e. forest, managed grassland and 'other'). Forest dominance of the fraction of net uptake CO_2 tracer (Fig. 5) at TTA coincides with crop senescence and harvest (Fig. 4). The relatively small mismatches shown here seem likely to be explained by seasonal variation in tower footprint as indicated by seasonal and interannual variation in prevailing wind direction (Fig. 7). Cropland is best represented by net uptake CO_2 flux tracers (Table 3) which is expected given the local dominance already discussed. However it should be noted that within an atmospheric inversion simulation the lack of a detectable seasonal cycle within atmospheric CO_2 concentrations would still convey information on surface net CO_2 fluxes.

5.4 Interannual variation

Interannual variation of the simulated seasonal cycles in surface net CO_2 uptake flux is poorly represented by net uptake CO_2 tracers simulated at TTA (Fig. 6). Interannual variation of net uptake CO_2 tracers simulated at TTA is greater than interannual variation in modelled land surface net CO_2 uptake flux. This suggests that interannual variation in atmospheric transport due to year to year variation in weather, not variation in land surface net CO_2 uptake, is the dominant driver of interannual variation in tall tower observations for the years simulated here. This inference is supported by the interannual variation in wind direction, for example during the growing season (May, June, July and August) in 2008 the there is a larger incidence of easterly winds altering the observation footprint of TTA (Fig. 7). This highlights the need for careful attention to atmospheric transport uncertainties and errors when carrying out atmospheric inversions. To detect a change in land surface activity the magnitude of the change must be greater than the variation in detection due to transport. Alternatively, an extended network of tall towers is required to gain spatially explicit information on land surface exchange (Lauvaux et al., 2012).

Net uptake CO_2 tracer concentrations for managed grassland and 'other' land covers simulated at TTA are less than 0.7 ppm and 0.2 ppm respectively. The accuracy limit for CO_2 detection of the equipment installed at TTA is 0.1 ppm. This suggests that limited real world information is present in TTA observations for managed grassland and 'other' land covers in the MODIS map. Therefore, it is also likely that TTA provides limited information in the real world for any ecosystem with limited activity or small spatial extent. Ineffective detection of 'other' vegetation is significant as 'other' land cover types include Scotland's uplands and peatland areas. Upland and peatland areas are highly important given the significant amount of carbon stored as soil organic matter in these soils, estimated to contain > 200 tC ha^{-1} (Bradley et al., 2005). However it should be noted that the MODIS land cover map used in WRF-SPA does contain errors, the upland and peatland cover for Scotland in the MODIS map is ∼3 % while more detailed mapping efforts of Scotland have estimated uplands and peatlands to cover a larger area (∼ 17 % The Macaulay Land Use Research Institute, 1993).

5.5 Future work

WRF-SPA estimates for ecosystem specific mean annual sequestration are broadly reasonable, however they should be considered with caution. This study does not estimate the SPA parameter uncertainties or uncertainties associated with atmospheric transport that may have a significant impact on the interpretation of sequestration estimates given here. As a result, estimates of ecosystem mean annual carbon sequestration should be considered only as indicators of consistency with other estimates. Therefore future work should involve an appropriate data driven uncertainty analysis of SPA parameters (i.e. data assimilation) and an attempt to assess atmospheric transport uncertainties.

WRF-SPA does not currently include a representation of forest management. Forest ecosystems are initialised with identical conditions that have been 'spun up' into steady state. As a result important differences in forest sequestration due to age class distribution and lateral transport of carbon due to forest harvest are not included. In future, a more detailed representation of forest processes should be included.

It remains to be investigated whether policy relevant land cover management can be detected at TTA (e.g. afforestation). WRF-SPA simulations presented here indicate that observations made at TTA are unable to reliably detect interannual variation of ecosystems. However tall towers are expected to be used for monitoring the effects of land surface management aimed at mitigating climate change (ICOS, 2012). Current Scottish Government policy is to increase Scotland's forest cover by 650,000 ha by 2050 (Forestry Commission Scotland, 2009). Through WRF-SPA the capability of current observations to detect changes in Scotland's regional carbon balance should be investigated.

6 Conclusions

Three specific questions were asked of WRF-SPA to investigate atmospheric observations of CO_2 made mostly within the PBL from TTA, Scotland.

(i) Does WRF-SPA more accurately simulated observed atmospheric CO_2 concentrations compared to a coarse resolution global atmospheric inversion model? WRF-SPA does more accurately simulate observed atmospheric CO_2 concentrations at TTA compared to CTE-CT. WRF-SPA better represents diurnal variation and a reduced bias between simulated atmospheric CO_2 concentrations and observations, particularly during the growing season. (ii) Can ecosystem specific CO_2 tracers be used to inform on which ecosystem processes and land covers are responsible for observed variations in atmospheric CO_2 concentrations? Ecosystem specific tracers have been successfully used to infer crops as responsible for a increase in the bias between WRF-SPA simulated atmospheric CO_2 concentrations at observations post harvest each year. Furthermore we have hypothesised that the cause of the error is the lack of a representation of uncultivated components of agricultural land not currently parameterised for in WRF-SPA. (iii) Can observations made at TTA detect variation in ecosystem carbon uptake, for ecosystems within the footprint of TTA, at seasonal and interannual time scales? A majority of seasonal variation in surface net CO_2 uptake flux is explained by net uptake CO_2 tracers for each ecosystem. However the amount of variation explained varied considerably between years. Moreover interannual variation was not well captured, potentially due to seasonal and inter annual variation in the prevailing wind direction. However for all other ecosystems interannual variation in atmospheric transport due to year to year variation in weather had a large impact on tall tower observations than interannual variation in surface uptake.

Acknowledgements. The authors would like to thank the PhD project funding body, National Centre for Earth Observation, a Natural Environment Research Council research centre. Tall tower Angus has been funded since 2004 by EU FP5, FP6 grants.

References

Ahmadov, R., Gerbig, C., Kretschmer, R., Koerner, S., Roedenbeck, C., Bousquet, P., and Ramonet, M.: Comparing high resolution WRF-VPRM simulations and two global CO_2 transport models with coastal tower measurements of CO_2, Biogeosciences, 6, 807–817, 2009.

Bradley, R., Milne, R., Bell, J., Lilly, A., Jordan, C., and Higgins, A.: A soil carbon and land use database for the United Kingdom, Soil Use Manage., 21, 363–369, doi:10.1079/SUM2005351, 2005.

Brunner, D., Henne, S., Keller, C. A., Reimann, S., Vollmer, M. K., O'Doherty, S., and Maione, M.: An extended Kalman-filter for regional scale inverse emission estimation, Atmos. Chem. Phys., 12, 3455–3478, doi:10.5194/acp-12-3455-2012, 2012.

Canadell, J. G., Le Quere, C., Raupach, M. R., Field, C. B., Buitenhuis, E. T., Ciais, P., Conway, T. J., Gillett, N. P., Houghton, R. A., and Marland, G.: Contributions to accelerating atmospheric CO_2 growth from economic activity, carbon intensity, and efficiency of natural sinks, P. Natl. Acad. Sci. USA., 104, 18 866–18 870, doi:10.1073/pnas.0702737104, 2007.

Cannell, M., Milne, R., Hargreaves, K., Brown, T., Cruickshank, M., Bradley, R., Spencer, T., Hope, D., Billett, M., Adger, W., and Subak, S.: National inventories of terrestrial carbon sources and sinks: The UK experience, Clim. Change, 42, 505–530, doi:10.1023/A:1005425807434, 1999.

Ciais, P., Reichstein, M., Viovy, N., Granier, A., Ogee, J., Allard, V., Aubinet, M., Buchmann, N., Bernhofer, C., Carrara, A., Chevallier, F., De Noblet, N., Friend, A., Friedlingstein, P., Grunwald, T., Heinesch, B., Keronen, P., Knohl, A., Krinner, G., Loustau, D., Manca, G., Matteucci, G., Miglietta, F., Ourcival, J., Papale, D., Pilegaard, K., Rambal, S., Seufert, G., Soussana, J., Sanz, M., Schulze, E., Vesala, T., and Valentini, R.: Europe-wide reduction in primary productivity caused by the heat and drought in 2003, Nature, 437, 529–533, 2005.

Farquhar, G. D. and von Caemmerer, S.: Modelling of photosynthetic response to the environment. Physiological Plant Ecology II. Encyclopedia of plant physiology, Springer-Verlag, Berlin, 1982.

Forestry Commission Scotland: The Scottish Government's Rational for Woodland Expansion, The scottish government strategy document, Forestry Commission, Edinburgh, EH12 7AT, Scotland, 2009.

Gerbig, C., Dolman, A. J., and Heimann, M.: On observational and modelling strategies targeted at regional carbon exchange over continents, Biogeosciences, 6, 1949–1559, 2009.

Gurney, K., Law, R., Denning, A., Rayner, P., Baker, D., Bousquet, P., Bruhwiler, L., Chen, Y., Ciais, P., Fan, S., Fung, I., Gloor, M., Heimann, M., Higuchi, K., John, J., Maki, T., Maksyutov, S., Masarie, K., Peylin, P., Prather, M., Pak, B., Randerson, J., Sarmiento, J., Taguchi, S., Takahashi, T., and Yuen, C.: To-

wards robust regional estimates of CO_2 sources and sinks using atmospheric transport models, Nature, 415, 626–630, doi: 10.1038/415626a, 2002.

Henne, S., Brunner, D., Folini, D., Solberg, S., Klausen, J., and Buchmann, B.: Assessment of parameters describing representativeness of air quality in-situ measurement sites, Atmos. Chem. Phys., 10, 3561–3591, 2010.

Hu, X.-M., Klein, P. M., and Xue, M.: Evaluation of the updated YSU planetary boundary layer scheme within WRF for wind resource and air quality assessments, J. Geophys. Res.-Atmos., 118, 1–16, doi:10.1002/jgrd.50823, 2013.

ICOS: Integrated Carbon Observing System: Stakeholders Handbook, A European Infrastructure - European Union, LSCE-Orme, CEA-Orme des Merisiers, F-91191 GIF-SUR-YVETTE CEDEX, 2012.

IPCC: Climate Change 2007: The Physical Basis. Contribution of Working Group I to the Fourth Assessment Report of the Intergovernmental Panel on Climate Change., S. Solomon, D. Qin, M. Manning, Z. Chen, M. Marquis, K. B. Averyt, M. Tignor and H. L. Miller (Eds). Cambridge University Press, United Kingdom and New York, NY, USA., Cambridge, United Kingdom and New York, NY, USA., 2007.

Janssens, I., Freibauer, A., Schlamadinger, B., Ceulemans, R., Ciais, P., Dolman, A., Heimann, M., Nabuurs, G., Smith, P., Valentini, R., and Schulze, E.: The carbon budget of terrestrial ecosystems at country-scale - a European case study, Biogeosciences, 2, 15–26, 2005.

Jones, H. G.: Plants and microclimate, Cambridge University Press, Cambridge, 1992.

Lauvaux, T., Schuh, A. E., Bocquet, M., Wu, L., Richardson, S., Miles, N., and Davis, K. J.: Network design for mesoscale inversions of CO_2 sources and sinks, Tellus Ser. B-Chem. Phys. Meteorol., 64, doi:10.3402/tellusb.v64i0.17980, 2012.

Luyssaert, S., Ciais, P., Piao, S. L., Schulze, E. D., Jung, M., Zaehle, S., Schelhaas, M. J., Reichstein, M., Churkina, G., Papale, D., Abril, G., Beer, C., Grace, J., Loustau, D., Matteucci, G., Magnani, F., Nabuurs, G. J., Verbeeck, H., Sulkava, M., van der Werf, G. R., Janssens, I. A., and CARBOEUROPE-IP Synth Team: The European carbon balance. Part 3: forests, Glob. Change Biol., 16, 1429–1450, doi:10.1111/j.1365-2486.2009.02056.x, 2010.

Mesoscale and Microscale Meteorology Division: Weather Research and Forecasting ARW Version 3 Modelling System User's Guide, User's guide, National Center for Atmospheric Research, Colorado, USA, 2011.

Miles, N. L., Richardson, S. J., Davis, K. J., Lauvaux, T., Andrews, A. E., West, T. O., Bandaru, V., and Crosson, E. R.: Large amplitude spatial and temporal gradients in atmospheric boundary layer CO_2 mole fractions detected with a tower-based network in the U.S. upper Midwest, J. Geophys. Res.-Biogeo., 2012.

Peters, W., Jacobson, A. R., Sweeney, C., Andrews, A. E., Conway, T. J., Masarie, K., Miller, J. B., Bruhwiler, L. M. P., Petron, G., Hirsch, A. I., Worthy, D. E. J., van der Werf, G. R., Randerson, J. T., Wennberg, P. O., Krol, M. C., and Tans, P. P.: An atmospheric perspective on North American carbon dioxide exchange: CarbonTracker, P. Natl. Acad. Sci. USA., 104, 18 925–18 930, 2007.

Peters, W., Krol, M. C., van der Werf, G. R., Houweling, S., Jones, C. D., Hughes, J., Schaefer, K., Masarie, K. A., Jacobson, A. R., Miller, J. B., Cho, C. H., Ramonet, M., Schmidt, M., Ciattaglia, L., Apadula, F., Helta, D., Meinhardt, F., di Sarra, A. G., Piacentino, S., Sferlazzo, D., Aalto, T., Hatakka, J., Strom, J., Haszpra, L., Meijer, H. A. J., van der Laan, S., Neubert, R. E. M., Jordan, A., Rodo, X., Morgui, J. A., Vermeulen, A. T., Popa, E., Rozanski, K., Zimnoch, M., Manning, A. C., Leuenberger, M., Uglietti, C., Dolman, A. J., Ciais, P., Heimann, M., and Tans, P. P.: Seven years of recent European net terrestrial carbon dioxide exchange constrained by atmospheric observations, Glob. Change Biol., 16, 1317–1337, doi:10.1111/j.1365-2486.2009.02078.x, 2010.

Pillai, D., Gerbig, C., Ahmadov, R., Roedenbeck, C., Kretschmer, R., Koch, T., Thompson, R., Neininger, B., and Lavric, J. V.: High-resolution simulations of atmospheric CO2 over complex terrain - representing the Ochsenkopf mountain tall tower, Atmos. Chem. Phys., 11, 7445–7464, doi:10.5194/acp-11-7445-2011, 2011.

Rigby, M., Manning, A. J., and Prinn, R. G.: Inversion of long-lived trace gas emissions using combined Eulerian and Lagrangian chemical transport models, Atmos. Chem. Phys., 11, 98879898, doi:10.5194/acp-11-9887-2011, 2011.

Skamarock, W. C., Klemp, J. B., Dudhia, J., Gill, D. O., Barker, D. M., Duda, M. G., Huang, X.-Y., Wang, W., and Powers, J. G.: A Description of the Advanced research WRF Version 3, 2008.

Smallman, T. L., Moncrieff, J. B., and Williams, M.: WRFv3.2-SPAv2: development and validation of a coupled ecosystem-atmosphere model, scaling from surface fluxes of CO_2 and energy to atmospheric profiles, Geosci. Model Dev., 6, 1079–1093, doi:10.5194/gmd-6-1079-2013, http://www.geosci-model-dev.net/6/1079/2013/, 2013.

Smith, P.: Carbon sequestration in croplands: the potential in Europe and the global context, Eur. J. Agron., 20, 229–236, doi:10.1016/j.eja.2003.08.002, 2004.

Steeneveld, G. J., Tolk, L. F., Moene, A. F., Hartogensis, O. K., Peters, W., and Holtslag, A. A. M.: Confronting the WRF and RAMS mesoscale models with innovative observations in the Netherlands: Evaluating the boundary layer heat budget, J. Geophys. Res.-Atmos., 116, doi:10.1029/2011JD016303, 2011.

Sus, O., Williams, M., Bernhofer, C., Beziat, P., Buchmann, N., Ceschia, E., Doherty, R., Eugster, W., Gruenwald, T., Kutsch, W., Smith, P., and Wattenbach, M.: A linked carbon cycle and crop developmental model: Description and evaluation against measurements of carbon fluxes and carbon stocks at several European agricultural sites, Agr. Ecosyst. Environ., 139, 402–418, 2010.

The Macaulay Land Use Research Institute: The land cover of Scotland 1988: Executive Summary, The scottish government strategy document, The Macaulay Land Use Research Institute, Aberdeen, AB9 2QJ, Scotland, iSBN 0 7084 0538 X, 1993.

The Scottish Government: Scottish Agricultural Census, A national statistics publication for scotland: Agricultural series, The Scottish Government, 2012.

Thomson, A. M., Hallsworth, S., and Malcolm, H.: Emissions and Removals of Greenhouse Gases from Land Use, Land Use Change and Forestry (LULUCF) for England, Scotland, Wales and Northern Ireland: 1990-2010, Department for Energy and Climate Change Contract GA0510, 2012.

Tolk, L. F., Peters, W., Meesters, A. G. C. A., Groenendijk, M., Vermeulen, A. T., Steeneveld, G. J., and Dolman, A. J.: Modelling

regional scale surface fluxes, meteorology and CO_2 mixing ratios for the Cabauw tower in the Netherlands, Biogeosciences, 6, 2265–2280, 2009.

Vermeulen, A. T., Hensen, A., Popa, M. E., van den Bulk, W. C. M., and Jongejan, P. A. C.: Greenhouse gas observations from Cabauw Tall Tower (1992-2010), Atmos. Meas. Tech., 4, 617–644, doi:10.5194/amt-4-617-2011, 2011.

Williams, M., Rastetter, E. B., Fernandes, D. N., Goulden, M. L., Wofsy, S. C., Shaver, G. R., Melillo, J. M., Munger, J. W., Fan, S. M., and Nadelhoffer, K. J.: Modelling the soil-plant-atmosphere continuum in a Quercus-Acer stand at Harvard Forest: the regulation of stomatal conductance by light, nitrogen and soil/plant hydraulic properties, Plant Cell Environ., 19, 911–927, 1996.

Williams, M., Schwarz, P. A., Law, B. E., Irvine, J., and Kurpius, M.: An improved analysis of forest carbon dynamics using data assimilation, Glob. Change Biol., 11, 89–105, 2005.

Williams, M., Malhi, Y., Nobre, A., Rastetter, E., Grace, J., and Pereira, M.: Seasonal variation in net carbon exchange and evapotranspiration in a Brazilian rain forest: a modelling analysis, Plant Cell Environ., 21, 953–968, 1998.

Williams, M., Law, B., Anthoni, P., and Unsworth, M.: Use of a simulation model and ecosystem flux data to examine carbon-water interactions in Ponderosa pine, Tree Physiol., 21, 287–298, 2001.

...

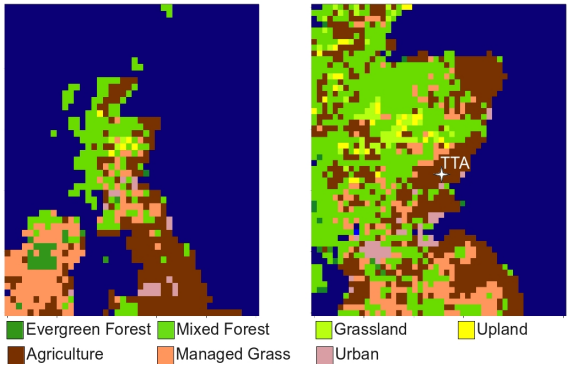

Fig. 1. Land classification map used covering the spatial extent of the model domain. The left panel is the parent domain at 18 x 18 km, right panel is nested domain at 6 x 6 km. The star indicates the location of tall tower Angus. The map used in WRF-SPA is a modified MODIS land cover map provided with the WRF model. The fractions of each land cover within the nested domain are crop = 36 %, evergreen forest = 1 %, mixed forest = 42 %, grassland = 2 %, managed grassland = 13 %, upland = 3 %, urban = 3 %.

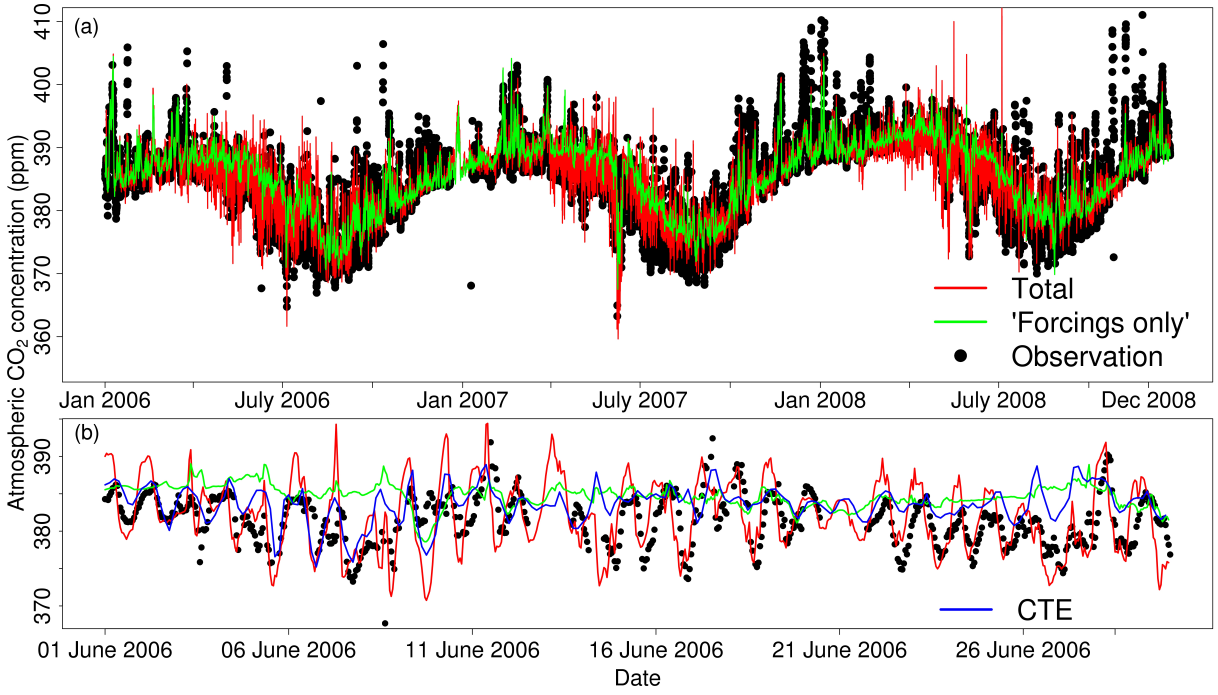

Fig. 2. Time series comparison between hourly observations of atmospheric CO_2 concentrations made at TTA and WRF-SPA simulated total atmospheric CO_2 and "forcings only" CO_2. Atmospheric CO_2 concentrations at 3 hourly time step from CTE-CT are also included in panel (b). Panel (a) shows that the simulated CO_2 time series (2006-2008) is mostly driven by forcings originating outside of the model domain as indicated by "forcings only" CO_2. Panel (b) shows an hourly (3 hourly for CTE-CT) time series for June 2006 highlighting that diurnal variation in simulated CO_2 is due to exchange with the biosphere within the simulated domain, as total atmospheric CO_2 captures this variation. WRF-SPA modelled total atmospheric CO_2 contains all model forcings and exchange with the simulated biosphere while "forcings only" CO_2 does not include biospheric exchange (i.e. total - biospheric fluxes).

Table 1. Tracer pools and definitions used by WRF-SPA. A non-interacting tracer does not have the potential to be exchanged with the land surface after its initial emission. Whereas an interacting tracer can be removed from the atmosphere, as it represents a physical mass of CO_2 added to the atmosphere through respiration.

Tracer	Description	Interacting tracer
1	Total CO_2 concentration, includes all sources and sinks of CO_2, for comparison to observations	Yes
2	Forest net CO_2 uptake	No
3	Anthropogenic emissions	Yes
4	Forcings only, i.e. anthropogenic emissions, ocean sequestration, initial and lateral boundary conditions only	No
5	Crop net CO_2 uptake	No
6	Ocean sequestration	No
7	Forest net CO_2 release	Yes
8	Crop net CO_2 release	Yes
9	Managed grassland net CO_2 release	Yes
10	Other vegetation net CO_2 release	Yes
11	Managed grassland net CO_2 uptake	No
12	Other vegetation net CO_2 uptake	No

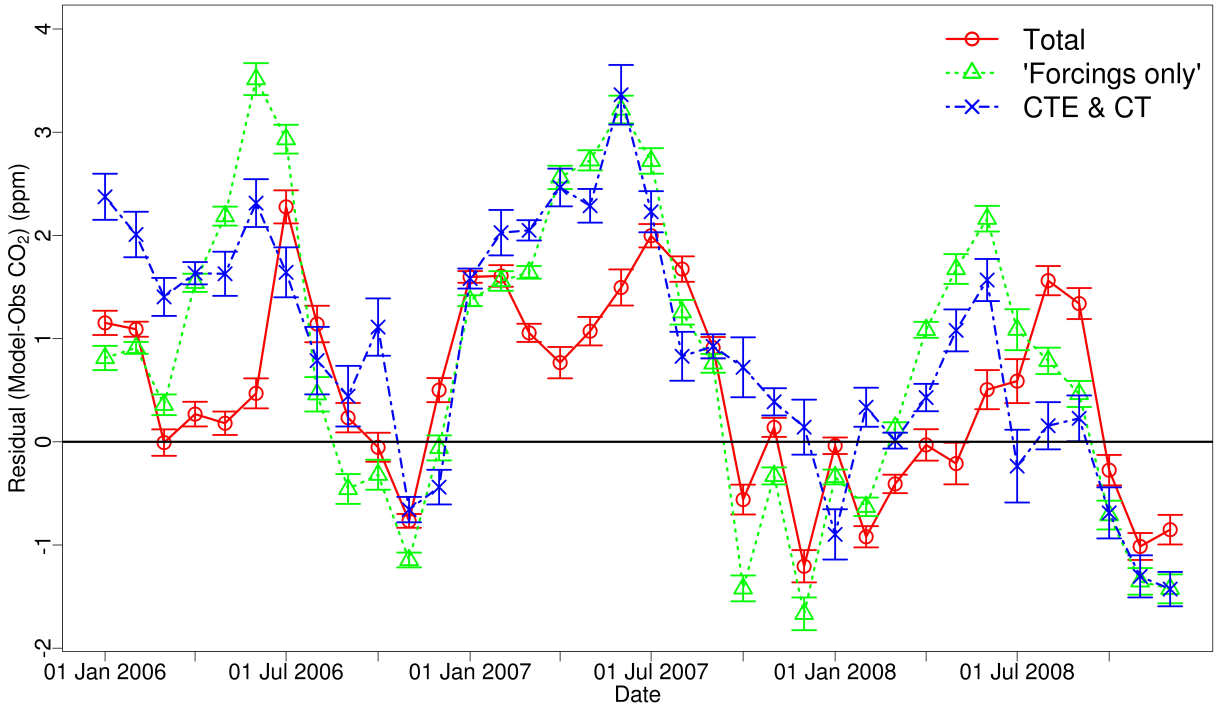

Fig. 3. Time series of monthly mean residual (Model-Obs) between observed, CTE-CT and WRF-SPA simulated total atmospheric CO_2 and "forcings only" concentrations. Highlights time periods during which the inclusion of the simulated biosphere results in a reduction in monthly mean bias. Error bars are $\pm$ 1 standard error, accounting of temporal and spatial uncertainty only.

Table 2. Parameter and model options used in WRF-SPA.

Basic equations	Non-hydrostatic, compressible Advanced Research WRF (ARW)
Radiative transfer scheme	Rapid Radiative Transfer Model for GCMs (RRTMG) for both long wave and short wave
Planetary boundary layer scheme	Yonsei University
Surface scheme	Monin-Obukov
Microphysics scheme	WSM 3-class simple ice
Cumulus parameterisation	Grell 3D ensemble scheme (coarse domain only)
Nesting	Two-way nesting
Model time step	Outer = 90 seconds, inner = 30 seconds
Domain, resolution	44 x 47, 18 km
	48 x 54, 6 km
	35 vertical levels
Domain centre	56.63° N, 3.35° W

Table 3. Summary of R^2 values from regression analysis of variation in surface net CO_2 uptake flux explained by tall tower detected net CO_2 uptake tracers. A combined 2006 to 2008 period is provided to give an indication of overall performance, while individual years allow for consideration of interannual variation in detection capability.

	Crop	Forest	Managed grassland	'Other'
2006-2008	0.94	0.72	0.72	0.77
2006	0.94	0.76	0.82	0.85
2007	0.94	0.74	0.58	0.71
2008	0.96	0.58	0.69	0.70

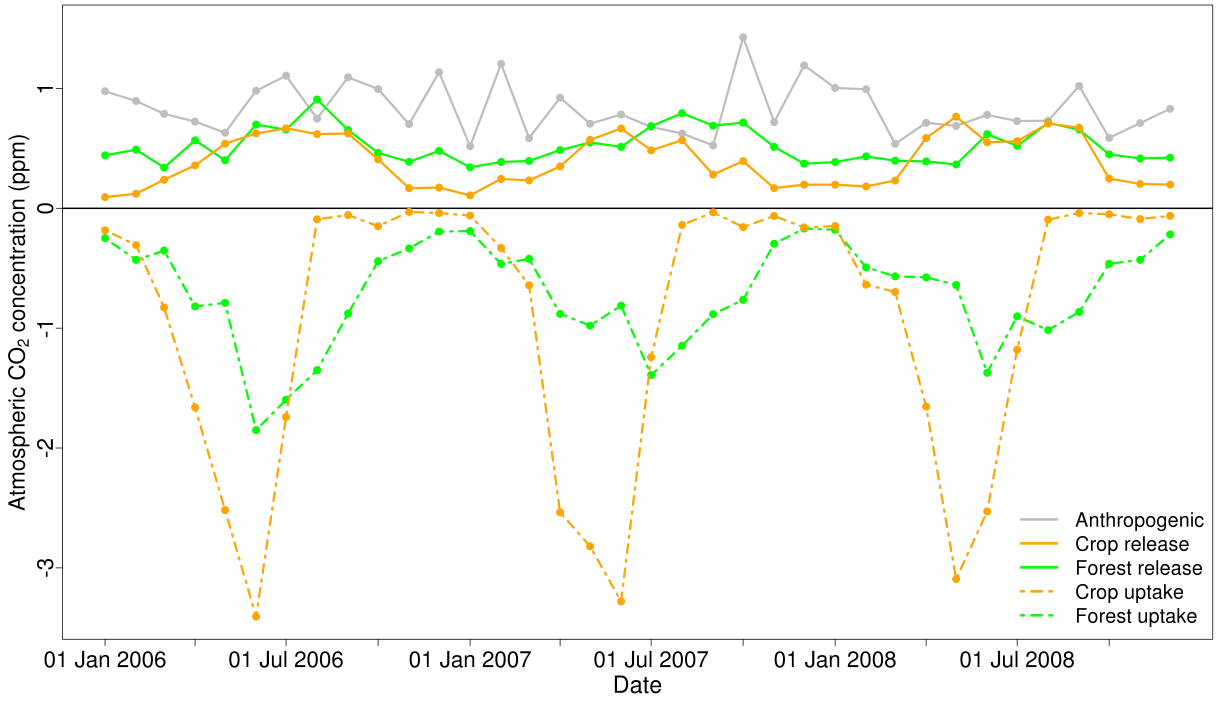

Fig. 4. Monthly mean mixing ratios for net uptake and net release CO_2 tracers, for crop and forest ecosystems, simulated at TTA. Highlights differences in detection of ecosystem processes at TTA, in particular the distinct seasonal cycle of cropland net uptake and net release CO_2 tracers compared to all other ecosystems. Managed grassland and 'other' ecosystems are not included due to their small magnitude contributions, never exceeding 0.7 ppm.

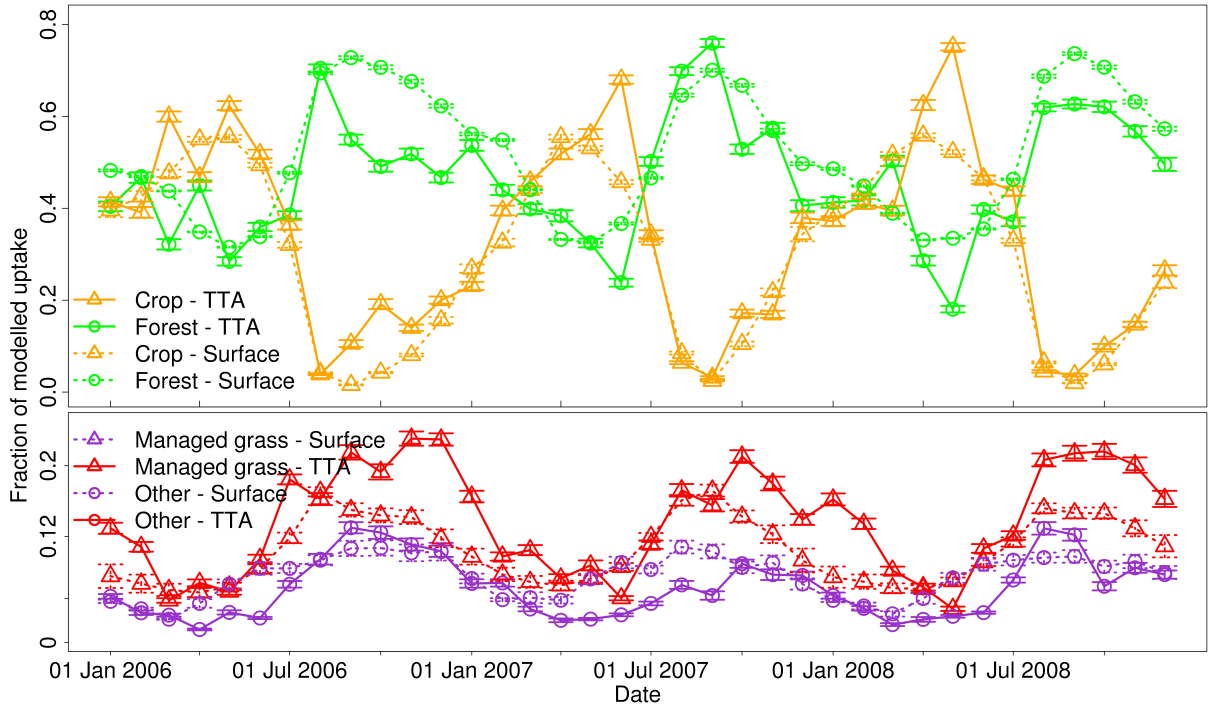

Fig. 5. Comparison between monthly mean ecosystem specific fraction of net uptake CO_2 tracers simulated at TTA and fraction of surface net CO_2 uptake flux. Where an ecosystems fraction of net uptake CO_2 tracer greater than the corresponding fraction of surface net CO_2 uptake flux, it would indicate that the ecosystem is over-represented in total atmospheric CO_2 concentrations. Where the reverse would indicate that the ecosystem was under-represented. Error bars are $\pm$ 1 standard error, accounting of temporal and spatial uncertainty only.

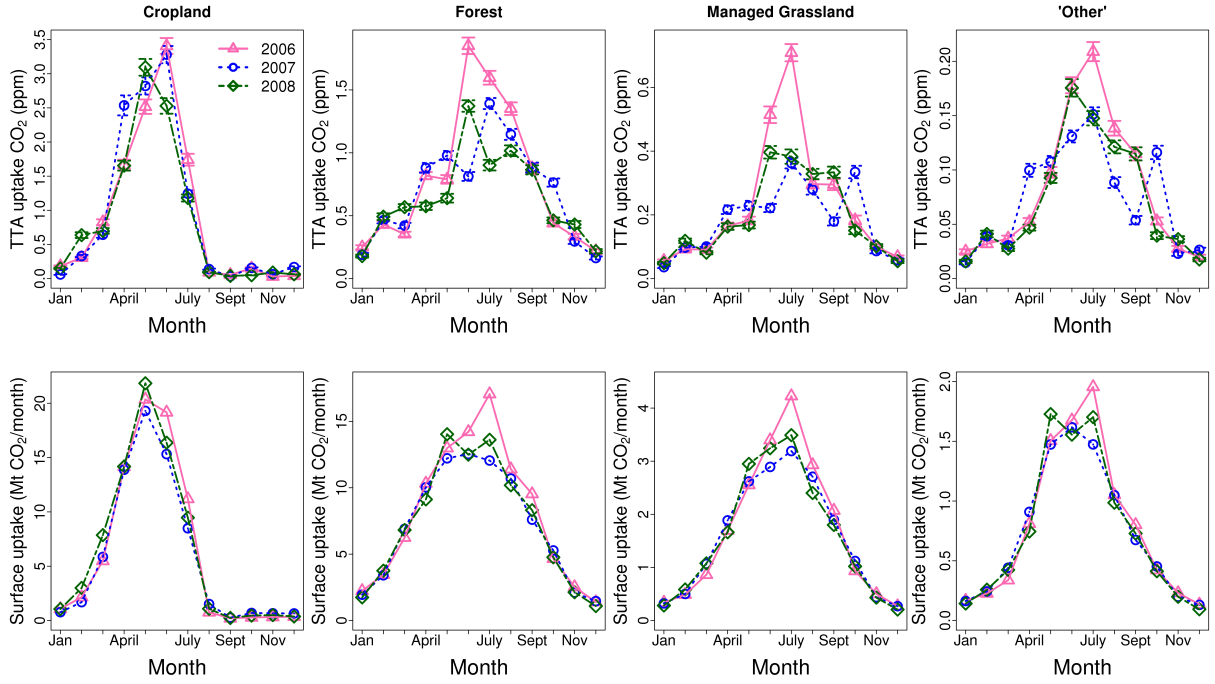

Fig. 6. Seasonal and interannual comparison between monthly mean net uptake CO_2 tracer simulated at TTA for crop, forest, managed grassland and 'other' (upper panel), and monthly sum surface net CO_2 uptake flux. Note the different scales between ecosystem types. Error bars are $\pm$ 1 standard error, accounting of temporal and spatial uncertainty only.

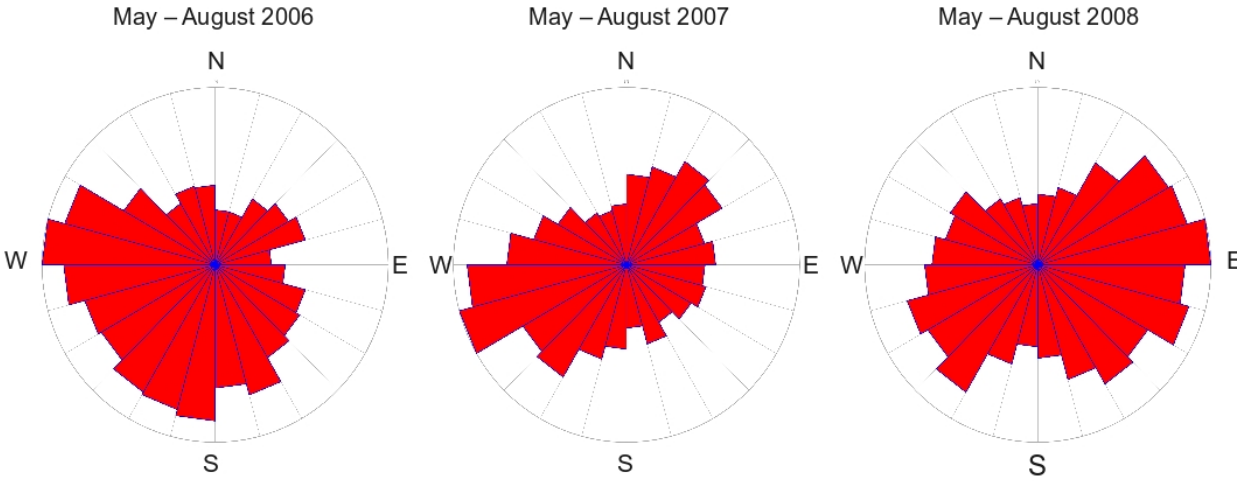

Fig. 7. Interannual comparison of growing season (May, June, July and August) prevailing wind direction at TTA. The wind rose shows the count of hourly wind directions simulated by WRF-SPA, where the direction indicated is the direction from which the wind is coming.

Chapter 4

Can the proposed afforestation of Scotland be detected by a tall tower? An experimental afforestation using WRF-SPA

Manuscript prepared for Biogeosciences
with version 4.2 of the LaTeX class copernicus.cls.
Date: 10 January 2014

Can tall tower networks detect policy relevant afforestation? A synthetic study

T. L. Smallman[1,2], **M. Williams**[1,2], **and J. B. Moncrieff**[1]

[1]School of GeoSciences, The University of Edinburgh, Edinburgh, EH9 3JN
[2]National Centre for Earth Observation, The University of Edinburgh, Edinburgh, EH9 3JN

Abstract. The coupled numerical weather model WRF-SPA has been used to investigate whether a policy relevant afforestation of Scotland can be detected by observations of atmospheric CO_2 concentrations made at tall tower Angus. Tall tower Angus is currently the only tall tower in Scotland operationally observing atmospheric CO_2 concentrations. In addition, five hypothetical tall towers were assessed to determine if alternate tower locations or a network of towers would improve detection of currently planned afforestation. Detectability of afforestation was assessed by comparing a control and experimentally afforested simulation over a three year period. The experimental simulation was afforested with an additional 650,000 ha of forest as specified in current Scottish Government policy. The policy estimates that afforestation will increase forest sequestration by $\sim$1.2 Mt C yr^{-1}. WRF-SPA simulated afforestation to increase forest sequestration by $\sim$1.8 Mt C yr^{-1}. Accounting for previous land use, the net terrestrial increase in sequestration was $\sim$1.4 Mt C yr^{-1}.

All tall towers were simulated to be able to detect the impact of afforestation on atmospheric CO_2 concentrations at seasonal time scales. However there was considerable interannual variation of the magnitude of the impact of afforestation. Prevailing wind direction varies considerably at seasonal and interannual time scales, therefore impacting the observation footprint of observations; providing a plausible reason for the variability in detectability. Detection of seasonal variation in ecosystem carbon uptake by tall tower observations was improved through the use of a network of tall towers (e.g. detection of seasonal variation of forest net CO_2 uptake flux using tall tower Angus alone R^2 = 0.72 and with a network R^2 = 0.92). An alternate tower to tall tower Angus was better able to detect the simulated changes in forest net CO_2 uptake flux due to afforestation (R^2 = 0.88) than tall tower Angus (R^2 = 0.75). Afforestation resulted in changes to the surface net radiation balance and the Bowen ratio. Moreover, changes in surface net radiation and fluxes drove changes in surface air temperature and moisture content, leading to increased mean annual precipitation within the afforested region.

Correspondence to: T. L. Smallman
(t.l.smallman@.ed.ac.uk)

1 Introduction

Terrestrial ecosystems play an important but as yet uncertain role in global climate and the global carbon cycle (IPCC, 2007). Currently the terrestrial biosphere absorbs a significant fraction of anthropogenic emissions of CO_2 (Canadell et al., 2007). However, the terrestrial biosphere is highly complex and dynamic creating a land surface that can be either a source or sink of CO_2, varying at seasonal and interannual time scales. Changes in climate and ecosystem composition have a significant impact on net ecosystem exchange of CO_2 (NEE). Furthermore, many ecosystems are now under human management, such as agriculture or forestry, increasing the complexity of ecosystem processes and having a significant impact on the carbon balance of the land surface (IPCC, 2007). A greater understanding of the drivers of variability of land surface sources and sinks is needed, in particular due to human management.

Afforestation is often considered to be part of mitigation strategies to increase carbon sequestration of the land surface and thereby reduce the accumulation of anthropogenic CO_2 in the atmosphere (IPCC, 2007; Kaplan et al., 2012). Several studies have investigated the effects of land use and land cover change (LULCC) (e.g., Arora and Montenegro, 2011) on CO_2 sequestration. Arora and Montenegro (2011) predicted that 100 % afforestation of current cropland would lead to a small cooling effect on global mean temperature ($\leq$0.45°C, i.e. a reduction in the predicted warming not a net cooling) and a reduction in mean atmospheric CO_2 con-

centrations of ∼93 ppm between 2010 and 2100 compared to a control simulation without afforestation. However, a 'more realistic' afforestation of 50 % of agricultural land in the northern temperate region was simulated to have a non-statistically significant cooling effect of 0.11°C and a reduction in mean atmospheric CO_2 concentrations of ∼20 ppm. The simulated cooling was mediated through an increase in global CO_2 sequestration and an increase in evapotranspiration particularly at low latitudes. The simulated cooling effect is small compared to historical deforestation and agricultural expansion which are simulated to have resulted in a net cooling effect on mean global air temperature of 1-2 °C through increased land surface albedo (Bala et al., 2007; Betts et al., 2007; Davin and de Noblet-Ducoudre, 2010; Kaplan et al., 2012). However, given that the simulated response of the land surface to increasing atmospheric CO_2 and climate change remains highly uncertain the response of the land surface due to LULCC should be closely examined (Friedlingstein et al., 2006; Sitch et al., 2008; Friedlingstein and Prentice, 2010; Qian et al., 2010). Moreover previous modelling studies which have investigated the impact of afforestation and deforestation have tended to consider global or large latitudinal scale LULCC (e.g. Betts et al., 2007; Arora and Montenegro, 2011). Policy relevant afforestation is unlikely to cover a majority available agricultural land, resulting in a globally averaged impact that is likely to be smaller in magnitude than those simulated by e.g. Arora and Montenegro (2011). Therefore the regional impact of policy relevant afforestation on atmospheric CO_2 concentrations and surface meteorological variables remains to be investigated.

The effectiveness of mitigation on CO_2 sequestration needs to be assessed using reliable and robust methodologies. Proposed methods include periodical forest inventories (Forestry Commission Scotland, 2009), remote sensing of above ground carbon (Le Toan et al., 2011; ESA, 2012) and atmospheric inverse modelling of atmospheric CO_2 concentrations (ICOS, 2012). Forest inventories are labour intensive while remotely sensed above-ground carbon fails to account for changes in below ground carbon stock, which represent a significant store of carbon (Bradley et al., 2005; Ostle et al., 2009). The response of soil carbon stocks is complex, varying depending on land use history and time since afforestation occurred (Paul et al., 2002; Ostle et al., 2009; Poeplau et al., 2011). Observations of atmospheric CO_2 concentration contain information on the net source sink distribution and magnitude of CO_2 exchange (Peters et al., 2010), and therefore include potentially important information on changes in soil carbon.

Atmospheric inversions are dependant on information contained within observations of atmospheric CO_2 concentrations, typically from aircraft and networks of tall towers, to infer surface CO_2 fluxes (Gurney et al., 2002; Peters et al., 2010; Lauvaux et al., 2012). In response to the requirement for observations made at tall towers, several regional networks have been established, such as the European Union supported integrated carbon observing system (ICOS, 2012). Observations made at tall towers can be influenced by a large area of the land surface. For example the Cabauw tower in the Netherlands, an area of ∼500 x 700 km around the tall tower is expected to contribute up to ∼ 50 % of the signal observed by the tower (Vermeulen et al., 2011).

Tall tower observations are, however, dominated by CO_2 exchange originating within the local area of a tower (∼100 or less km) (Gerbig et al., 2009; Vermeulen et al., 2011; Lauvaux et al., 2012; Miles et al., 2012). While observations are dominated by near field exchange, inversion studies have shown that the regional level net carbon balance can be detected using a relatively sparse network of tall towers (Lauvaux et al., 2012). However the spatial distribution of regional sources and sinks estimated by atmospheric inversion are dependent on the density and location of tall towers within an observing network (Lauvaux et al., 2012). Therefore it remains unclear whether tall towers observations are able to detect variation in surface CO_2 exchange due to changes in ecosystem composition which occurs at sub-regional scales and attribute simulated variation to a specific ecosystem type (e.g. policy relevant afforestation).

Afforestation represents a potentially significant change in ecosystem heterogeneity and ecosystem processes, altering NEE, surface energy balance and near surface atmospheric transport (Avissar, 1998; Bonan, 2008; Schomburg et al., 2012). Changes in atmospheric transport may have an impact on the ability of observations made at tall towers to detect changes in surface exchange. Therefore the spatial distribution of ecosystem cover of the land surface needs to be realistically modelled to accurately predict regional scale exchange and atmospheric transport (Avissar, 1998; Schomburg et al., 2012).

The forward running mesoscale model, WRF-SPA (Smallman et al., 2013a), was used to investigate the detectability of afforestation of Scotland by observations of atmospheric CO_2 concentrations made at tall tower Angus (TTA). WRF-SPA has previously been used to simulate Scotland and has been validated against observations at a range of spatial scales from surface fluxes of CO_2 to aircraft and observations made at tall towers (Smallman et al., 2013a,b). TTA is currently Scotland's only tall tower operationally observing atmospheric CO_2 concentrations. The impact of afforestation was assessed by comparing a control simulation (i.e. with no land cover change) and a experimentally afforested simulation.

In addition to TTA, five alternate tall towers were assessed for their ability to detect changes in atmospheric CO_2 due to the simulated afforestation. The alternate towers are existing telecommunication towers that are not currently equipped for measuring atmospheric CO_2 concentrations. The inclusion of alternate towers allows for an assessment of whether an individual tower, other than Angus, or a network of tall towers are better able to detect afforestation. The ability of the

tall towers to detect afforestation is assessed through the use of ecosystem specific CO_2 tracers which are simulated by WRF-SPA.

WRF-SPA uses ecosystem specific CO_2 tracers to represent net release and net uptake of CO_2 by the land surface (Smallman et al., 2013b). The net CO_2 uptake tracers simulated at each tall tower have been compared to the simulated surface uptake to assess the ability of an individual tower or network to detect seasonal variation in ecosystem uptake. Furthermore the ability of towers to detect changes in forest net CO_2 uptake specifically due to afforestation has also been assessed.

The overall aim of this paper is to use ecosystem specific CO_2 tracers to investigate whether current observations at tall tower Angus, or a network of tall towers are best able to detect policy relevant afforestation. A unique aspect of this study is the attempt to use ecosystem tracers of CO_2 exchange to inform on development of tall tower observing networks.

Using WRF-SPA simulations we aim to answer specific questions:

i. Does afforestation result in a change in atmospheric CO_2 concentrations which is detectable by current observations made at a tall tower Angus?

ii. Can detection of afforestation on forest CO_2 uptake be improved through use of an alternate tall tower or a network of tall towers?

iii. Can detection of seasonal variation in ecosystem CO_2 uptake be improved through use of a tall tower network?

iv. Does changing Scotland's ecosystem composition, i.e. afforestation, alter atmospheric transport, and if so, does this affect detection capability?

v. Does afforestation result in changes to surface meteorological variables?

2 Model description: WRF-SPA

WRF-SPA (Smallman et al., 2013a) is a coupling between the mesoscale model Weather Research and Forecasting (WRF) and the mechanistic terrestrial ecosystem model Soil Plant Atmosphere (SPA). WRF provides a state-of-the-art representation of atmospheric dynamics, while SPA generates realistic ecosystem-atmosphere exchanges through coupled hydrological, carbon and energy cycles to drive atmospheric transport.

2.1 WRF

The Weather Research & Forecasting model (WRFv3.2) (http://www.mmm.ucar.edu/wrf/users/, accessed 19/10/2009 15:00) is a well supported and rapidly developing high resolution non-hydrostatic meteorological model (Skamarock et al., 2008). WRF is designed to be highly adaptable with a modular structure to allow for tailoring to specific uses. The model has been extensively validated over a range of locations around the world (e.g. Borge et al., 2008; Zhang, 2008; Ahmadov et al., 2007; Wang et al., 2009) and performs well in comparison to other commonly used mesoscale meteorological models (e.g. Sarrat et al., 2007; Steeneveld et al., 2011).

2.2 SPA

The Soil Plant Atmosphere (SPA) model is a high vertical resolution terrestrial ecosystem model (up to 10 canopy layers and 20 soil layers). SPA provides surface fluxes of heat, water and CO_2 in response to meteorological drivers through a close coupling of its hydrological and carbon cycles, based on a mechanistic representation of ecosystem processes (Williams et al., 1996). A brief description of the SPA model is given below. Detailed descriptions of the major SPA developments can be found in Williams et al. (1996, 1998, 2001, 2005); Sus et al. (2010); Smallman et al. (2013a).

WRF provides SPA with meteorological drivers including air temperature, precipitation, vapour pressure deficit (VPD), wind speed, friction velocity, atmospheric CO_2 mixing ratios, air pressure, short and long wave incoming radiation. SPA currently has parameters for 8 vegetation types (evergreen forest, deciduous forest, mixed forest, arable cropland, managed grassland, grassland, upland and urban) suitable for UK application and 13 soil types impacting soil hydrology. Vegetation cover is specified by the MODIS land cover map provided with WRFv3.2, while soil classifications are from the default WRF soil cover maps (Mesoscale and Microscale Meteorology Division, 2011).

The Farquhar model of photosynthesis (Farquhar and von Caemmerer, 1982), the Penman-Monteith model of leaf transpiration (Jones, 1992) and the leaf energy balance are coupled via a mechanistic model of stomatal conductance. Stomatal conductance is modelled by linking atmospheric demand for water and available water supply from the soil through plant hydraulics creating a soil-plant-atmosphere continuum (Williams et al., 1996, 2001). SPA maximises photosynthesis per unit foliar nitrogen within a minimum leaf water potential constraint to prevent cavitation (Williams et al., 1996). SPA uses a detailed parameterisation of canopy processes, including multi-layer canopy radiative transfer (Williams et al., 1998), above and within canopy momentum decay and leaf level boundary layer conductance for heat and water vapour exchange (Smallman et al., 2013a).

Plant phenology is described by a box carbon model to simulate the main ecosystem carbon (C) pools (Williams et al., 2005; Sus et al., 2010). C pools are foliage, structural wood carbon, fine roots, labile, soil organic matter (SOM) and surface litter. Crops have two additional C pools; storage organ C (i.e. harvestable C) and dead foliar C (still standing). The C pools within WRF-SPA are 'spun-up' as de-

scribed in Smallman et al. (2013a), using meteorology which is broadly representative of the median meteorological conditions in Scotland. The carbon model provides a direct coupling between the plant carbon cycle and plant phenology, specifically foliar and fine root C. Foliar C determines the leaf area index (LAI) while fine root C impacts water uptake potential.

2.3 Atmospheric CO_2 tracers

WRF-SPA has been modified with the addition of several atmospheric CO_2 tracer pools (Table 1). CO_2 tracer transport is simulated within the model domain concurrently with meteorological variables (feedback on atmospheric radiative transfer due to variable CO_2 is neglected as its impact is expected to be small at $\sim$3 %).

We compared simulated atmospheric CO_2 with an active biosphere versus simulated without a biosphere ("forcings only"). "Forcings only" CO_2 tracer contains IC, LBC, anthropogenic emissions and ocean sequestration of CO_2 (i.e. CO_2 exchange not calculated by WRF-SPA) but no exchange with the SPA simulated biosphere. Comparison between the total atmospheric CO_2 concentration and "forcings only" CO_2 concentration allow for isolations of the impact due to inclusion of the simulated biosphere. Furthermore, CTE (2006-2007) and CT (2008) atmospheric CO_2 concentrations are compared to TTA observations to assess how well CTE-CT simulates atmospheric CO_2 at a tower not included in the inversion model.

2.3.1 Ecosystem specific tracers

The ecosystem specific tracers of net uptake and net release of CO_2 are used to investigate the information content on these processes contained within the total atmospheric CO_2 concentrations simulated at TTA. Note that LBCs for the outer domain have been set with zero inflow and zero-gradient outflow for ecosystem specific net uptake and net release CO_2 tracers. Zero gradient inflow / outflow allow tracers to easily leave the domain and prevent artificial influx to the CO_2 tracer fields. A brief description of the ecosystem specific tracers is given below, for a detailed description see Smallman et al. (2013b).

The land surface can be either a net source or net sink of atmospheric CO_2, varying both spatially and temporally. Whether the land surface is a net sink or source of CO_2 is determined by the net result of photosynthetic and respiratory processes. Atmospheric CO_2 concentrations represent a spatial and temporal integration of the net flux of CO_2 between the land surface and the lower atmosphere. Therefore, when the simulated surface flux of CO_2 represents a net removal of CO_2 from the atmosphere, an ecosystem specific 'net uptake CO_2 tracer' is released into the simulated atmosphere at the same rate as the 'surface net CO_2 uptake flux' (i.e. rate of NEE). Correspondingly, when the surface net CO_2 uptake flux represents a net addition of CO_2 to the atmosphere an ecosystem specific 'net release CO_2 tracer' is released.

The net uptake CO_2 tracers are considered to be non-interacting / non-interactive, while the net release CO_2 tracers are interacting / interactive. The net uptake CO_2 tracers are non-interacting as they represent a removal of atmospheric CO_2 and as such cannot interact with the land surface. After their emission from the surface the net uptake CO_2 tracers are transported through the model atmosphere. Conversely, net release CO_2 tracers represent an addition of a physical mass of CO_2 to the atmosphere via respiration, which can therefore be subsequently removed from the atmosphere by photosynthesis after its initial release. Allowing the removal of a net release CO_2 tracer prevents a respiratory signal from being simulated at TTA which in reality does not reach TTA due to being consumed en route in a physically consistent manor.

Net release CO_2 tracers are removed from the atmosphere if they are present in the lowest model atmospheric level and the land surface below represents a net removal of CO_2. If there are multiple ecosystem specific net release CO_2 tracers present in the same model atmosphere grid box, then removal is determined by the relative fraction of each ecosystem specific tracer. For example, to determine the removal of crop net release CO_2 tracer

$$\gamma \uparrow t_{crop} rm = \frac{\uparrow t_{crop}}{\uparrow t_{crop} + \uparrow t_{forest} + \uparrow t_{grass} + \uparrow t_{other}} \quad (1)$$

where $\gamma \uparrow t_{crop} rm$ is the fraction of surface CO_2 flux (i.e. NEE) to be applied to the crop net release CO_2 tracer. $\uparrow t_{crop}$ is the crop net release (as indicated by the direction of the arrow and t indicates it being a tracer) CO_2 tracer concentration, similarly for forest, managed grassland and 'other' land cover types.

2.4 Model domain

WRF-SPA modelled two domains with two-way nesting; the outer domain has a resolution of 18 km x 18 km and inner domain 6 km x 6 km (Fig. 1). Model output presented is from the inner domain only.

The main features of the WRF model set up are presented in Table 2. All meteorological data required e.g., soil temperature and moisture content for initialisation, atmospheric initial conditions and lateral boundary conditions were taken from the Global Forecasting System (GFS) reanalysis product (http://www.emc.ncep.noaa.gov/). GFS data are available at 1°x 1° longitude / latitude resolution with 6 hourly time steps (available from http://rda.ucar.edu/datasets/ds083.2/).

2.5 Experimental afforestation

Detectability of afforestation was assessed by comparing control and experimentally afforested simulations. The control simulation used the MODIS land cover map provided

with WRF, to represent the current day forest cover. The experimentally afforested simulation used the default land cover map with an additional 650,000 ha of forest cover. As specified in the Scottish Government's afforestation policy the afforested area was ∼60 % as evergreen plantation and ∼40 % mixed forest (Forestry Commission Scotland, 2009). The policy estimates that planned afforestation will add ∼1.2 MtC yr^{-1} to Scotland's current forest sequestration (Forestry Commission Scotland, 2009), representing ∼9 % of Scotland's net greenhouse gas emissions in 2009 (The Scottish Government, 2011).

The experimental design aims to assess whether the end point of planned afforestation, i.e. due to increased forest cover only, is detectable and to consider the development of an observing network for this specific purpose. Therefore the afforested simulation uses the same initial and lateral boundary conditions for meteorological and atmospheric CO_2 variables which removes climatic effects on biogeochemical processes (i.e. photosynthesis and respiration). Afforested areas are assumed to be the same as forest areas already simulated by WRF-SPA with no parameterisation of forestry management. Therefore the system here does not consider the impact of forest age, changes in spatial distribution over time or the effect on soil carbon stocks due to disturbance. Forests in WRF-SPA are spun-up over a 30 year period (Smallman et al., 2013a), which is appropriate given the mode forest age class in Scotland is the 21–40 year class.

Afforested areas were selected at random within the southern and eastern areas of Scotland. These areas are identified as having the greatest potential for land available for afforestation (Forestry Commission Scotland, 2009). As specified in the afforestation policy a preference against afforestation of agricultural land was applied. If an agricultural site was randomly selected for afforestation the site would only be afforested if there was not an adjacent non-cropland area.

3 Tall tower observations

Observations of atmospheric CO_2 concentration are from tall tower Angus (TTA) near Dundee, Scotland (56.56 N, 2.99 W). Angus' observation height is 222 m above the ground and 537 m above sea level. TTA is equipped for continuous measurement of atmospheric CO_2 concentrations producing 30 minute observations which have been averaged to hourly time scales for comparison with WRF-SPA. TTA has been operational since the end of 2005 to present. Observations made at TTA have an accuracy limit of 0.1 ppm, therefore for a change in atmospheric CO_2 concentration to be detectable, the change must be greater than 0.1 ppm.

TTA was part of the CHIOTTO network during the period of analysis reported here (EVK2-CT-2002-00163) and as such was fully integrated into the calibration and validation methodologies of that project. The data continues to be quality controlled under the InGOS project (http://www.ingos-infrastructure.eu/, accessed 09/12/2013, 16:30 UTC).

Five telecommunication tall towers not currently equipped for measurement of atmospheric CO_2 concentrations have been included in the analysis as hypothetical alternatives to tall tower Angus (Table 3). Four of the towers are located in the experimentally afforested region (Blackhill, Darvel, Durris and Selkirk). The fifth tower (Knockmore) is located down wind of the forest dominated western areas of Scotland (Fig. 1).

3.1 Tall tower footprint

Currently there are no published assessment of TTA's or any of the hypothetical towers observation footprints, however the footprint of Mace Head, located on the west coast of Ireland has been assessed in multiple studies (e.g. Henne et al., 2010; Rigby et al., 2011; Brunner et al., 2012). Mace Head is exposed to similar meteorological conditions in north west Europe, and therefore we expect a similar footprint. Henne et al. (2010) calculated a 12 hour inversion, estimating the footprint of Mace Head to be the land surface within ∼195 km of the tower. Therefore, if a similar footprint is assumed for TTA ∼98 % of the inner domain's land surface is within the footprint of TTA. Assuming a similar footprint for each of the hypothetical tall towers also leads to the majority of the simulated land surface within the inner domain to be included. Critically all tall towers footprints would include the afforested region of Scotland.

4 Results

Simulated afforestation increased forest CO_2 sequestration by 1.8 Mt C yr^{-1}, larger than the expected increase of ∼1.2 Mt C yr^{-1} specified in the Scottish Government policy. The net increase in terrestrial sequestration, after accounting for previous land use of the afforested areas was 1.4 Mt C yr^{-1}. The control and afforested simulations are highly correlated (R^2 = 0.98, bias = -0.014 ppm), with a small annual bias indicating little impact on CO_2 present at tall tower Angus due to afforestation at annual time scales. The root mean square error (rmse = 0.73 ppm) is comparatively large which may indicate greater hour-to-hour variability.

4.1 Tall tower Angus

At seasonal time scales there is a detectable (absolute value >0.1 ppm) difference in atmospheric CO_2 present at TTA between the control and afforested simulations (Fig. 2). Afforestation results in a detectable reduction in atmospheric CO_2 concentrations, including a reduction of up to 0.75 ppm during July and August at TTA. The magnitude of the seasonal bias due to afforestation varies between years, with the largest occurring in 2006. In contrast, during April and

September there is a detectable increase in atmospheric CO_2 concentrations due to afforestation, with the largest occurring in 2006.

Investigation of ecosystem specific net uptake CO_2 tracers show an increase in forest net uptake CO_2 tracer simulated at TTA (Fig. 3). Net uptake CO_2 tracer for crops, managed grassland and 'other' land covers are reduced in the afforested simulation (Fig. 3). A comparison between net uptake CO_2 tracers and the simulated surface net CO_2 uptake flux provides an indication of how well observations made at TTA represent variation of ecosystem specific surface exchange. There is little impact on how well seasonal variation in ecosystem specific net uptake CO_2 tracers, simulated at TTA, explain seasonal variation of the simulated surface net CO_2 uptake flux (Fig. 3). Maintenance of seasonal information in TTA observations is supported by statistical analysis comparing seasonal variation for surface net CO_2 uptake flux explained by net uptake CO_2 tracers at TTA. Forest (R^2= 0.72 and 0.78), cropland (R^2= 0.93 and 0.91), managed grassland (R^2= 0.73 and 0.71) and 'other' (R^2= 0.77 and 0.78) each showed little difference between the control and afforested simulations respectively.

4.2 Alternate tall towers

The seasonal and interannual variations simulated in atmospheric CO_2 concentrations due to afforestation are consistent between the alternate tall towers and TTA (Fig. 2). However there is considerable variation in the magnitude of the difference between the control and afforested simulations. The variability results in several towers being simulated to not have a detectable difference in atmospheric CO_2 concentrations due to afforestation, most clearly seen in 2007 and 2008 (Fig. 2).

Each tall tower was assessed for its ability to detect differences in forest CO_2 exchange between the control and afforested simulations. This was achieved through regression analysis of the difference between the control and afforested simulations for forest net uptake CO_2 tracer simulated at each tower and the difference between the simulated forest surface net CO_2 uptake flux. A network of tall towers (Blackhill and Selkirk) are statistically best able to detect changes in forest surface net CO_2 uptake flux due to the simulated afforestation (R^2 = 0.90). Individually both Blackhill (R^2= 0.88) and Selkirk (R^2= 0.86) are able to explain the majority of variation due to afforestation. Angus was not included in the network, however it is worth noting that Angus was simulated to detect a large amount of variation in forest surface net CO_2 uptake flux due to afforestation (R^2= 0.75). There is strong seasonality in the magnitude of the difference between simulations for forest net CO_2 uptake. The greatest impact occurs during the peak of the growing season (Fig. 4).

Analysis of the prevailing wind conditions at each tower shows that at both annual and seasonal time scales all towers are exposed to similar conditions. There is little apparent difference between the prevailing wind direction at annual time scales, however there was considerable interannual variation in prevailing wind conditions at seasonal time scales particularly during the growing season (i.e. May, June, July and August) (Fig. 5). During 2006 the wind direction varies between westerly and southerly, while in 2007 wind direction includes increased contributions from northerly and easterly directions. In 2008 easterly winds are more dominant during the growing season. The simulated interannual variation in seasonal wind direction will have a considerable impact on the footprint of the tall tower observations.

Improved detection of ecosystem seasonal variation of surface net CO_2 uptake flux was achieved through use of a network of tall towers (Table 4). Stepwise multiple linear regression was used to assess the 'best' observing network to detect seasonal variation in surface net CO_2 uptake flux, for both the control and afforested simulations. Networks typically consist of three towers, with a minimum of one and a maximum of four towers used (Table 4). The 'best' network for each ecosystem varies between the control and afforested simulations (except managed grassland), although in each case there are common towers. Variation in the 'best' network is expected as a result of changes in ecosystem spatial distribution and possible changes in atmospheric transport due to changes in near surface turbulent mixing. Knockmore is most frequently included in ecosystem observing networks followed by TTA. Durris is least often included in observing networks.

Tall towers Angus, Blackhill and Knockmore were assessed as a potential observing network for Scotland (Table 5). Angus is included as the only tower currently operational. Blackhill is included as the tower which individually best detects the impact of the simulated afforestation on forest CO_2 uptake, while Knockmore is included as the tall tower that is most commonly included in observing networks for ecosystem variation (Table 4). The selected ecosystem specific observing network varies between the control and afforested simulations, however all three towers are included in multiple observing networks (Table 5). Using these three towers it is possible to explain the majority of seasonal variation of ecosystem surface net CO_2 uptake flux with little degradation compared to having all towers available for selection. Of these three towers only Blackhill significantly contributes to detection of changes to forest CO_2 uptake due to afforestation.

4.3 Changes in atmospheric transport

A comparison of the anthropogenic emissions CO_2 tracer between the control and afforested simulations was used to indicate changes in atmospheric transport due to afforestation. Anthropogenic emissions were identical between both simulations and once emitted they did not interact further with the land surface, thus allowing anthropogenic CO_2 tracer to

act as a passive indicator of changes in atmospheric transport. Anthropogenic emissions CO_2 tracer was highly correlated (R^2 = 0.96, rmse = 0.18 ppm, bias = 0.02 ppm, afforested-control) between the control and afforested simulations . The mean percentage difference (percentage equivalent of the rmse) was 5.3 % and the mean percentage bias was 2.8 %. Similar differences were found at each of the alternate tall towers (data not shown). While differences between simulations were small they do indicate some changes in atmospheric transport due to afforestation.

Near surface atmospheric transport i.e. planetary boundary layer (PBL) mixing, is driven by surface net radiation and its partitioning to turbulent exchange of latent and sensible heat between the surface and the atmosphere. Comparison of afforested locations with their corresponding location in the control simulation shows modest hour to hour variation in PBL height (R^2= 0.87, rmse = 165.6 m, bias = -19.7 m). Net radiation (R^2= 0.94, rmse = 37.7 W m^{-2}, bias = 3.8 W m^{-2}) remained well correlated with an increase in mean annual bias between the control and afforested simulations for afforested locations. There is also a moderate change in net radiation where the rmse indicate hourly variation. Partitioning to latent (R^2 = 0.78, rmse = 46.4 W m^{-2}, bias = 18.7 W m^{-2}) and sensible heat (R^2 = 0.84, rmse = 40.2 W m^{-2}, bias = -15.1 W m^{-2}) are more significantly affected by afforestation. Partitioning to latent heat has increased and correspondingly sensible heat has decreased, as indicated by the mean annual bias.

4.4 Changes to surface meteorology

The simulated afforestation resulted in a reduction in land surface mean annual surface air temperature (R^2= 0.99, rmse = 0.42 °C, bias = -0.06 °C) and an increase in mean annual surface water vapour content (R^2 = 0.89, rmse = 1.3 g/kg, bias = 0.58 g/kg). The impact of afforestation is broadly localised to the afforested region with a maximum change in air temperature of -0.16°C (or ∼1.8 %) and maximum increase in mean annual surface water vapour of 2 g/kg (or ∼18.6 %) (Fig. 6). Both the reduction in surface air temperature and the increase in surface water vapour contribute to a reduction in the vapour pressure deficit (VPD, R^2 = 0.98, rmse = 40.2 Pa, bias = -10.9 Pa). Reduced VPD is also broadly localised to the afforested region and appears to be dominated by changes in surface air temperature, based on comparison with the mean annual surface air temperature map (Fig. 6). Mean annual precipitation was simulated to increase (R^2 = 0.99 , rmse = 87.5 mm, bias = 29.9 mm). Consistent with surface meteorological variables, increases in precipitation occurs primarily within the afforested region, with a maximum increase in mean annual accumulation of precipitation due to afforestation of 118 mm (∼ 7.6 %) (Fig. 6).

5 Discussion and conclusions

WRF-SPA has been used to investigate the detectability of a policy relevant afforestation of Scotland using observations made at a tall tower. WRF-SPA simulated increase in surface forest sequestration is greater than expected in the Scottish Government's policy (Forestry Commission Scotland, 2009), it is however of a similar magnitude. Therefore, it is reasonable to expect that changes in tall tower observations simulated here due to afforestation should also be of broadly realistic magnitude.

All tall towers were found to detect changes in atmospheric CO_2 concentrations of a magnitude greater than the observations accuracy limit in at least one of the years simulated here (Fig. 2). Atmospheric CO_2 concentrations simulated at Knockmore showed the smallest magnitude difference due to afforestation. Lower detection at Knockmore is consistent with its location outside of the afforested area. Afforestation leads to a reduction in atmospheric CO_2 concentrations during the peak of the growing season which is consistent with the simulated increase in surface sequestration. This suggests that current observations at tall tower Angus, and a number of alternate towers, are able to detect currently planned policy relevant afforestation of Scotland. However the magnitude of the reduction varied considerable between towers and between years, often falling below the detection limit. A probable explanation for the variation in detectability is variation in prevailing wind direction, particularly during the growing season (Fig. 5). The variable and small magnitude impact on simulated atmospheric CO_2 concentration wold seem to indicate the limited ability of observations made at tall towers to detect afforestation, however analysis of ecosystem specific CO_2 tracers indicate otherwise.

5.1 Detection of afforestation

Explicit detection of the impact of afforestation on forest surface net CO_2 uptake flux is improved through the use of a network of tall towers (Fig. 4). This is consistent with the conclusions of other studies which investigated tall tower observing networks (e.g. Lauvaux et al., 2012). Blackhill and Selkirk were selected through stepwise regression as best able to explain the effect of afforestation policy relevant forest surface net CO_2 uptake flux. While TTA is not included in the network it should be noted that net uptake CO_2 tracers indicate that a majority of seasonal variation due to afforestation can be explained by net uptake CO_2 tracers simulated at TTA. Observations made at Blackhill explain a similar amount of variation for forest surface net CO_2 uptake flux due to afforestation as the 'best' network (Fig. 4). Observations made at Selkirk also 'detect' a majority of variation in forest surface net CO_2 uptake flux due to afforestation. Good detection of afforestation is consistent with the central location of Darvel and, in particular, Blackhill within the afforested region (Fig. 1). Moreover Selkirk was simulated to

consistently show a significant change in atmospheric CO_2 concentrations due to afforestation (Fig. 2). Therefore, the addition of Blackhill or Selkirk towers to a national network may potentially be valuable in monitoring currently planned afforestation of Scotland.

5.2 Detection of seasonal variation

Detection of seasonal variation of surface net CO_2 uptake CO_2 for Scotland's dominant ecosystems is improved through the use of a network of tall towers (Fig. 3 and Table 4). The statistically determined 'best' networks varied between ecosystems; the frequency that each tower occurred within a network also varied considerably. Knockmore was most frequently included in observing networks, indicating that Knockmore should be considered for inclusion in any future extension of the tall tower observing network of Scotland. TTA was the third most frequently included tower indicating that TTA, as Scotland's currently operating tall tower, is well placed for observing Scotland as a whole. Blackhill has been shown to be potentially important for the detection of afforestation it is the second most commonly included tower in observing networks. However the variation between selected 'best' network highlights that optimum network design is likely governed by a networks intended purpose. Furthermore, the selected networks varied for each ecosystem between the control and afforested simulations. Creating further uncertainty regarding how robust any network is to future changes in land cover composition.

Tall towers Angus, Blackhill and Knockmore were considered as part of a reduced observing network, to assess the feasibility of a compromise network between the detection of afforestation and seasonal variation of ecosystem surface net CO_2 uptake flux more generally. The reduced network was able to detect the majority of seasonal variation for each ecosystem and changes in forest surface net CO_2 uptake flux due to afforestation (Table 5). Effective detection with a reduced network is consistent with previous studies (e.g. Lauvaux et al., 2012). This suggests that the methodology used here to optimise a tall tower observing network for specific purpose, i.e. observing specific ecosystem or change in management, may be a viable alternative to network analysis through multiple atmospheric inversions. However, this conclusion needs to be tested in comparison with atmospheric inversion analysis of the towers used here.

5.3 Changes to atmospheric transport

Atmospheric transport, and in particular PBL development, is closely coupled to surface energy balance and its partitioning between turbulent exchange of latent and sensible heat (Schomburg et al., 2012). As expected the simulated afforestation resulted in increased latent heat flux and a reduction in sensible heat exchange (Davin and de Noblet-Ducoudre, 2010; Betts, 2011). Forest ecosystems typically have a larger leaf area impacting rainfall interception and transpiration, and deeper roots to access water. These changes had only a small apparent impact on atmospheric transport, indicated by small proportional differences in anthropogenic emissions CO_2 tracer detected at each of the tall towers between the control and afforested simulations.

5.4 Changes to surface meteorology

The simulated impact of afforestation on surface meteorology are due to the land cover change only, as these simulations take no account of the impact of increased atmospheric CO_2 concentration or climate change which are expected to occur over the coming decades. The net effect of afforestation at temperate latitudes remains uncertain, primarily due to differing response of simulations to reduced albedo, increased evapotranspiration and associated feedbacks through, for example changes in cloud cover and precipitation (Bonan, 2008). The simulated cooling effect seen here is consistent with increased evaporation within the afforested area (Fig. 6). The cooling effect is also consistent with the simulated results over Scotland from a long term global scale afforestation experiment (Arora and Montenegro, 2011). The simulated increase of net radiation is consistent with the expectations of afforestation (Betts, 2011). Therefore, the net cooling effect indicates that increased latent heat flux is the dominant response over increased net radiation.

Afforestation resulted in a change in the magnitude of mean annual precipitation, particularly within the afforested region (Fig. 6). The increased precipitation occurs broadly in the same region as areas of reduced VPD, indicating that VPD is the underlying driver. This study does not include the effect of climate change or increased atmospheric CO_2 concentrations, however the simulations here indicate that it is possible for policy relevant afforestation to have an impact on precipitation over Scotland, and therefore potentially on surface run off and flood risk.

5.5 Caveats and future work

We expect that the overall conclusion, that afforestation is likely to be detectable by observations of atmospheric CO_2 concentrations made at tall towers to be robust, however there are a number of important caveats. The afforested area is assumed to be fully grown, with no parameterisation for forest management practices. Therefore the effect of ecosystem age and variations in the spatial distribution of ecosystems over time are neglected. Furthermore, only one potential afforestation map was simulated whereas in reality both the spatial distribution of the afforested areas and ecosystem composition will vary over time due to human management and successional processes. Given that the optimal network for specific ecosystems varied between the control and afforested simulation, it is also likely that the optimal network

will vary over time. Critically we consider detection over a relatively short period of time, both reducing the interannual variation that the tall towers are exposed to and lacking a consideration of future climate change on ecosystem processes.

There are a number of potential areas for further research. The most important next step is a comparison with atmospheric inversion simulations to assess the key assumption made here, that improved detection of seasonal cycles can be used to generate an optimal observing network. Subsequent work could then include an assessment of how observation height impacts detectability, the effect of multiple possible afforestation distributions and critically longer simulations. Longer simulations offer the ability to assess the impact on detection of afforestation due to the inclusion of forest management allowing development of a realistic age class distribution and time varying spatial distributions. This could also include the effects of management of soil carbon stocks. Increased release of CO_2 from soils due to afforestation could reduce the magnitude of the difference in atmospheric CO_2 concentration between control and afforested simulations. Furthermore, a longer simulation also allows for the inclusion of impacts on ecosystem processes due to climate change.

5.6 Conclusions

Specific questions were asked of WRF-SPA. (i) Does afforestation result in a change in atmospheric CO_2 concentrations which is detectable by current observations made at a tall tower Angus? Simulated afforestation resulted in a change in total atmospheric CO_2 concentrations of a magnitude which is detectable at Angus and all alternate towers however the magnitude of the difference between the control and afforested simulations varied considerably between years and towers. (ii) Can detection of afforestation on forest net CO_2 uptake be improved through use of an alternate tall tower or network? Detection of afforestation can be improved through the use of a tall tower network, however the Blackhill tower alone is able to detect a similar amount of variation in forest net CO_2 uptake as the selected 'best' network. (iii) Can detection of seasonal variation in ecosystem CO_2 uptake be improved through use of a tall tower network? Detection of seasonal variation in ecosystem carbon net CO_2 uptake can be improved through the use of a tall tower network. The most frequently included towers in the simulated observing networks are Knockmore and Blackhill, while Angus is third most frequently included. Therefore the maintenance of Angus and the addition of Knockmore or Blackhill to a national observing network are potentially important for future observations of Scotland's carbon balance. As indicated by the majority of seasonal variation being explained by a reduced network consisting of Angus, Blackhill and Knockmore. (iv) Does changing Scotland's ecosystem composition, i.e. afforestation, significantly alter atmospheric transport? Afforestation leads to small changes in atmospheric transport through increases in surface net radiation and a change in the relative amounts of latent and sensible heat exchanges. (v) Does afforestation result in changes to surface meteorological variables? Afforestation results in a cooling and wetting of the near surface air resulting in changes in precipitation magnitude primarily within the afforested region.

Through WRF-SPA simulations we have demonstrated that observations of atmospheric CO_2 concentrations made at tall towers are potentially useful tools for understanding seasonal and interannual ecosystem CO_2 exchange. The method for assessing observation networks for both specific and generalist purposes may also provide useful information of policy makers in understanding the impacts of planned land cover change and management.

Acknowledgements. The authors would like to thank the project funding body, National Centre for Earth Observation, a Natural Environment Research Council research centre. Tall tower Angus has been funded since 2004 by EU FP5, FP6 grants.

References

Ahmadov, R., Gerbig, C., Kretschmer, R., Koerner, R., Neininger, B., Dolman, A. J., and Sarrat, C.: Mesoscale covariance of transport and CO_2 fluxes: Evidence from observations and simulations using the WRF-VPRM coupled atmosphere-biosphere model, J. Geophys. Res.-Atmos., 112, D11, 2007.

Arora, V. K. and Montenegro, A.: Small temperature benefits provided by realistic afforestation efforts, Nat. Geosci., 4, 514–518, doi:10.1038/NGEO1182, 2011.

Avissar, R.: Which type of soil vegetation atmosphere transfer scheme is needed for general circulation models: a proposal for a higher order scheme, J. Hydrol., 212213, 136 – 154, doi:10.1016/S0022-1694(98)00227-3, 1998.

Bala, G., Caldeira, K., Wickett, M., Phillips, T. J., Lobell, D. B., Delire, C., and Mirin, A.: Combined climate and carbon-cycle effects of large-scale deforestation, Proc. Natl. Acad. Sci. U. S. A., 104, 6550–6555, doi:10.1073/pnas.0608998104, 2007.

Betts, R. A.: CLIMATE SCIENCE Afforestation cools more or less, Nat. Geosci., 4, 504–505, doi:10.1038/ngeo1223, 2011.

Betts, R. A., Falloon, P. D., Goldewijk, K. K., and Ramankutty, N.: Biogeophysical effects of land use on climate: Model simulations of radiative forcing and large-scale temperature change, Agr. Forest Meteorol., 142, 216–233, 2007.

Bonan, G. B.: Forests and Climate Change: Forcings, Feedbacks, and the Climate Benefits of Forests, Science, 320, 1444–1449, 2008.

Borge, R., Alexandrov, V., del Vas, J. J., Lumbreras, J., and Rodriguez, E.: A comprehensive sensitivity analysis of the WRF model for air quality applications over the Iberian Peninsula, Atmos. Environ., 42, 8560–8574, doi:10.1016/j.atmosenv.2008.08.032, 2008.

Bradley, R., Milne, R., Bell, J., Lilly, A., Jordan, C., and Higgins, A.: A soil carbon and land use database for the United Kingdom, Soil Use Manage., 21, 363–369, doi:10.1079/SUM2005351, 2005.

Brunner, D., Henne, S., Keller, C. A., Reimann, S., Vollmer, M. K., O'Doherty, S., and Maione, M.: An extended Kalman-filter for regional scale inverse emission estimation, Atmos. Chem. Phys., 12, 3455–3478, doi:10.5194/acp-12-3455-2012, 2012.

Canadell, J. G., Le Quere, C., Raupach, M. R., Field, C. B., Buitenhuis, E. T., Ciais, P., Conway, T. J., Gillett, N. P., Houghton, R. A., and Marland, G.: Contributions to accelerating atmospheric CO_2 growth from economic activity, carbon intensity, and efficiency of natural sinks, Proc. Natl. Acad. Sci. U. S. A., 104, 18 866–18 870, doi:10.1073/pnas.0702737104, 2007.

Davin, E. L. and de Noblet-Ducoudre, N.: Climatic Impact of Global-Scale Deforestation: Radiative versus Nonradiative Processes, J. Clim., 23, 97–112, doi:10.1175/2009JCLI3102.1, 2010.

ESA: Report for Mission Selection: Biomass, ESA SP-1324/1 (3 volume series), European Space Agency, Noordwijk, The Netherlands, 2012.

Farquhar, G. D. and von Caemmerer, S.: Modelling of photosynthetic response to the environment. Physiological Plant Ecology II. Encyclopedia of plant physiology, Springer-Verlag, Berlin, 1982.

Forestry Commission Scotland: The Scottish Government's Rational for Woodland Expansion, The scottish government strategy document, Forestry Commission, Edinburgh, EH12 7AT, Scotland, 2009.

Friedlingstein, P. and Prentice, I. C.: Carbon-climate feedbacks: a review of model and observation based estimates, Curr. Opin. Environ. Sustainability, 2, 251–257, 2010.

Friedlingstein, P., Cox, P., Betts, R., Bopp, L., Von Bloh, W., Brovkin, V., Cadule, P., Doney, S., Eby, M., Fung, I., Bala, G., John, J., Jones, C., Joos, F., Kato, T., Kawamiya, M., Knorr, W., Lindsay, K., Matthews, H. D., Raddatz, T., Rayner, P., Reick, C., Roeckner, E., Schnitzler, K. G., Schnur, R., Strassmann, K., Weaver, A. J., Yoshikawa, C., and Zeng, N.: Climate-carbon cycle feedback analysis: Results from the C_4MIP model intercomparison, J. Climate, 19, 3337–3353, doi:10.1175/JCLI3800.1, 2006.

Gerbig, C., Dolman, A. J., and Heimann, M.: On observational and modelling strategies targeted at regional carbon exchange over continents, Biogeosciences, 6, 1949–1559, 2009.

Gurney, K., Law, R., Denning, A., Rayner, P., Baker, D., Bousquet, P., Bruhwiler, L., Chen, Y., Ciais, P., Fan, S., Fung, I., Gloor, M., Heimann, M., Higuchi, K., John, J., Maki, T., Maksyutov, S., Masarie, K., Peylin, P., Prather, M., Pak, B., Randerson, J., Sarmiento, J., Taguchi, S., Takahashi, T., and Yuen, C.: Towards robust regional estimates of CO_2 sources and sinks using atmospheric transport models, Nature, 415, 626–630, doi:10.1038/415626a, 2002.

Henne, S., Brunner, D., Folini, D., Solberg, S., Klausen, J., and Buchmann, B.: Assessment of parameters describing representativeness of air quality in-situ measurement sites, Atmos. Chem. Phys., 10, 3561–3591, 2010.

ICOS: Integrated Carbon Observing System: Stakeholders Handbook, A European Infrastructure - European Union, LSCE-Orme, CEA-Orme des Merisiers, F-91191 GIF-SUR-YVETTE CEDEX, 2012.

IPCC: Climate Change 2007: Synthesis Report. Contribution of Working Groups I, II and III to the Fourth Assessment Report of the Intergovernmental Panel on Climate Change, Core Writing Team, Pachauri, R.K. and Reisinger, A. (Eds.)., IPCC, Geneva, Switzerland., 2007.

Jones, H. G.: Plants and microclimate, Cambridge University Press, Cambridge, 1992.

Kaplan, J. O., Krumhardt, K. M., and Zimmermann, N. E.: The effects of land use and climate change on the carbon cycle of Europe over the past 500 years, Glob. Change Biol., 18, 902–914, doi:10.1111/j.1365-2486.2011.02580.x, 2012.

Lauvaux, T., Schuh, A. E., Bocquet, M., Wu, L., Richardson, S., Miles, N., and Davis, K. J.: Network design for mesoscale inversions of CO_2 sources and sinks, Tellus Ser. B-Chem. Phys. Meteorol., 64, doi:10.3402/tellusb.v64i0.17980, 2012.

Le Toan, T., Quegan, S., Davidson, M. W. J., Balzter, H., Paillou, P., Papathanassiou, K., Plummer, S., Rocca, F., Saatchi, S., Shugart, H., and Ulander, L.: The BIOMASS mission: Mapping global forest biomass to better understand the terrestrial carbon cycle, Remote Sens. Environ., 115, 2850–2860, doi:10.1016/j.rse.2011.03.020, 2011.

Mesoscale and Microscale Meteorology Division: Weather Research and Forecasting ARW Version 3 Modelling System User's Guide, User's guide, National Center for Atmospheric Research, Colorado, USA, 2011.

Miles, N. L., Richardson, S. J., Davis, K. J., Lauvaux, T., Andrews, A. E., West, T. O., Bandaru, V., and Crosson, E. R.: Large amplitude spatial and temporal gradients in atmospheric boundary layer CO_2 mole fractions detected with a tower-based network in the U.S. upper Midwest, J. Geophys. Res.-Biogeosci., 117, doi:10.1029/2011JG001781, 2012.

Ostle, N., Levy, P., Evans, C., and Smith, P.: UK land use and soil carbon sequestration, Land Use Policy, 26, S274 – S283, doi:10.1016/j.landusepol.2009.08.006, land Use Futures, 2009.

Paul, K., Polglase, P., Nyakuengama, J., and Khanna, P.: Change in soil carbon following afforestation, Forest Ecol. Manag., 168, 241–257, doi:10.1016/S0378-1127(01)00740-X, 2002.

Peters, W., Krol, M. C., van der Werf, G. R., Houweling, S., Jones, C. D., Hughes, J., Schaefer, K., Masarie, K. A., Jacobson, A. R., Miller, J. B., Cho, C. H., Ramonet, M., Schmidt, M., Ciattaglia, L., Apadula, F., Helta, D., Meinhardt, F., di Sarra, A. G., Piacentino, S., Sferlazzo, D., Aalto, T., Hatakka, J., Strom, J., Haszpra, L., Meijer, H. A. J., van der Laan, S., Neubert, R. E. M., Jordan, A., Rodo, X., Morgui, J. A., Vermeulen, A. T., Popa, E., Rozanski, K., Zimnoch, M., Manning, A. C., Leuenberger, M., Uglietti, C., Dolman, A. J., Ciais, P., Heimann, M., and Tans, P. P.: Seven years of recent European net terrestrial carbon dioxide exchange constrained by atmospheric observations, Glob. Change Biol., 16, 1317–1337, doi:10.1111/j.1365-2486.2009.02078.x, 2010.

Poeplau, C., Don, A., Vesterdal, L., Leifeld, J., Van Wesemael, B., Schumacher, J., and Gensior, A.: Temporal dynamics of soil organic carbon after land-use change in the temperate zone - carbon response functions as a model approach, Glob. Change Biol., 17, 2415–2427, doi:10.1111/j.1365-2486.2011.02408.x, 2011.

Qian, H., Joseph, R., and Zeng, N.: Enhanced terrestrial carbon uptake in the Northern High Latitudes in the 21st century from the Coupled Carbon Cycle Climate Model Intercomparison Project model projections, Glob. Change Biol., 16, 641–656, doi:10.1111/j.1365-2486.2009.01989.x, 2010.

Rigby, M., Manning, A. J., and Prinn, R. G.: Inversion of long-lived trace gas emissions using combined Eulerian and Lagrangian

chemical transport models, Atmos. Chem. Phys., 11, 98879898, doi:10.5194/acp-11-9887-2011, 2011.

Sarrat, C., Noilhan, J., Dolman, A. J., Gerbig, C., Ahmadov, R., Tolk, L. F., Meesters, A. G. C. A., Hutjes, R. W. A., Ter Maat, H. W., Perez-Landa, G., and Donier, S.: Atmospheric CO_2 modeling at the regional scale: an intercomparison of 5 meso-scale atmospheric models, Biogeosciences, 4, 1115–1126, 2007.

Schomburg, A., Venema, V., Ament, F., and Simmer, C.: Disaggregation of screen-level variables in a numerical weather prediction model with an explicit simulation of subgrid-scale land-surface heterogeneity, Meteorol. Atmos. Phys., 116, 81–94, doi: 0.1007/s00703-012-0183-y, 2012.

Sitch, S., Huntingford, C., Gedney, N., Levy, P. E., Lomas, M., Piao, S. L., Betts, R., Ciais, P., Cox, P., Friedlingstein, P., Jones, C. D., Prentice, I. C., and Woodward, F. I.: Evaluation of the terrestrial carbon cycle, future plant geography and climate-carbon cycle feedbacks using five Dynamic Global Vegetation Models (DGVMs), Glob. Change Biol., 14, 2015–2039, 2008.

Skamarock, W. C., Klemp, J. B., Dudhia, J., Gill, D. O., Barker, D. M., Duda, M. G., Huang, X.-Y., Wang, W., and Powers, J. G.: A Description of the Advanced research WRF Version 3, 2008.

Smallman, T. L., Moncrieff, J. B., and Williams, M.: WRFv3.2-SPAv2: development and validation of a coupled ecosystem-atmosphere model, scaling from surface fluxes of CO_2 and energy to atmospheric profiles, Geosci. Model Dev., 6, 1079–1093, doi:10.5194/gmd-6-1079-2013, http://www.geosci-model-dev.net/6/1079/2013/, 2013a.

Smallman, T. L., Williams, M., and Moncrieff, J. B.: Can seasonal and interannual variation in landscape CO_2 fluxes be detected by atmospheric observations of CO_2 concentrations made at a tall tower?, Biogeosciences Discussions, 10, 14 301–14 331, doi:10.5194/bgd-10-14301-2013, http://www.biogeosciences-discuss.net/10/14301/2013/, 2013b.

Steeneveld, G. J., Tolk, L. F., Moene, A. F., Hartogensis, O. K., Peters, W., and Holtslag, A. A. M.: Confronting the WRF and RAMS mesoscale models with innovative observations in the Netherlands: Evaluating the boundary layer heat budget, J. Geophys. Res.-Atmos., 116, doi:10.1029/2011JD016303, 2011.

Sus, O., Williams, M., Bernhofer, C., Beziat, P., Buchmann, N., Ceschia, E., Doherty, R., Eugster, W., Gruenwald, T., Kutsch, W., Smith, P., and Wattenbach, M.: A linked carbon cycle and crop developmental model: Description and evaluation against measurements of carbon fluxes and carbon stocks at several European agricultural sites, Agr. Ecosyst. Environ., 139, 402–418, 2010.

The Scottish Government: Scottish Greenhouse Gas Emissions 2009, Tech. rep., Scottish Government Statistician Group, Environment Statistics, Rural and Environment Science and Analytical, Services Rural Payments and Inspections Directorate 1F-South, Victoria Quay, Edinburgh, EH6 6QQ, 2011.

Vermeulen, A. T., Hensen, A., Popa, M. E., van den Bulk, W. C. M., and Jongejan, P. A. C.: Greenhouse gas observations from Cabauw Tall Tower (1992-2010), Atmos. Meas. Tech., 4, 617–644, doi:10.5194/amt-4-617-2011, 2011.

Wang, Y., Long, C. N., Leung, L. R., Dudhia, J., McFarlane, S. A., Mather, J. H., Ghan, S. J., and Liu, X.: Evaluating regional cloud-permitting simulations of the WRF model for the Tropical Warm Pool International Cloud Experiment (TWP-ICE), Darwin, 2006, J. Geophys. Res.-Atmos., 114, 1 – 21, doi: 10.1029/2009JD012729, 2009.

Williams, M., Rastetter, E. B., Fernandes, D. N., Goulden, M. L., Wofsy, S. C., Shaver, G. R., Melillo, J. M., Munger, J. W., Fan, S. M., and Nadelhoffer, K. J.: Modelling the soil-plant-atmosphere continuum in a Quercus-Acer stand at Harvard Forest: the regulation of stomatal conductance by light, nitrogen and soil/plant hydraulic properties, Plant Cell Environ., 19, 911–927, 1996.

Williams, M., Schwarz, P. A., Law, B. E., Irvine, J., and Kurpius, M.: An improved analysis of forest carbon dynamics using data assimilation, Glob. Change Biol., 11, 89–105, 2005.

Williams, M., Malhi, Y., Nobre, A., Rastetter, E., Grace, J., and Pereira, M.: Seasonal variation in net carbon exchange and evapotranspiration in a Brazilian rain forest: a modelling analysis, Plant Cell Environ., 21, 953–968, doi:10.1046/j.1365-3040.1998.00339.x, 1998.

Williams, M., Law, B., Anthoni, P., and Unsworth, M.: Use of a simulation model and ecosystem flux data to examine carbon-water interactions in ponderosa pine, Tree Physiol., 21, 287–298, 2001.

Zhang, Y.: Online-coupled meteorology and chemistry models: history, current status, and outlook, Atmos. Chem. Phys., 8, 2895–2932, 2008.

...

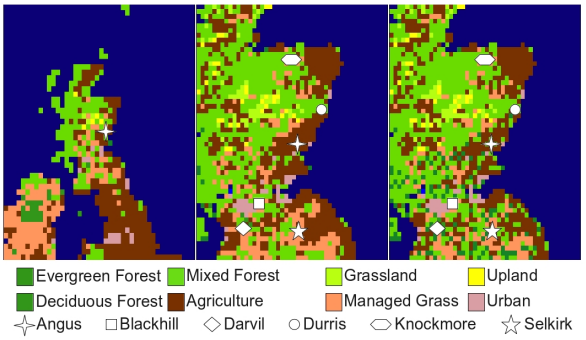

Fig. 1. Land classification map showing the spatial extent of the model domain. The left panel is the parent domain at 18 x 18 km, the centre and right panels show the nested domain at 6 x 6 km resolution. The centre panel shows the control simulation with current day land cover. The right panel shows the land cover map used in the afforested simulation, with additional forest cover in the south and eastern areas of Scotland. The symbols show the locations of the tall towers assessed in this study.

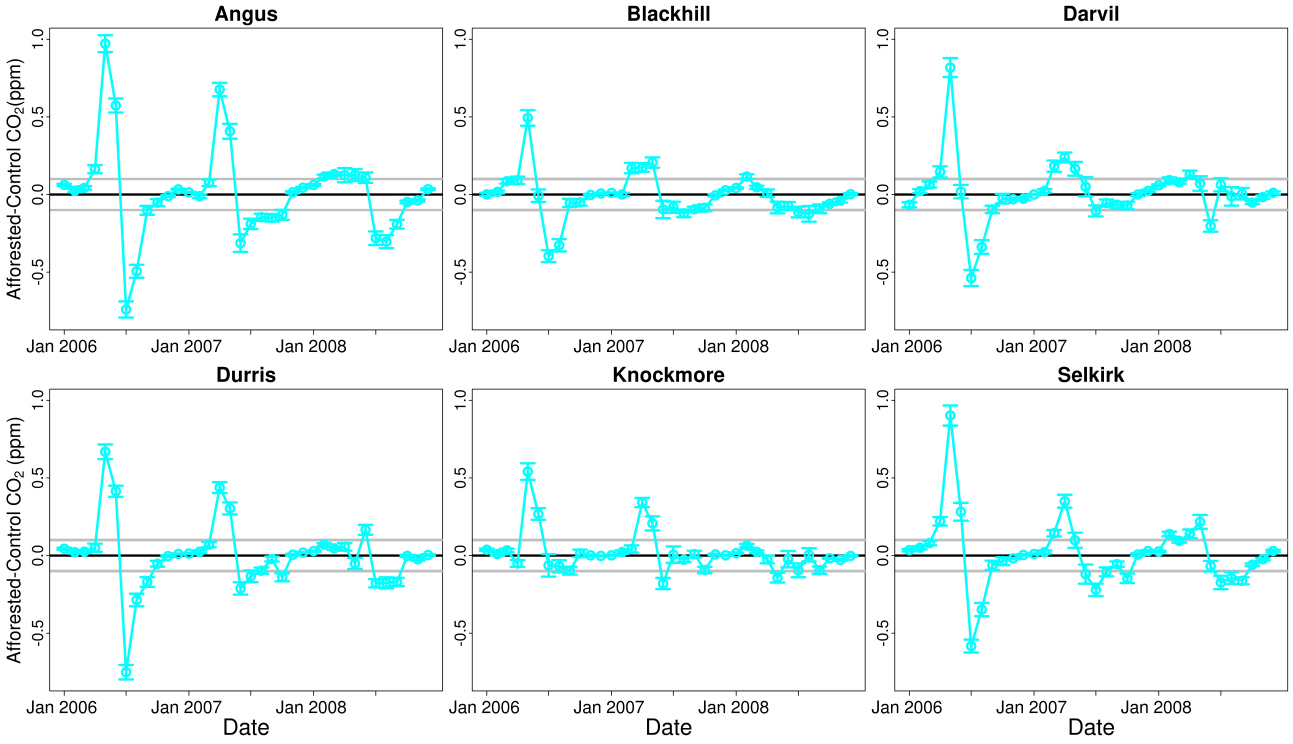

Fig. 2. Monthly mean residual in atmospheric CO_2 concentrations simulated to be at tall tower Angus between the control and afforested simulations. Also included are monthly mean residuals for the five alternate tall tower locations which could in the future be used for observation of atmospheric CO_2 concentrations. Residuals which are outside of the grey lines are of a magnitude which is considered to be detectable by observations. The grey lines indicate $\pm$ the accuracy limit (0.1 ppm) of observation equipment at tall tower Angus. Error bars are $\pm$ 1 standard error accounting for temporal variation only.

Table 1. Tracer pools and definitions used by WRF-SPA. A passive tracer does not have the potential to be exchanged with the land surface after its initial emission. Whereas a non-passive tracer can be removed from the atmosphere, as it represents a physical mass of CO_2 added to the atmosphere through respiration.

Tracer	Description	Passive tracer
1	Total CO_2 concentration, includes all sources and sinks of CO_2, for comparison to observations	No
2	Forest net CO_2 uptake	Yes
3	Anthropogenic emissions	Yes
4	Forcings only, i.e. anthropogenic emissions, ocean sequestration, initial and lateral boundary conditions only	Yes
5	Crop net CO_2 uptake	Yes
6	Ocean sequestration	Yes
7	Forest net CO_2 release	No
8	Crop net CO_2 release	No
9	Managed grassland net CO_2 release	No
10	Other vegetation net CO_2 release	No
11	Managed grassland net CO_2 uptake	Yes
12	Other vegetation net CO_2 uptake	Yes

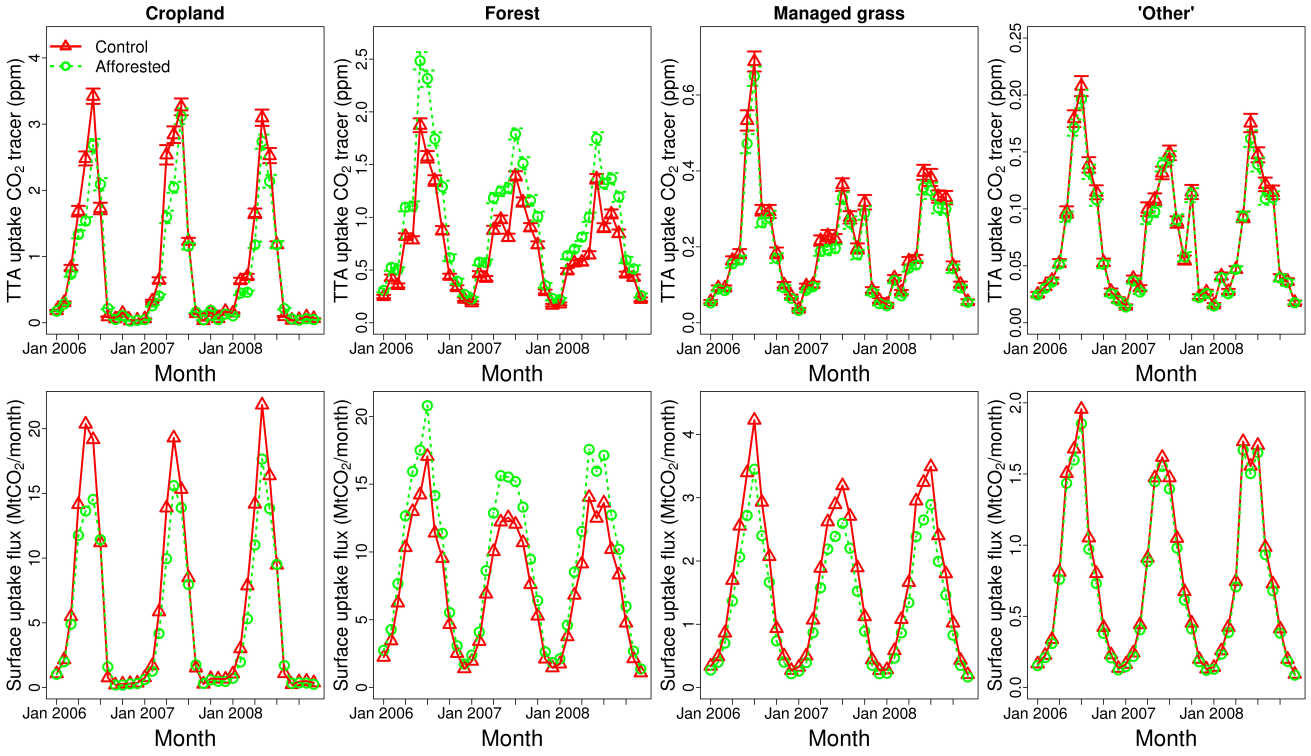

Fig. 3. Modelled monthly mean net CO_2 uptake tracer simulated at tall tower Angus (top) and simulated land surface net CO_2 uptake (bottom). Surface net CO_2 uptake is the domain sum value for the land cover specified. Allows comparison of changes in surface uptake due to afforestation with changes in uptake tracer detected at tall tower Angus. This comparison allows us to ascertain whether observations reflect the actual changes in surface uptake. Error bars are $\pm$1 standard error for temporal variability only.

Table 2. Parameter and model options used in WRF-SPA

Basic equations	Non-hydrostatic, compressible Advanced Research WRF (ARW)
Radiative transfer scheme	Rapid Radiative Transfer Model for GCMs (RRTMG) for both long wave and short wave
Planetary boundary layer scheme	Yonsei University
Surface scheme	Monin-Obukov
Land surface model	Soil Plant Atmosphere (SPA)
Microphysics scheme	WSM 3-class simple ice
Cumulus parameterisation	Grell 3D ensemble scheme (coarse domain only)
Nesting	Two-way nesting
Domain, resolution	44 x 47, 18 km
	48 x 54, 6 km
	35 vertical levels
Domain centre	56.63° N, 3.35° W

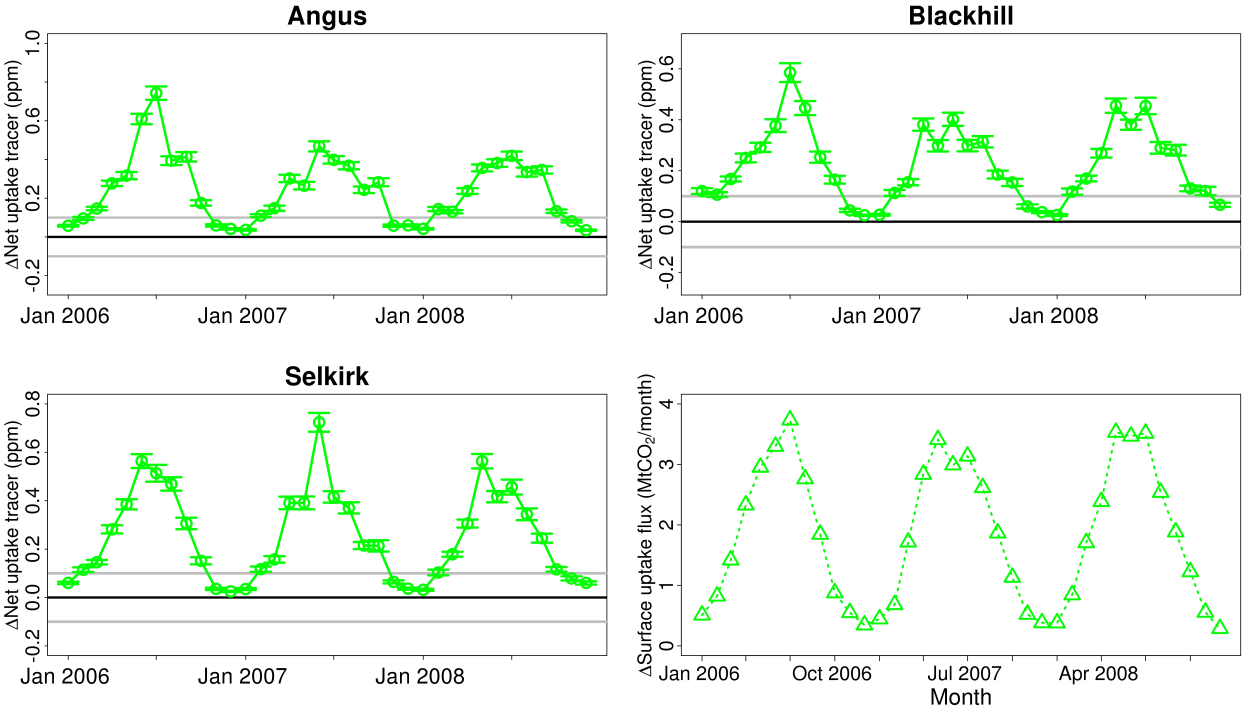

Fig. 4. Monthly mean difference between afforested and control simulation for net uptake CO_2 tracer for forests. The towers shown were determined to contribute significantly to detection of differences in seasonal variation in forest net CO_2 uptake due to afforestation. The lower right panel shows the difference between the control and afforested simulations for the simulate forest surface net CO_2 uptake, i.e. the net uptake CO_2 tracers simulated at the tall towers are attempting to explain the variation seen in this graph. Grey lines indicate $\pm$0.1 ppm which is the accuracy limits for detection of atmospheric CO_2 concentrations at tall tower Angus, therefore variations in forest net uptake CO_2 tracers must be of a magnitude >0.1 ppm to be detectable. Error bars are $\pm$1 standard error for temporal variability only.

Table 3. Hypothetical tall towers used in this study. Provided is the tower latitude longitude coordinates, observation height above the ground level and observation height above sea level.

Tall Tower	Height (m) above ground	Height (m) above sea level	Location
Blackhill	306	555	55.9 N, 3.9 W
Darvel	152	441	55.6 N, 4.3 W
Durris	322	644	57.0 N, 2.4 W
Knockmore	107	462	57.5 N, 3.1 W
Selkirk	238	529	55.6 N, 2.8 W

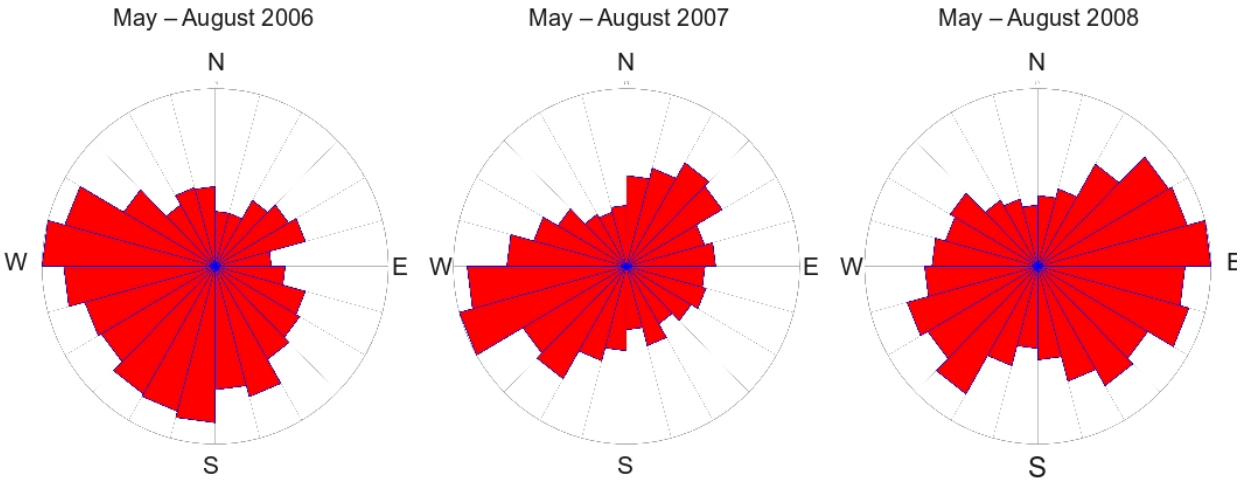

Fig. 5. Interannual comparison of growing season (May, June, July and August) prevailing wind direction at TTA. The wind rose for TTA only is shown as it is indicative of the prevailing wind conditions experiences by all tall towers. The wind rose shows the count of hourly wind directions simulated by WRF-SPA, where the direction indicated is the direction from which the wind is coming.

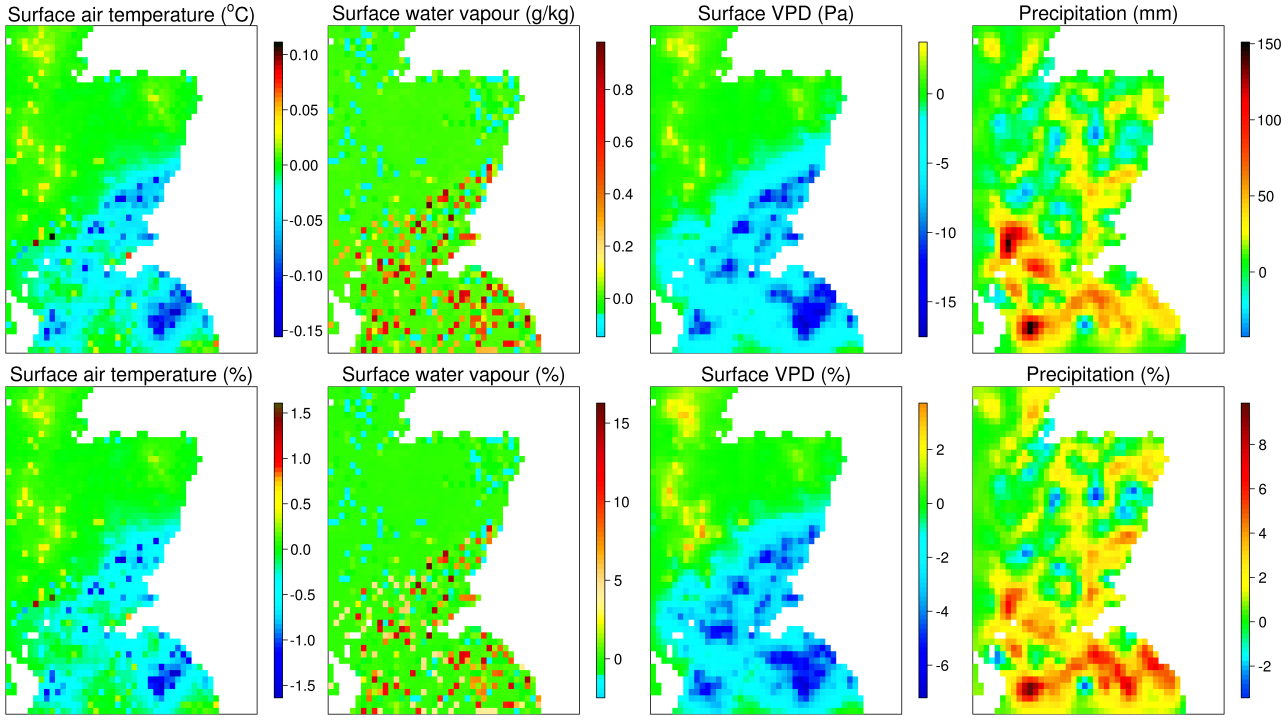

Fig. 6. Shows the spatial distribution of changes to meteorological variables over the land surface due to afforestation. The upper row shows the difference between mean annual values in the appropriate meteorological units. The lower row shows the percentage change for each meteorological variable to indicate the relative size of the impact of afforestation.

Table 4. Summary of R^2 values from regression analysis of variation in surface net CO_2 uptake flux explained by tall tower detected net CO_2 uptake tracers for both the control and afforested simulations. Angus was included separately as it is the only tower currently operational. Tower network provides the best R^2 value achieved from a network constructed from the available hypothetical towers and Angus. Towers used specifies the towers which were statistically selected to be included with a network for detection of a specific ecosystem. The analysis was carried out for the control and afforested simulations to determine if the optimal network changes as a result of afforestation.

	Angus	Tower network	Towers used
Control			
Cropland	0.93	0.96	Blackhill, Darvel, Knockmore
Forest	0.72	0.92	Angus, Darvel, Knockmore
Managed grassland	0.73	0.94	Angus, Knockmore, Selkirk
'Other'	0.77	0.85	Darvel, Blackhill
Afforested			
Cropland	0.91	0.97	Blackhill, Darvel, Durris, Knockmore
Forest	0.78	0.92	Angus, Blackhill, Knockmore
Managed grassland	0.71	0.93	Angus, Knockmore, Selkirk
'Other'	0.78	0.85	Blackhill

Table 5. Summary of R^2 values from regression analysis using net uptake CO_2 tracers detected at tall towers to explain either changes in forest surface net CO_2 uptake flux due to afforestation or seasonal variation in ecosystem surface net CO_2 uptake flux. Only Angus, Blackhill and Knockmore towers were used in this analysis. Angus is included as it is currently operational, Blackhill is included as it was best able to detect changes in forest carbon uptake due to afforestation and Knockmore is used as it was included in the greatest number of networks to detect seasonal variation in the dominant ecosystems. Towers used indicates the combination of tall tower observations that provided the best explanation of surface CO_2 uptake. The analysis is split between the control and afforested simulations to determine if there is an impact on detectability of seasonal variation of ecosystem surface net CO_2 uptake flux due to afforestation.

	Tower network	Towers used
Afforestation detection	0.88	Blackhill
Control		
Cropland	0.95	Knockmore
Forest	0.91	Angus, Blackhill, Knockmore
Managed grassland	0.87	Blackhill, Knockmore
'Other'	0.83	Angus, Blackhill, Knockmore
Afforested		
Cropland	0.95	Knockmore
Forest	0.92	Angus, Blackhill, Knockmore
Managed grassland	0.84	Blackhill, Knockmore
'Other'	0.85	Blackhill

Chapter 5

Discussion

The overall objective of this thesis is two fold. First, the development of a new coupled mesoscale model, WRF-SPA. Second, to use WRF-SPA to explore our understanding of ecosystem relevant information contained within observations of atmospheric CO_2 concentrations.

This thesis is composed of three main research chapters (2, 3 & 4) covering: (i) Development of a coupled atmosphere-ecosystem model that includes a mechanistic representation of the terrestrial ecosystem and its validation against multi-scale datasets, from site level observations to measurements made at tall tower Angus and aircraft profiles. (ii) An investigation of how each ecosystem's contribution to atmospheric CO_2 concentrations vary at seasonal and interannual time scales. (iii) An experimental afforestation to assess the detectability of policy relevant national scale afforestation of Scotland by observations of atmospheric CO_2 concentration made at tall towers.

The WRF-SPA model was used to simulate Northern Britain, with a focus on Scotland for a 7 year period between 2002 and 2008. WRF-SPA output was validated against observations made at multiple spatial and temporal scales. These scales include site level eddy covariance, aircraft profiles and observations made at a tall tower.

Four key hypotheses were addressed in this thesis, leading to the following overall conclusions:

H1 The addition of a mechanistic LSM will lead to improvements in the prediction of surface exchanges compared with the less mechanistic NOAH LSM.

C1 The coupling of SPA and WRF resulted in an improved representation of seasonality of surface fluxes observed at three eddy covariance sites in Scotland.

H2 The mechanistic representation of surface fluxes and feedbacks simulated by SPA will drive realistic atmospheric transport.

C2 WRF-SPA has been shown to simulate realistic atmospheric transport in comparison with multi-annual datasets of atmospheric CO_2 concentrations observed at tall tower Angus and aircraft profiles.

H3 Observations of atmospheric CO_2 concentrations made at tall tower Angus contain information representative of seasonal and interannual variations of ecosystem activity at the national scale.

C3 WRF-SPA simulations indicate that observations made at tall tower Angus contain information that describe a majority of seasonal and interannual variation of ecosystem net CO_2 uptake for the major ecosystem land covers within the observation footprint of the tower. However, interannual variation is poorly detected by observations made at tall tower Angus potentially due to seasonal and interannual variation in prevailing wind conditions.

H4 Afforestation will result in a reduction in atmospheric CO_2 concentration of a magnitude greater than observation detection limits.

C4 An experimental afforestation simulated using WRF-SPA indicated that policy relevant afforestation of Scotland will result in a seasonally varying reduction in atmospheric CO_2 concentrations that is detectable by current observations made at tall tower Angus.

5.1 Scaling from site to regional observations

The coupling and validation of WRF-SPA was described in Chapters 2–4. Validation used multi-annual observations of surface fluxes, aircraft profiles and observations made at tall tower Angus. WRF-SPA validation was done at sites that included an evergreen plantation forest, a grazed grassland and a spring barley cropland. These sites represent the dominant ecosystems in Scotland. Further validation included a comparison with an unmodified WRFv3.2 (hereafter referred to as WRF), which used the NOAH land surface model (LSM), to assess the impact of including SPA. Aircraft observation of atmospheric CO_2, made over central Scotland, and observations of atmospheric CO_2 made at tall tower Angus, provided validation of surface CO_2 exchange at larger spatial scales and atmospheric transport.

WRF-SPA compared well with WRF at hourly time scales with an improved perfor-

mance at seasonal time scales, particularly at the arable cropland site. The comparison with WRF is important as WRF is considered to be one of the best mesocale models available (e.g. Sarrat et al., 2007; Steeneveld et al., 2011), therefore we can infer that WRF-SPA is also comparable to contemporary mesoscale models. WRF-SPA was able to simulate both surface fluxes of heat, water and CO_2 exchange and atmospheric CO_2 concentrations. However the validation process also highlighted areas of improvement in WRF-SPA's representation of evergreen forests and uncultivated vegetation associated to agricultural land.

The land cover map used in WRF-SPA and the lack of a labile carbon pool were identified as issues in the representation of evergreen forests. The land cover map used in WRF-SPA is a modified MODIS map provided with WRF, however the map significantly overestimates the forest cover of Scotland. The MODIS map estimates forest cover to be $\sim$43 % whereas Scotland's actual forest cover is $\sim$17 % (National Forest Inventory, 2011). The overestimate of forest cover contributes to the overestimation of regional CO_2 draw down simulated during summer 2004 (Chapter 2). The MODIS map was used in the thesis due to the time required for the WRF-SPA coupling and model development. However due to the overestimates of forest cover the MODIS map should be replaced with a more realistic representation of UK ecosystem composition, such as the UK land cover map 2007 (LCM 2007, `http://www.ceh.ac.uk/LandCoverMap2007.html`).

Comparison between site level observations of net ecosystem exchange of CO_2 (NEE) and WRF-SPA showed a delay in growth at Griffin forest during the early part of the growing season (Chapter 2). The early season lag is a known issue with the evergreen carbon model in SPA, due to a lack of a labile carbon pool. Labile carbon is accumulated during the course of the growing season and is used for rapid growth of foliage during the spring. Without a labile pool, foliar growth is limited in spring time to carbon available from photosynthesis at that time (Williams et al., 2005). Therefore future development of the SPA model will include addition of a labile carbon pool for evergreen systems.

Investigation of model-data mismatches at tall tower Angus identified increases in er-

ror post harvest in each year simulated here (Chapter 3). The increase in error was associated with senescence and subsequent crop harvest, processes which in SPA are known to be broadly realistic (Sus et al., 2010). However, WRF-SPA does not simulate uncultivated vegetation associated with croplands (e.g. fallow land, hedgerows and forest patches), which in Scotland represent 36 % of agricultural holdings (The Scottish Government, 2012). Uncultivated components of agricultural land have previously been identified as significant stores of carbon (Smith, 2004; Smith et al., 2008). This thesis shows that these components have a significant impact on regional carbon balance at seasonal time scales. The uncultivated components are likely to be perennial systems and critically are less intensively managed than arable crops, resulting in a longer growing season.

As with forest systems, a new high resolution land cover map is required to distinguish fallow land and forest patches to improve the representation of crop systems. Furthermore, if the land cover map was combined with Scottish and UK Government agricultural census data, crop specific parameters could be used, which would likely reduce errors in the simulation of agricultural systems caused by WRF-SPA's simplistic representation of arable systems (with just two crop parameterisations).

Validation against multi-scale observations has been key to the identification of several areas for future model development, highlighting the need to continue collection of these data. Forward running models, such as WRF-SPA, represent the synthesis of our current understanding of both atmospheric and ecosystem processes. Analysis of model-observation errors provide an important opportunity to identify misrepresented or absent processes, both when they occur and which ecosystems are contributing to observations at that time e.g. the identification of increased model-data error which occurs after harvest in every year simulated by WRF-SPA (Chapter 3).

The ability to identify missing processes or errors in representation would be enhanced by using forward running models in conjunction with atmospheric inversion modelling. For example, a forward running model, such as WRF-SPA, can identify time periods of increased error between simulated atmospheric CO_2 concentrations and observations, however it may not always be clear which ecosystems or processes are responsible

for an increase in error. An inverse model could be driven by meteorological fields provided by WRF-SPA and used to determine where the air present in observations came into close contact with the surface. Therefore between both inverse and forward running models it is possible to identify both the timing of model-data errors and the spatial origin of fluxes that resulted in errors, allowing for targeted research.

5.2 Seasonal and interannual variation in ecosystem contributions to observations

Seasonal and interannual variation of ecosystem contributions to tall tower observations were investigated in Chapters 3 & 4. Ecosystem specific tracers of net uptake and net release of CO_2 were used to upscale surface exchange of CO_2 to observations made at tall towers. The CO_2 tracers allowed variation in observations of atmospheric CO_2 concentrations to be related to surface processes.

Observations at tall tower Angus were representative of seasonal and interannual variation of net CO_2 uptake for the dominant ecosystems within the footprint of observations (Chapter 3). The preservation of seasonal and interannual information about ecosystems within the observation footprint of the tall tower is consistent with both observational and atmospheric inversion studies (Gerbig et al., 2009; Vermeulen et al., 2011; Lauvaux et al., 2012a; Miles et al., 2012). Furthermore interannual variation in weather, in particular prevailing wind direction, was found to have a larger impact on interannual variation in simulated observations at tall tower Angus than interannual variation in the simulated land surface, for the years simulated. This highlights the importance of realistic simulation of atmospheric transport when using atmospheric CO_2 to infer surface CO_2 fluxes, such as in atmospheric inversions (Lauvaux et al., 2012a,b).

Seasonal variation of ecosystem specific net CO_2 uptake could be effectively detected through use of a network of tall towers (Chapter 4). As Angus is currently the only tall tower operationally observing atmospheric CO_2 concentrations in Scotland, five telecommunication tall towers (not currently equipped for observing atmospheric CO_2

concentrations) were included as hypothetical observing tall towers. The 'best' network selected varied between ecosystems; moreover the number of times each tower was included in an observing network varied between two and six suggesting that some towers are more broadly useful. A reduced network of three tall towers, including Angus, was analysed, given that it is unlikely that Scottish research infrastructure could support six tall towers. The reduced network was still able to detect the majority of seasonal variation for all ecosystems. This suggests that it is possible to both determine the optimum network for observing ecosystem processes but also that smaller, more practical networks, are able to provide significant information. The towers included in the reduced network were Knockmore, Angus and Blackhill. Knockmore was the tower most frequently included in ecosystem specific observing networks. Angus was included as it is currently operational and second most frequently included in observing networks. Blackhill was included here as Blackhill was best able to detect changes to forest net CO_2 uptake due to simulated policy relevant afforestation of Scotland (Chapter 4).

The approach used in Chapter 4 has a potentially important advantage over the more commonly used atmospheric inversion modelling. Using WRF-SPA, multiple possible networks were assessed using a single forward running simulation, whereas using atmospheric inversion each combination of network design must be separately simulated (e.g. Lauvaux et al., 2012a). However, the approach using WRF-SPA is dependent on the assumption that optimising detection of ecosystem seasonal variation will lead to the same optimum network as determined by atmospheric inversion. This assumption must be tested as part of ongoing development of WRF-SPA. Due to the significant impact of atmospheric transport on inversion estimates, a robust comparison would necessitate the use of identical atmospheric transport between the simulations. A potential means to achieve this would be to couple a Lagrangian particle dispersion model (e.g. STILT) to WRF-SPA, creating WRF-SPA-STILT similar to WRF-VPRM-STILT (Nehrkorn et al., 2010). However given the continued uncertainty in simulated meteorology, multiple different paired simulations using different meteorology is required, in an attempt to quantify transport errors.

5.3 Detection of national scale afforestation

In Chapter 4 the detectability of afforestation of Scotland, by observations of atmospheric CO_2 concentrations made at tall tower Angus and five hypothetical tall towers, was assessed. The five hypothetical towers are telecommunication tall towers which are not currently equipped for measurement of atmospheric CO_2 concentrations. Tall towers Angus, Blackhill, Darvel, Durris and Selkirk are located within the afforested area while Knockmore is located in the North of Scotland.

Tall tower Angus and all hypothetical towers were simulated to be able to detect changes in atmospheric CO_2 concentrations due to afforestation in at least one of the years simulated. Atmospheric CO_2 concentrations simulated at Knockmore showed the smallest magnitude difference due to afforestation. Lower detection is consistent with its location outside of the afforested area. Afforestation leads to a reduction in atmospheric CO_2 concentrations during the peak of the growing season which is consistent with the simulated increase in surface sequestration.

Further analysis determined the 'best' network of tall towers to detect the changes in forest net CO_2 uptake due to afforestation. Tall towers Blackhill and Selkirk were able to explain the majority of variation in forest carbon uptake due to afforestation (R^2 = 0.90). While Angus is not included in the 'best' network, observation made at Angus were simulated to explain a majority of variation in forest carbon uptake due to afforestation (R^2 = 0.75). Blackhill and Selkirk were able to detect a similar amount of variation in forest net CO_2 uptake due to afforestation as both towers combined (R^2 = 0.88 and R^2 = 0.86 respectively). Therefore either tall tower may be an important tower for detection of currently planned afforestation of Scotland.

The 'best' observing network varies depending on both its intended use and changes in ecosystem composition. For example Blackhill was simulated to be best able to detect the simulated afforestation (Chapter 4). Knockmore was most frequently included in ecosystem observing networks, but was least capable of detecting changes to atmospheric CO_2 concentrations due to afforestation. Furthermore the ecosystem specific

networks varied between the control and afforested simulations.

A network consisting of Angus, Blackhill and Knockmore was used to assess the robustness of a realistic compromise network for detection of ecosystem net CO_2 uptake as a whole and of planned afforestation. Angus was included as it is currently operational, Blackhill and Knockmore were included as they were the most important towers for detection of afforestation and ecosystem seasonal variation respectively. The reduced network was able to explain a majority of seasonal variation for all ecosystems simulated by WRF-SPA for both the control and afforested simulations. Blackhill alone significantly contributed to the detection of variation in forest net CO_2 uptake due to afforestation. The 'best' network for detection of seasonal variation varies between ecosystems, however it is possible to explain a majority of seasonal variation using a realistic compromise network, for the simulations here.

The methodology described in Chapter 4 has been used to assess multiple tall tower observing networks, for both specific and general purposes. However, the approach used with WRF-SPA relies on the assumption that optimising detection of ecosystem variation will generate the same network as atmospheric inversion modelling. If this assumption is validated, WRF-SPA becomes a powerful tool for assessing observing networks required for a variety of network purposes.

There are however a number of additional assumptions made in the afforestation experiment. The experiment assumes that the afforested areas are fully grown and there is no parameterisation of forest management practices (for full description see Chapter 4). Therefore the selected best network may only be true for the afforested map used here. Moreover no assessment has been made of how detectable afforestation may be at an earlier stage of forest development. However these assumptions do not undermine the central conclusion that policy relevant afforestation of Scotland should be detectable at a network of tall towers.

The afforestation experiment in Chapter 4 also allowed for an investigation of the impact of afforestation on atmospheric transport and surface meteorological variables. Afforestation was simulated to result in a small reduction in mean annual planetary

boundary layer (PBL) height e.g. due to changes in surface net radiation and partitioning to turbulent fluxes. Simulated afforestation led to increased net radiation and increased partitioning of net radiation to latent heat over sensible heat for the afforested locations.

The increase in latent heat flux is greater than the increase in net radiation of the afforested region, resulting in cooler surface air temperatures and increased surface water vapour content. These changes to surface meteorological variables resulted in a reduction of the surface vapour pressure deficit, in turn driving an increase in mean annual accumulated precipitation of up to 118 mm within the afforested region (Chapter 4). It is important to note that these simulated results are due to land cover change only, as they do not include the effects of climate change or increased atmospheric CO_2 concentrations on ecosystem processes. Furthermore, these results are from a single afforestation simulation and therefore may not be robust. However, the simulated change in surface air temperature is consistent with changes in surface air temperature simulated by more robust global afforestation experiment by Arora and Montenegro (2011). Finally it is also worth noting that the simulated reduction in surface air temperature (mean annual reduction of 0.06°C, maximum reduction of 0.16°C) is more than an order of magnitude less than simulated climate change (an increase of between 2.0°C and 4.5°C by 2100) (IPCC, 2007).

5.4 Conclusions

This thesis set out to answer a number of specific research questions which were addressed through the development, validation and experimental use of the WRF-SPA model.

(Q1) Can WRF-SPA realistically model surface meteorological variables and fluxes across a multi-annual period? We have shown that WRF-SPA can realistically model surface observations at hourly time scales which are comparable to WRF.

(Q2) Does WRF-SPA scale realistically from the surface measurements to regional

scale observations, specifically aircraft profiles? We have shown across multiple years and across seasons that WRF-SPA realistically scales from surface observations to observed atmospheric CO_2 concentration profiles.

(Q3) Does WRF-SPA lead to an improvement in surface fluxes compared to the unmodified WRFv3.2? We have demonstrated that at monthly means WRF-SPA predicts more realistic seasonal behaviour than WRFv3.2.

(Q4) Does WRF-SPA more accurately simulated observed atmospheric CO_2 concentrations compared to a coarse resolution global atmospheric inversion model? WRF-SPA does more accurately simulate observed atmospheric CO_2 concentrations at TTA compared to CTE-CT. WRF-SPA better represents diurnal variation and a reduced bias between simulated atmospheric CO_2 concentrations and observations, particularly during the growing season.

(Q5) Can ecosystem specific CO_2 tracers be used to inform on which ecosystem processes and land covers are responsible for observed variations in atmospheric CO_2 concentrations? Ecosystem specific tracers have been successfully used to infer crops as responsible for a increase in the bias between WRF-SPA simulated atmospheric CO_2 concentrations at observations post harvest each year. Furthermore we have hypothesised that the cause of the error is the lack of a representation of uncultivated components of agricultural land not currently parameterised for in WRF-SPA.

(Q6) Can observations made at TTA detect variation in ecosystem carbon uptake, for ecosystems within the footprint of TTA, at seasonal and interannual time scales? A majority of seasonal variation in surface net CO_2 uptake flux is explained by net uptake CO_2 tracers for each ecosystem. However the amount of variation explained varied considerably between years. Moreover interannual variation was not well captured, potentially due to seasonal and inter annual variation in the prevailing wind direction. However for all other ecosystems interannual variation in atmospheric transport due to year to year variation in weather had a large impact on tall tower observations than interannual variation in surface uptake.

(Q7) Does afforestation result in a change in atmospheric CO_2 concentrations which is detectable by current observations made at a tall tower Angus? Simulated afforestation resulted in a change in total atmospheric CO_2 concentrations of a magnitude which is detectable at Angus and all simulated towers for the majority of years simulated here.

(Q8) Can detection of afforestation on forest net CO_2 uptake be improved through use of an alternate tall tower or a network of tall towers? Detection of afforestation can be improved through the use of a tall tower network, however the Blackhill tower alone is able to detect a similar amount of variation for forest net CO_2 uptake as the selected 'best' network.

(Q9) Can detection of seasonal variation in ecosystem net CO_2 uptake be improved through use of a tall tower network? Detection of seasonal variation in ecosystem net CO_2 uptake can be improved through the use of tall tower networks. The most commonly included towers in the simulated observing networks are Knockmore and Angus. Therefore the maintenance of Angus and the addition of Knockmore to a national observing network are potentially important for future observations of Scotland's carbon balance. As indicated by the majority of seasonal variation being explained by a reduced network of Angus, Blackhill and Knockmore.

(Q10) Does changing Scotland's ecosystem composition, i.e. afforestation, alter atmospheric transport? Afforestation leads to small changes in atmospheric transport through increases in surface net radiation and a change in the Bowen ratio.

(Q11) Does afforestation result in changes to surface meteorological variables? Afforestation leads to a cooling effect in mean annual air temperatures within the afforested region of Scotland. Combined with increases in surface atmospheric water vapour content, due to increased latent heat flux, the vapour pressure deficit was also reduced. The collective effect of these changes was an increase in precipitation broadly within the afforested region.

5.5 Further work

WRF-SPA simulations have identified a number of avenues for future work to improve the representation of key systems such as arable agriculture and forests. WRF-SPA has also shown itself to be a capable model, able to answer a wide range of research questions from investigation of observations and land cover change experiments. This section identifies the key steps for future model development of WRF-SPA, but also further research questions and experimental designs.

5.5.1 Improvements to WRF-SPA

To improve the representation of both forest and agricultural systems the current default MODIS land cover map should be replaced. A replacement land cover map, such as the LCM2007 (`http://www.ceh.ac.uk/LandCoverMap2007.html`) would provide a realistic forest area and spatial distribution. The LCM2007 is extremely high resolution (25 m), providing an improved representation of agricultural land for high resolution simulations or to inform on sub-grid variability for model tiling of the land surface. Accounting for fine scale variation in agricultural systems will allow inclusion of uncultivated components of agricultural land which have been highlighted as important for simulating regional CO_2 exchange at seasonal time scales (Chapter 3). Agricultural census data could also be combined with land cover maps to inform on crop type present, crop rotation and inter crop vegetation further reducing model error.

The addition of a labile carbon pool is needed to improve the representation of evergreen ecosystems in WRF-SPA. Inclusion of a labile carbon pool will correct the delay in phenological development seen in the early growing season for evergreen forests (Chapter 2). This modification requires parameterisations to determine timings for when labile carbon turnover and allocation to foliage should begin, but also when leaf fall should occur. Typically foliar turnover and allocation are determined by the current air temperature relative to a minimum or maximum tolerated temperature for a specific plant functional type (Sitch et al., 2008; Levis et al., 2012). In recent years large multi-

annual databases, such as the CarboEurope network (`www.carboeurope.org/`), have been developed containing a large number of measurements of ecosystem flux and meteorological conditions. Using this data, there is an opportunity to parametrise foliar bud-burst and turnover rates based on a range of environmental drivers from multiple sites using data assimilation (DA) methodologies (e.g. Williams et al., 2005; Sus et al., 2013). DA methods, such as Markov chain Monte Carlo (MCMC) Metropolis Hastings would allow for exploration of the best model to parametrise phenological processes for each ecosystem, including an estimate of uncertainty in the parameterisation (Ziehn et al., 2012).

Critically all land cover parameters could be improved through re-parameterisation via model data fusion techniques. MCMC is a methodology based on Bayesian statistics to solve for model parameters but the method also generates statistically robust uncertainties of both model parameters (e.g. litter turnover rate) and model outputs (e.g. net carbon balance) (Ziehn et al., 2012). Future WRF-SPA development could occur in two phases, first the offline parameterisation of SPA ecosystem parameters using multi-annual multi-site datasets. This data assimilation procedure would provide uncertainties that could be propagated, through model iteration, into the full WRF-SPA model giving uncertainty estimates of atmospheric CO_2 concentrations for validation with aircraft and tall tower based observations. Second, the full WRF-SPA model could be used in conjunction with the data constrained SPA parameters (as priors); these parameters could then be further constrained for regional applicability based on tall tower and aircraft observations. Earth observation (EO) data could also be used to provide large spatial scale information, such as LAI estimates from MODIS. EO could provide validation of the optimised WRF-SPA model or could be fed into the data assimilation itself. Such a data-model fusion framework could achieve something similar to atmospheric inverse modelling, however the approach presented here for WRF-SPA is more mechanistic, potentially highlighting further areas of model development and improved understanding of ecosystem biogeochemical and biogeophysical processes.

5.5.2 Model experiments

There is considerable potential in using WRF-SPA to investigate optimum tall tower observing networks for specific purposes. However prior to any further network analysis with WRF-SPA, the networks generated in Chapter 4 need to be validated in comparison with those generated by atmospheric inversion using the same atmospheric transport as WRF-SPA. If the networks prove to be in agreement, there are a number of possible experiments which could be undertaken with WRF-SPA.

The afforestation experiment could be more fully explored, using multiple possible afforestation distributions, varied composition of forest type and the inclusion of forestry management practices. The ecosystem specific networks varied between the control and afforested simulations indicating an impact of both variation in atmospheric transport but also ecosystem composition. Through multiple simulations, each with a new randomly selected afforestation map, a robust assessment could be made of the most important tall towers for observing Scotland's carbon cycle. An investigation could also be made of the impact of forest type on detectability. Scottish Government policy called for afforestation to be 60 % evergreen plantation and 40 % mixed natural forest (Forestry Commission Scotland, 2009). Due to differences in photosynthetic capacity and management practices, these systems may have a significantly different impact on the regional carbon balance. The afforested proportions could be varied to investigate the optimum composition to maximum carbon sequestration.

The inclusion of forest management practices will allow for a more realistic forest age class composition, particularly if long term simulations are used. Simulating the whole afforestation period, from the current day to 2050, with realistic afforestation rates and management has a number of advantages over the afforestation experiment carried out here. Simulating forest growth will allow an assessment of how detectability changes through the course of the afforestation experiment and how the optimum observing network varies over time. Critically these simulations will allow simulation of soil carbon loss due to disturbance from the afforestation itself. Moreover the effect of climate change on ecosystem processes could also be included.

So far the analysis of tall tower observing networks has considered existing towers as hypothetical locations for observations, with observations assumed to be made at the top of these towers. However no attempt has been made to consider alternate locations which do not have a tower (e.g. the possibility of constructing a new tower). Also, no attempt has been made to investigate the effect of varying observation height. Future work could consider the value added through multiple observation height at an individual location in comparison with single observation heights at multiple locations. Furthermore this analysis could consider increasing observation height as a means to improve observation of surface processes from a limited number of locations. This is particularly relevant given on going development of a differential absorption LiDAR (DIAL) at the University of Edinburgh. The DIAL is capable of collecting near continuous measurements of vertical profiles of atmospheric CO_2 concentrations extending several kilometres into the troposphere.

A synthetic experiment using both WRF-SPA and an atmospheric inversion model could be used to assess the value of the DIAL system over existing tall tower observations. WRF-SPA could generate synthetic DIAL observations to feed into the atmospheric inversion, while at the same time providing a realistic "truth" of surface fluxes used to generate the synthetic observations. An atmospheric inversion model, such as WRF-STILT (Nehrkorn et al., 2010), could then use different combinations of observations from varying heights to determine the error reduction compared to the simulated "truth".

Finally, tall tower Angus has been operational since the end of 2005 to present. In this thesis only three years (2006-2008) of the last seven years of observations were investigated using WRF-SPA. Therefore, a substantial amount of observations remain to investigated, which through comparison with WRF-SPA or other models may yield further ecosystem process knowledge.

References

Arora, V. K. and A. Montenegro, 2011: Small temperature benefits provided by realistic afforestation efforts. *Nat. Geosci.*, **4**, 514–518, doi:10.1038/NGEO1182.

Forestry Commission Scotland, 2009: The Scottish Government's Rational for Woodland Expansion. The scottish government strategy document, Forestry Commission, Edinburgh, EH12 7AT, Scotland.

Gerbig, C., A. J. Dolman, and M. Heimann, 2009: On observational and modelling strategies targeted at regional carbon exchange over continents. *Biogeosciences*, **6**, 1949–1559.

IPCC, 2007: Climate Change 2007: Synthesis Report. Contribution of Working Groups I, II and III to the Fourth Assessment Report of the Intergovernmental Panel on Climate Change. Core Writing Team, Pachauri, R.K. and Reisinger, A. (Eds.)., IPCC, Geneva, Switzerland. pp 104.

Lauvaux, T., A. E. Schuh, M. Bocquet, L. Wu, S. Richardson, N. Miles, and K. J. Davis, 2012a: Network design for mesoscale inversions of CO_2 sources and sinks. *Tellus Ser. B-Chem. Phys. Meteorol.*, **64**, doi:10.3402/tellusb.v64i0.17980.

Lauvaux, T., A. E. Schuh, M. Uliasz, S. Richardson, N. Miles, A. E. Andrews, C. Sweeney, L. I. Diaz, D. Martins, P. B. Shepson, and K. J. Davis, 2012b: Constraining the CO_2 budget of the corn belt: exploring uncertainties from the assumptions in a mesoscale inverse system. *Atmos. Chem. Phys.*, **12**, 337–354.

Levis, S., G. B. Bonan, E. Kluzek, P. E. Thornton, A. Jones, W. J. Sacks, and C. J. Kucharik, 2012: Interactive crop management in the Community Earth System Model (CESM1): Seasonal influences on land-atmosphere fluxes. *J. Clim.*, **25**, 4839–4859.

Miles, N. L., S. J. Richardson, K. J. Davis, T. Lauvaux, A. E. Andrews, T. O. West, V. Bandaru, and E. R. Crosson, 2012: Large amplitude spatial and temporal gradients in atmospheric boundary layer CO2 mole fractions detected with a

tower-based network in the U.S. upper Midwest. *J. Geophys. Res.-Biogeosci.*, **117**, doi:10.1029/2011JG001781.

National Forest Inventory, 2011: National forest inventory woodland area statistics: Scotland. Forestry commission statistical release, Forestry Commission, Edinburgh, EH12 7AT, Scotland.

Nehrkorn, T., J. Eluszkiewicz, S. C. Wofsy, J. C. Lin, C. Gerbig, M. Longo, and S. Freitas, 2010: Coupled weather research and forecasting-stochastic time-inverted lagrangian transport (WRF-STILT) model. *Meteorol. Atmos. Phys.*, **107**, 51–64, doi:10.1007/s00703-010-0068-x.

Sarrat, C., J. Noilhan, A. J. Dolman, C. Gerbig, R. Ahmadov, L. F. Tolk, A. G. C. A. Meesters, R. W. A. Hutjes, H. W. Ter Maat, G. Perez-Landa, and S. Donier, 2007: Atmospheric CO_2 modeling at the regional scale: an intercomparison of 5 meso-scale atmospheric models. *Biogeosciences*, **4**, 1115–1126.

Sitch, S., C. Huntingford, N. Gedney, P. E. Levy, M. Lomas, S. L. Piao, R. Betts, P. Ciais, P. Cox, P. Friedlingstein, C. D. Jones, I. C. Prentice, and F. I. Woodward, 2008: Evaluation of the terrestrial carbon cycle, future plant geography and climate-carbon cycle feedbacks using five Dynamic Global Vegetation Models (DGVMs). *Glob. Change Biol.*, **14**, 2015–2039.

Smith, P., 2004: Carbon sequestration in croplands: the potential in Europe and the global context. *European Journal of Agronomy*, **20**, 229–236, doi:10.1016/j.eja.2003.08.002.

Smith, P., D. Martino, Z. Cai, D. Gwary, H. Janzen, P. Kumar, B. McCarl, S. Ogle, F. O'Mara, C. Rice, B. Scholes, O. Sirotenko, M. Howden, T. McAllister, G. Pan, V. Romanenkov, U. Schneider, S. Towprayoon, M. Wattenbach, and J. Smith, 2008: Greenhouse gas mitigation in agriculture. *Philos. Trans. R. Soc. B-Biol. Sci.*, **363**, 789–813, doi:10.1098/rstb.2007.2184.

Steeneveld, G. J., L. F. Tolk, A. F. Moene, O. K. Hartogensis, W. Peters, and A. A. M. Holtslag, 2011: Confronting the WRF and RAMS mesoscale models with innova-

tive observations in the Netherlands: Evaluating the boundary layer heat budget. *J. Geophys. Res.-Atmos.*, **116**, doi:10.1029/2011JD016303.

Sus, O., M. W. Heuer, T. P. Meyers, and M. Williams, 2013: A data assimilation framework for constraining upscaled cropland carbon flux seasonality and biometry with modis. *Biogeosciences*, **10**, 2451–2466, doi:10.5194/bg-10-2451-2013.

Sus, O., M. Williams, C. Bernhofer, P. Beziat, N. Buchmann, E. Ceschia, R. Doherty, W. Eugster, T. Gruenwald, W. Kutsch, P. Smith, and M. Wattenbach, 2010: A linked carbon cycle and crop developmental model: Description and evaluation against measurements of carbon fluxes and carbon stocks at several European agricultural sites. *Agr. Ecosyst. Environ.*, **139**, 402–418.

The Scottish Government, 2012: Scottish agricultural census. A national statistics publication for scotland: Agricultural series, The Scottish Government.

Vermeulen, A. T., A. Hensen, M. E. Popa, W. C. M. van den Bulk, and P. A. C. Jongejan, 2011: Greenhouse gas observations from Cabauw Tall Tower (1992-2010). *Atmos. Meas. Tech.*, **4**, 617–644, doi:10.5194/amt-4-617-2011.

Williams, M., P. A. Schwarz, B. E. Law, J. Irvine, and M. Kurpius, 2005: An improved analysis of forest carbon dynamics using data assimilation. *Glob. Change Biol.*, **11**, 89–105.

Ziehn, T., M. Scholze, and W. Knorr, 2012: On the capability of Monte Carlo and adjoint inversion techniques to derive posterior parameter uncertainties in terrestrial ecosystem models. *Glob. Biogeochem. Cycle*, **26**, doi:10.1029/2011GB004185.

Appendix A

WRFv3.2-SPAv2: Development and validation of a coupled ecosystem-atmosphere model, scaling from surface fluxes of CO_2 and energy to atmospheric profiles

This appendix provides additional information regarding the coupling between WRF and SPA, creating WRF-SPA, and further description of the CO_2 preprocessor programs. The preprocessors are used to input Carbon Tracker 3D CO_2 mixing ratios, ocean and anthropogenic flux maps to provide WRF-SPA with initial and boundary conditions for CO_2. The key subroutines are highlighted in the text, while minor changes are presented in a list format including the file path and line number. Finally the differences between running WRF-SPA an unmodified WRFv3.2 will be described.

The source code for WRF-SPA and the two CO_2 preprocessors used with WRF-SPA are provided on the attached CD. All cited subroutines are provided with a file path location referenced to the root directory of the CD. The source code has been extensively annotated and where modifications have been made to the WRF model the notation "TLS:" has been added.

As part of the coupling process the SPA model was upgraded to include both new and improved parameterisations. These modifications have been incorporated into an offline version of SPA which is freely available for download from the SPA subversion repository under the "iterative_canopy" branch (`https://sourced.ecdf.ed.ac.uk/projects/geos/SPA/browser/branches/iterative_canopy`).

A.1 Coupling between WRF and SPA

A direct coupling approach was used in the formation of WRF-SPA, resulting in a fully integrated modelling system. A direct coupling allowed SPA to make use of the existing WRF spatial memory for storing, processing and outputting spatially distributed surface states and fluxes.

SPA specific states and variable are declared within the WRF model framework through the existing registry system. These variables are added to the WRF registry via a new file, registry.co2, which is called by WRF during the compilation process. The new variables are passed down the default calling path to the surface_driver() which is responsible for controlling land surface processes within WRF. SPA is called from the

surface_driver() through lsm_spa(), a modified version of the original SPA top level SPA_DALEC programme file. lsm_spa() has been extensively modified to sit as a module file within WRF and is responsible for controlling the exchange of variables between the WRF and SPA models. lsm_spa() remains the top level control subroutine for SPA, being responsible for loading SPA plant and soil parameters, calling the SPA model itself and preparation of SPA outputs to WRF.

The majority of the coupling interface occurs in two subroutines, update_SPA() and update_WRF(). These subroutines load spatially distributed state variables and meteorological data from the WRF spatial grid to SPA. These subroutines are also responsible for the conversion of WRF generated meteorological inputs into appropriate drivers for SPA and for converting SPA outputs into surface diagnostic variables and fluxes required by WRF. For example, WRF transports atmospheric CO_2 as kg CO_2 per kg dry air, whereas SPA requires atmospheric CO_2 in part per million by volume. Furthermore, these subroutines also carry out sanity checks of both WRF inputs and SPA outputs to facilitate debugging.

To minimize the number modifications to WRF, SPA is initialised during the first model time step (i.e. the first time SPA is called by WRF) rather than as part of the pre-existing WRF initialisation procedures. SPA state initialisation is dependent on the vegetation and soil cover types, which is determined in INIT() for all ecosystem except arable cropland. Arable crops are initialised separately in crop_init() due to the large number of unique parameters required for the crop development model. Due to the large number of model parameters used in SPA, parameters are re-loaded at each time step rather than stored in the WRF-SPA memory. Parameter input is carried out in param_load() and crop_param(), again distinguishing between cropland and other ecosystems due to the parameter requirements for crops. It is possible to concatenate all four subroutines using conditional statements, however separate subroutines were maintained to preserve greatest similarity with the original SPA code for subsequent updates.

WRF was modified to accommodate SPA's multi-layer canopy and high vertical resolution representation of the soil. New canopy layer (ab) and deep soil (core) dimensions were added to the model registry, registry.dimspec. Critically the subroutine

responsible for the initialisation of the simulated soil temperature and moisture profiles, init_soil_depth_2() was modified to hard code SPA's 20 soil layers with 10 cm thickness.

A.1.1 Modified subroutines

This section contains two lists relating to modifications made for WRF-SPA. The first relates to the location of subroutines mentioned in the coupling description above and the second contains the location of minor code modifications made to WRF for the WRF-SPA coupling.

A.1.1.1 Location of references subroutines

registry.co2: /WRF-SPA/WRF-SPAv1.8/Registry/registry.co2

registry.dimspec: /WRF-SPA/WRF-SPAv1.8/Registry/registry.dimspec

surface_driver(): /WRF-SPA/WRF-SPAv1.8/phys/module_surface_driver.F

lsm_spa(): /WRF-SPA/WRF-SPAv1.8/phys/SPA_DALEC.F

update_SPA(): /WRF-SPA/WRF-SPAv1.8/phys/spa_COUPLE.F

update_WRF(): /WRF-SPA/WRF-SPAv1.8/phys/spa_COUPLE.F

INIT(): /WRF-SPA/WRF-SPAv1.8/phys/spa_io_spa_dalec.F

crop_init(): /WRF-SPA/WRF-SPAv1.8/phys/spa_io_spa_dalec.F

param_load(): /WRF-SPA/WRF-SPAv1.8/phys/spa_COUPLE.F

crop_load(): /WRF-SPA/WRF-SPAv1.8/phys/spa_COUPLE.F

init_soil_depth_2(): /WRF-SPA/WRF-SPAv1.8/share/module_soil_pre.F

A.1.1.2 List of minor modifications

WRF-SPA/WRF-SPAv1.8/Registry/registry.co2: a new registry file has been added, contains definitions of new CO_2 related fluxes and mixing ratios. Additional SPA variable have also been added. New namelist variables have also been added to define the number of canopy layers, crop spin up and the level of detail in error messages used for debugging.

WRF-SPA/WRF-SPAv1.8/Registry/Registry.EM_CHEM: Line 438, "include registry.co2" inserted to add new variables and states.

WRF-SPA/WRF-SPAv1.8/Registry/registry.dimspec: Line 44, new dimension added (30day) for calculating rolling mean temperature used in crop phenology. New dimension wetting layers (wet) is used by SPA to define sections of soil profile which have water remaining in them.

WRF-SPA/WRF-SPAv1.8/phys/Makefile: Line 102, SPA subroutine files and coupling specific files have been added to the makefile for compilation. The prefix 'spa' is used to distinguish these files, except the primary control SPA_DALEC module. Line 230, dependencies for SPA files have been declared.

WRF-SPA/WRF-SPAv1.8/dyn_em/Makefile: Line 306, dependency added to module_force_scm.F for module_first_rk_step_part1.F, not present in WRFv3.2. However it is unknown why this dependency is needed to compile WRF-SPA.

WRF-SPA/WRF-SPAv1.8/dyn_em/start_em.F: Line 1030, conditional statement to prevent initialisation of default atmospheric chemistry when chem_opt == 99.

WRF-SPA/WRF-SPAv1.8/dyn_em/module_first_rk_step_part1.F: This module is responsible for calling a number of WRF model components including the surface_driver(). Line 473, SPA specific and atmospheric CO_2 variables have also been added to the surface_driver() subroutine, variables are passed with reference to the grid (allocatable type) which defines the WRF memory.

WRF-SPA/WRF-SPAv1.8/phys/module_surface_driver.F/: Multiple lines with prefix "TLS:", SPA specific variables added to subroutine call and declared within module. lsm_spa() call replaces NOAH LSM call as the default LSM model.

WRF-SPA/WRF-SPAv1.8/chem/chem_driver.F: Line 426, CASE argument for CO2_TRACER has been added, enables calls to the subroutines responsible for CO_2 tracer transport. Line 684, added calls to subroutines co2_source and co2_biogenic which are responsible for exchange of CO_2 between the surface and the lower atmosphere. Check point set to ensure that namelist option chem_opt==99 has been selected allowing simulation of CO_2 transport. Line 855, case statement has been added to include the CO2_TRACER, this prevents the aerosol optical properties from being calculated which are not needed. Line 881 and 1062, case statement have been added photolysis rates and hydrolysis rates respectively.

WRF-SPA/WRF-SPAv1.8/chem/module_chem_utilities.F: Contains subroutines responsible for actual CO_2 exchange between the surface and the lowest atmospheric model level.

WRF-SPA/WRF-SPAv1.8/chem/module_input_chem_data.F: Line 1907, hard coded model options to ensure that WRF-SPA always searches for CO_2 fields from wrfbdy_d01 file. Line 2833, 'get_last_gas' set to zero to prevent error when case(CO2_TRACER) is true.

WRF-SPA/WRF-SPAv1.8/chem/chemics_init.F: Line 187, conditional statements which prevent the use of the MODIS land cover map with WRF chemistry modules has been commented out. This is appropriate as all chemistry options except those used for transporting CO_2 have been turned off. Line 287, conditions calling ozone functions has been turned off.

WRF-SPA/WRF-SPAv1.8/share/module_check_a_mundo.F: Line 120, conditional statement to check that the 20 soil layers required by SPA have been provided.

WRF-SPA/WRF-SPAv1.8/share/solve_interface.F: Line 46, conditional statement which calls chem modules to begin CO_2 emission and transport if conditional statement chem_opt == 99 is true.

WRF-SPA/WRF-SPAv1.8/main/nup_em.F: Line 635, addition of warning flag to ensure that simulations which were initialised with CO_2 present in the atmosphere are also present in a restarted simulation.

WRF-SPA/WRF-SPAv1.8/main/real_em.F: Line 441, check point added to prevent real.exe from running with any chemistry option that does not enable the CO_2 tracers in chem_opt==99. Line 509, A warning message that CO_2 has not been initialised has also been added.

A.2 Differences running WRF-SPA and WRFv3.2

WRFv3.2 provides the model framework into which SPA was coupled. As a result the operation of WRF-SPA is nearly identical to that of WRFv3.2. However there are a number of differences in the operation of WRF-SPA to accommodate the addition of SPA and the provision of atmospheric CO_2 initial and lateral boundary conditions.

A.2.1 Changes to namelist.input

Several namelist.input options are required to have specific values to allow WRF-SPA to function. There are also a number of new SPA specific options which have been added and are detailed below.

In WRF-SPA, as with WRFv3.2, separate time steps can be specified for the simulation of atmospheric transport and other model components, such as planetary boundary layer (PBL) processes which includes the land surface exchange. SPA is designed to work at a time step which is exactly divisible into one hour, therefore requiring both the simulated atmospheric transport and PBL time steps to be exactly divisible into one hour. While these time steps can hold different values from each other, the time step for atmospheric transport must exactly divide into the PBL time step to prevent errors developing in SPA's internal time management. These conditions must be met for each model domain simulated.

The namelist.input options below are those which are specific to WRF-SPA or have

fixed values:

num_soil_layers = 20: the default number of soil layers used in SPA.

num_canopy_layers = 10: the default number of canopy layers used in SPA.

spa_forest_man = 0: 2 = loads replacement land cover map used in afforestation experiment.

spa_crop_spin_flag = 0: 1 = initiates first crop sowing immediately upon beginning simulation rather than, 0 = waiting till environmentally defined sowing date.

co2_flux_update_freq = 30: time in minutes between WRF-SPA updates the anthropogenic and ocean flux values.

spa_debug = 0: alters the amount of debug output that SPA generates. 0 = fail messages only, 1 = all debug code, 2 = energy balance code (inc. light subs), 3 = leaf subroutines, 4 = soil profile.

A.2.2 Initialisation differences between WRFv3.2 and WRF-SPA

The process for compiling WRF-SPA and running the model are nearly identical to WRFv3.2. There are additional stages required to provide WRF-SPA with CO_2 fields for initial and lateral boundary conditions, and CO_2 surface flux maps. The basic approach to compiling, preparing and running WRF-SPA are described below.

Compile WRF-SPA and run real.exe as detailed in the WRFv3.2 users guide. Empty fields for initial and lateral boundary conditions for atmospheric CO_2 are generated by real.exe. The first preprocessor, co2_wrf described in section A.3.1, should now be executed to downscale global atmospheric CO_2 fields to the WRF-SPA simulation domain and load them into the existing initial and boundary condition files. The preprocessor requires input for the time period of the simulation and file paths to the real.exe generated files wrfinput_d01, wrfbdy_d01 and to the global field CO_2 data. The CO_2 preprocessor is designed to extract all other information needed to carry out the prepa-

ration of CO_2 fields for WRF-SPA from the files generated by real.exe.

The second CO_2 preprocessor, fluxes_co2 described in section A.3.2, is responsible for downscaling global field surface fluxes of anthropogenic and ocean CO_2 to the WRF-SPA domain. Unlike co2_wrf, the downscales fluxes are output into newly created files which WRF-SPA is able to read in automatically based on the provided 'co2_flux_update_freq' set in the namelist.input. The preprocessor requires input of the time period for the simulation and file paths to the real.exe generated files wrfinput_d01 and to the global field CO_2 flux data. The CO_2 preprocessor is designed to extract all other information needed to carry out the preparation of CO_2 flux maps for WRF-SPA from the files generated by real.exe.

Once the CO_2 preprocessors have created the CO_2 fields WRF-SPA is ready to be operated as specified in the WRFv3.2 user guide. All WRF-SPA relevant outputs added via the registry.co2 have been set to be output to the default WRF output files or to auxiliary output2. The file name for auxiliary output2 is specified in the namelist.input (e.g. auxhist2_outname = "wrf_spa_out_d<domain>_<date>_p1") at domain specified intervals (e.g. auxhist2_interval = 60,60).

A.3 CO_2 preprocessor

WRFv3.2 is not designed to simulate the exchange or transport of CO_2 between the atmosphere and the surface. Atmospheric fields of CO_2 have have been added to allow for transport of CO_2 and SPA provides surface exchange of biospheric CO_2, however there remains a need for a mechanism to downscale global 3D CO_2 fields to provide initial and lateral boundary conditions for WRF-SPA. In addition, as SPA only simulates biospheric CO_2 exchange, anthropogenic emissions due to fossil fuel combustion and ocean exchange are included as flux maps. Two CO_2 preprocessors have been developed to downscale CO_2 fields to the WRF-SPA domain.

The programmes are written in Fortran 90. One programme deals with calculation of initial and lateral boundary conditions. The second programme determines the surface

flux maps for anthropogenic and oceanic CO_2 exchange.

A.3.1 Initial and lateral boundary conditions

Initial (IC) and lateral boundary conditions (LBC) are downscaled from Carbon Tracker Europe (CTE, `http://www.carbontracker.eu/`) global atmospheric CO_2 fields, at 1°x 1° resolution fields with a 3 hour interval period. The downscaled variables were input into the standard WRF initial (IC) and lateral boundary condition (LBC) files wrfinput_d01, wrfinput_d02 and wrfbdy_d01. This approach removed the need to develop new input / output system specifically for atmospheric CO_2.

The downscaling occurs in two stages, first in the horizontal and second in the vertical. Horizontal downscaling uses a 4 point weighted mean based on the longitude / latitude co-ordinates of the CTE global fields and WRF-SPA domain. Horizontal downscaling was carried out at each atmospheric level in the CTE global fields. Vertical downscaling uses linear interpolation between CTE atmospheric levels to those required by WRF-SPA. Air pressure values are provided with CTE CO_2 fields and are also present in WRF initial condition input files generated by the WRF preprocessor (WPS). Atmospheric CO_2 was interpolated to the WRF-SPA vertical atmospheric heights based on air pressure between CTE and WRF-SPA initial conditions providing common points of reference.

WRF-SPA uses 12 atmospheric CO_2 fields including total atmospheric CO_2, "forcings only" CO_2 and ecosystem specific tracers representing net release and net uptake of CO_2 (see Chapter 2, 3 and 4 for further information). IC and LCB are only assigned for total atmospheric CO_2 and "forcings only" CO_2, as these pools, respectively, represent the prediction of actual atmospheric CO_2 and transport CO_2 originating from boundary conditions only (i.e. no exchange with the biosphere). LBC for the outer domain have been set with zero inflow and zero-gradient outflow for all CO_2 fields, except total atmospheric CO_2 and "forcings only" CO_2 (Chapter 2), to allow for tracers to easily leave the domain and prevent artificial influx from outside the domain.

The source code, written in Fortran 90 for the IC and LCB preprocessor can be found on the attached CD.

File path: /WRF-SPA/co2_preprocessor/lcb_co2_input/co2_wrf

A.3.2 Anthropogenic emissions and ocean flux of CO_2

Anthropogenic CO_2 emissions and ocean CO_2 exchange are not simulated by the SPA land surface model, these fluxes are provided as inputs from CTE flux maps. As with the IC and LBC, surface fluxes were available at 1°x 1° horizontal resolution at 3 hour intervals. Surface fluxes are calculated as rates and added to the lowest atmospheric layer in WRF-SPA.

Unlike IC and LBC variables which are added to the pre-existing WRF initial and boundary condition files, CO_2 fluxes were output to newly generated files. The spatially explicit surface flux values are read by WRF-SPA, stored within the WRF-SPA memory and used at each model time step. The flux values are held constant between each update from the surface flux input files.

CTE global surface flux fields are downscaled to the WRF-SPA domain using a 4 point weighted mean based on the latitudinal and longitudinal co-ordinates provided in each the CTE and WRF-SPA domains. This approach results in a flux map which concentrates emissions closer to the emissions centre reducing with distance from the centre point. This is analogous to high emissions in a city centre to lower emissions as you approach urban limits. The 4 point weighted mean approach does not conserve mass between the CTE estimates and the downscaled estimates. However the error between the downscaled values and CTE estimate is of a similar magnitude to that of the uncertainty ascribed to CTE estimates (data not shown). Downscaling based on nearest neighbour is also available. The code has been designed to allow for subsequent addition of further downscaling methodologies.

The source code is available on the attached CD is fully commented to allow for subsequent development.

File path: /WRF-SPA/co2_preprocessor/surface_fluxes_co2_eachstep/fluxes_wrf

Appendix B

WRFv3.2-SPAv2: Model parameters

WRF-SPA: supplementary material

T. L. Smallman, J. B. Moncrieff and M. Williams
School of GeoScience,
University of Edinburgh,
Edinburgh, EH9 3JN

June 11, 2013

WRF-SPA uses parameters which represent the dominant UK ecosystems (evergreen forest, deciduous forest, mixed forest, managed grassland, grassland, arable cropland and urban). In this supplementary material these parameters are detailed along with further information as to their origin. The parameters used are broadly consistent with previous SPA studies, derived from a combination of site specific and data assimilation studies.

Table 1 and Table 2 provide ecosystem specific variables for the parameters that are broadly common to all ecosystems, while Table 3 details arable crop specific parameters. Table 4 and Table 5 provide descriptions of each parameters used by WRF-SPA.

Table 1: Vegetation parameters required by WRF-SPA for evergreen forest, deciduous forest, mixed forest and managed grassland. All parameters are consistent with those found in previous SPA papers. Evergreen parameters are derived from Williams et al. [2001], O'Neill et al. [2002], Medlyn et al. [2005], Fox et al. [2009] and deciduous forest parameters are derived from Williams et al. [1996], Waring et al. [1998], Fox et al. [2009]. Mixed forest parameters are a modified version of the evergreen parameter set. Managed grassland parameters are derived from Williams et al. [2000], Fox et al. [2009] and modified with information from a managed grassland at Easter Bush and Wullschleger [1993]. '-' indicate that a parameter is not used in the representation of a given land cover type. Two values are given for characteristic leaf dimension for ecosystem covers which include needle leaf vegetation. The first values is needle width and the second is cone diameter.

Parameter	Unit	Evergreen forest	Deciduous forest	Mixed forest	Managed grassland
Canopy height	m	12	15	12	0.3
Average foliar N conc.	gN m^{-2}	2.25	2.1	2.25	1.0
Minimum leaf water potential	MPa	-1.7	-2.5	-2.0	-1.9
Characteristic leaf dimension	m	0.002, 0.045	0.08	0.002, 0.045	0.01
Water use efficiency	-	1.0007	1.007	1.0007	1.007
Leaf capacitance	mmol m^{-2} leaf area MPa^{-1}	4000	8000	4000	2000
Stem Conductivity	mmol m^{-1} s^{-1} MPa^{-1}	20	30	20	5
Root resistivity	MPa s g $mmol^{-1}$	20	20	20	10
Ratio of Vcmax to foliar N	μmolC gN^{-1} $s^{-}1$	21.3	14	17.5	43
Ratio of Jmax to foliar N	μmolC gN^{-1} $s^{-}1$	44.4	36	47	85
Leaf carbon per area	gC m^{-2}	120	55	114	30
Max root depth	m	1.4	1.5	1.4	0.6
Root depth coefficient	gC m^{-2}	100	100	100	50
Root radius	m	0.0005	0.0001	0.0005	0.0001
Emissivity		0.96	0.96	0.96	0.96
Foliar PAR reflectance	fraction	0.11	0.11	0.11	0.16
Foliar PAR transmittance	fraction	0.16	0.16	0.16	0.16
Foliar NIR reflectance	fraction	0.16	0.43	0.16	0.43
Foliar NIR transmittance	fraction	0.26	0.26	0.26	0.26
Soil PAR reflectance	fraction	0.033	0.033	0.033	0.033
Soil NIR reflectance	fraction	0.023	0.023	0.023	0.023
Litter decomposition rate	$hour^{-1}$	$4.0x10^{-6}$	$1.5x10^{-7}$	$4.0x10^{-6}$	$4.0x10^{-6}$
Soil heterotropic temperature response coefficient	-	0.0693	0.0693	0.0693	0.0693
GPP allocation to autotrophic respiration	fraction	0.47	0.32	0.47	0.47
NPP allocation to foliage	fraction	0.30	0.70	0.32	0.50
NPP root	fraction	0.43	0.457	0.43	0.75
Foliage turn over	$hour^{-1}$	$6.4x10^{-5}$	$2.3x10^{-3}$	$1.0x10^{-4}$	$3.3x10^{-4}$
Structural turn over	$hour^{-1}$	$2.5x10^{-6}$	$2.5x10^{-6}$	$2.5x10^{-6}$	$2.5x10^{-4}$
Root turn over	$hour^{-1}$	$1.0x10^{-4}$	$2.8x10^{-4}$	$1.4x10^{-4}$	$2.6x10^{-4}$
Leaf loss to litter	fraction	-	0.45	-	-
Litter mineralisation	$hour^{-1}$	0.001	0.001	0.001	0.001
SOM mineralisation	$hour^{-1}$	$1.0x10^{-6}$	$1.0x10^{-6}$	$1.0x10^{-6}$	$1.0x10^{-6}$
Labile turn over	$hour^{-1}$	-	$5.0x10^{-3}$	-	-
Labile cost	$hour^{-1}$	-	0.129	-	-
Autotrophic turnover	$hour^{-1}$	0.07	0.07	0.07	0.07
Growing degree days	$^{\circ}C$ day^{-1}	-	250	-	-
Minimum temperature	$^{\circ}C$	-	5	-	-
Max foliar carbon	gC m^{-2}	-	270	-	-

Table 2: Vegetation parameters required by WRF-SPA for grassland, upland, arable crop and urban. All parameters are consistent with those found in previous SPA papers. Grassland is a modified version of the managed grassland parameterisation and adjusted reflectance similar to JULES [Best et al., 2011]. Upland parameters are derived from Williams et al. [2000], Fox et al. [2009]. Crop parameters for both winter wheat and winter barley are from Sus et al. [2010] with updated reflectance values from Nagler et al. [2003]. Vcmax and Jmax coefficients and leaf carbon per area are for winter wheat / winter barley. Urban cover is assumed to be a low density evergreen forest with a reduced emissivity. Emissivity was assumed to be the same as the value used by the default WRFv3.2 land surface scheme. '-' indicate that a parameter is not used in the representation of a given land cover type.

Parameter	Unit	Grassland	Upland	Crop	Urban
Canopy height	m	0.5	0.3	1.2	12
Average foliar N conc.	gN m^{-2}	1.0	2.0	1.0	1.0
Minimum leaf water potential	MPa	-1.9	-1.5	-1.9	-1.7
Characteristic leaf dimension	m	0.01	0.01	0.013	0.04
Water use efficiency	-	1.007	1.0007	1.007	1.0007
Leaf capacitance	mmol m^{-2} leaf area MPa^{-1}	2000	2000	2000	4000
Stem Conductivity	mmol m^{-1} s^{-1} MPa^{-1}	5	2	5	30
Root resistivity	MPa s g $mmol^{-1}$	10	200	10	20
Ratio of Vcmax to foliar N	μmolC gN^{-1} $s^{-}1$	43	20.8	64/79	17.5
Ratio of Jmax to foliar N	μmolC gN^{-1} $s^{-}1$	83	47.9	137/157	47
Leaf carbon per area	gC m^{-2}	30	120	19.5/15	45
Max root depth	m	0.6	0.4	1.5	1.6
Root depth coefficient	gC m^{-2}	50	100	50	100
Root radius	m	0.0001	0.0001	0.0001	0.0001
Emissivity		0.96	0.96	0.96	0.88
Foliar PAR reflectance	fraction	0.10	0.10	0.11	0.20
Foliar PAR transmittance	fraction	0.16	0.16	0.16	0.16
Foliar NIR reflectance	fraction	0.58	0.58	0.38	0.50
Foliar NIR transmittance	fraction	0.26	0.26	0.26	0.26
Soil PAR reflectance	fraction	0.033	0.033	0.033	0.033
Soil NIR reflectance	fraction	0.023	0.023	0.023	0.023
Litter decomposition rate	$hour^{-1}$	$1.5x10^{-7}$	$1.0x10^{-7}$	$2.8x10^{-5}$	$4.0x10^{-4}$
Soil heterotropic temperature response		0.0693	0.0693	0.0693	0.0693
GPP allocation to autotrophic respiration	fraction	0.46	0.50	0.44	0.47
NPP allocation to foliage	fraction	0.60	0.70	varied by DS	0.32
NPP root	fraction	0.60	0.70	varied by DS	0.43
Foliage turn over	$hour^{-1}$	$2.3x10^{-3}$	$2.0x10^{-4}$	varied by DS	$1.5x10^{-4}$
Structural turn over	$hour^{-1}$	$2.3x10^{-3}$	$2.0x10^{-5}$	varied by DS	$2.5x10^{-6}$
Root turn over	$hour^{-1}$	$2.8x10^{-4}$	$2.0x10^{-5}$	varied by DS	$2.8x10^{-4}$
Leaf loss to litter	fraction	-	-	-	-
Litter mineralisation	$hour^{-1}$	0.001	0.0001	$2.8x^{-4}$	0.001
SOM mineralisation	$hour^{-1}$	$1.0x10^{-6}$	$1.0x10^{-6}$	$2.28x10^{-6}$	$1.0x10^{-6}$
Labile turn over	$hour^{-1}$	-	-	$6.25x10^{-3}$	-
Labile cost	$hour^{-1}$	-	-	0.21	-
Autotrophic turnover	$hour^{-1}$	0.07	0.07	0.07	0.07
Growing degree days	$^{\circ}C$ day^{-1}	-	-	125	-
Minimum temperature	$^{\circ}C$	-	-	-	-
Max foliar carbon	gC m^{-2}	-	-	-	-

Table 3: Winter arable crop specific parameters required by WRF-SPA, the parameters are common to both winter wheat and winter barley. All other parameters are consistent with those described in Sus et al. [2010], except litter reflectance values which are taken from Nagler et al. [2003].

Parameter	Unit	Value
Post harvest leaf residue	fraction	0.1
Post harvest stem residue	fraction	0.1
DR coefficient pre-flowering	day^{-1}	0.04
DR coefficient post-flowering	day^{-1}	0.035
Minimum development temperature	°C	0
Optimum development temperature	°C	24
Maximum development temperature	°C	35
Minimum temperature for vernalization	°C	-1.3
Optimum temperature for vernalization	°C	4.9
Maximum temperature for vernalization	°C	15.7
Vernalization days	days	22.5
Self shading LAI	m^2m^{-2}	4
Maximum rate of self shading turnover	$hour^{-1}$	0.00125
Critical photoperiod	hours	8.25
Photoperiod sensitivity	-	0.25
Litter PAR reflectance	fraction	0.30
Litter NIR reflectance	fraction	0.50

Table 4: Description of vegetation parameters required by WRF-SPA.

Parameter	Unit	Description
Canopy height	m	Height of canopy top
Average Foliar N conc.	gN m^{-2}	Average foliar nitrogen concentration
Minimum leaf water potential	MPa	Minimum leaf water potential tolerated
Characteristic leaf dimension	m	Leaf diameter and / or cone diameter
Water use efficiency	-	Regulates maximum possible stomatal conductance
Leaf capacitance	mmol m^{-2} leaf area MPa^{-1}	Leaf water storage capacity
Stem Conductivity	mmol m^{-1} s^{-1} MPa^{-1}	Plant stem conductivity for water
Root resistivity	MPa s g $mmol^{-1}$	Root hydraulic resistance to water
Max root depth	m	Maximum soil depth that roots can reach
Root depth coefficient	gC m^{-2}	Root mass required to reach 50 % of max depth
Root radius	m	Average root radius
Foliar PAR reflectance	fraction	Leaf photosynthetically active radiation reflectance
PAR transmittance	fraction	Leaf photosynthetically active radiation transmittance between canopy layers
Foliar NIR reflectance	fraction	Leaf near infra-red radiation reflectance
NIR transmittance	fraction	Leaf near infra-red radiation transmittance between canopy layers
Soil PAR reflectance	fraction	Soil surface photosynthetically active radiation reflectance
Soil NIR reflectance	fraction	Soil surface near infra-red radiation reflectance
Litter decomposition rate	$hour^{-1}$	Litter decomposition rate constant
Soil heterotropic temperature response		Adjusts heterotropic respiration based on mean daily temperature (Q10 = 2.0)
GPP allocation to autotrophic respiration	fraction	Fraction of gross primary productivity allocated for respiration for plant maintenance
NPP allocation to foliage	fraction	Net primary productivity allocated to foliage
NPP root	fraction	Net primary productivity allocated to roots after allocation to foliage
Foliage turn over	$hour^{-1}$	Hourly turnover rate of foliage carbon
Structural turn over	$hour^{-1}$	Hourly turnover rate for structural / wood carbon
Root turn over	$hour^{-1}$	Hourly turnover rate for fine root carbon
Leaf loss to litter	fraction	Fraction of foliar turn over that goes to litter, remainder to labile
Litter mineralisation	$hour^{-1}$	Hourly mineralisation rate for soil organic carbon
SOM mineralisation	$hour^{-1}$	Hourly mineralisation rate for soil organic carbon
Labile turn over	$hour^{-1}$	Hourly turnover rate for labile carbon
Labile cost	$hour^{-1}$	Fraction of labile carbon allocated to foliage lost through respiration
Autotrophic turnover	$hour^{-1}$	Hourly turnover rate for carbon allocated to plant maintenance
Growing degree days	°C day^{-1}	Threshold of accumulated daily mean air temperatures for development
Minimum temperature	°C	Temperature threshold below which foliage turnover begins
Max foliar carbon	gC m^{-2}	Maximum total foliar carbon allowed

Table 5: Description for parameters specific to arable crops.

Parameter	Unit	Description
Post harvest leaf residue	fraction	Fraction of foliage carbon left as surface litter after harvest
Post harvest stem residue	fraction	Fraction of stem carbon left as surface litter after harvest
DR coefficient pre-flowering	day^{-1}	Development rate constant before flowering
DR coefficient post-flowering	day^{-1}	Development rate constant after flowering
Minimum development temperature	°C	Minimum temperature at which development occurs
Optimum development temperature	°C	Optimum temperature at which development occurs
Maximum development temperature	°C	Maximum temperature at which development occurs
Vernalization days	days	Number of days when plant is 50 % vernalized
Self shading LAI	m^2m^{-2}	Leaf area index at which foliage turnover occurs due to self shading
Maximum rate of self shading turnover	$hour^{-1}$	maximum rate of foliage turnover due to self shading
Critical photoperiod	hours	Minimum photoperiod required for development
Litter PAR reflectance	fraction	Post harvest litter reflectance for photosynthetically active radiation
Litter NIR reflectance	fraction	Post harvest litter reflectance for near infra-red radiation

References

M. J. Best, M. Pryor, D. B. Clark, G. G. Rooney, R. L. H. Essery, C. B. Menard, J. M. Edwards, M. A. Hendry, A. Porson, N. Gedney, L. M. Mercado, S. Sitch, E. Blyth, O. Boucher, P. M. Cox, C. S. B. Grimmond, and R. J. Harding. The Joint UK Land Environment Simulator (JULES), model description - Part 1: Energy and water fluxes. *Geosci. Model Dev.*, 4(3):677–699, 2011. doi: 10.5194/gmd-4-677-2011.

Andrew Fox, Mathew Williams, Andrew D. Richardson, David Cameron, Jeffrey H. Gove, Tristan Quaife, Daniel Ricciuto, Markus Reichstein, Enrico Tomelleri, Cathy M. Trudinger, and Mark T. Van Wijk. The REFLEX project: Comparing different algorithms and implementations for the inversion of a terrestrial ecosystem model against eddy covariance data. *Agric. For. Meteorol.*, 149(10):1597–1615, 2009. doi: 10.1016/j.agrformet.2009.05.002.

BE Medlyn, P Berbigier, R Clement, A Grelle, D Loustau, S Linder, L Wingate, PG Jarvis, BD Sigurdsson, and RE McMurtrie. Carbon balance of coniferous forests growing in contrasting climates: Model-based analysis. *Agric. For. Meteorol.*, 131(1-2):97–124, 2005. doi: 10.1016/j.agrformet.2005.05.004.

PL Nagler, Y Inoue, EP Glenn, AL Russ, and CST Daughtry. Cellulose absorption index (CAI) to quantify mixed soil-plant litter scenes. *Remote Sens. Environ.*, 87(2-3):310–325, OCT 15 2003. ISSN 0034-4257. doi: 10.1016/j.rse.2003.06.001.

A. L. O'Neill, J. A. Kupiec, and P. J. Curran. Biochemical and reflectance variation throughout a sitka spruce canopy. *Remote Sensing of Environment*, 80:134–142, 2002.

O. Sus, M. Williams, C. Bernhofer, P. Beziat, N. Buchmann, E. Ceschia, R. Doherty, W. Eugster, T. Gruenwald, W. Kutsch, P. Smith, and M. Wattenbach. A linked carbon cycle and crop developmental model: Description and evaluation against measurements of carbon fluxes and carbon stocks at several European agricultural sites. *Agr. Ecosyst. Environ.*, 139(3, SI):402–418, NOV 15 2010.

RH Waring, JJ Landsberg, and M Williams. Net primary production of forests: a constant fraction of gross primary production? *Tree Physiol.*, 18(2):129–134, 1998.

M. Williams, E. B. Rastetter, D. N. Fernandes, M. L. Goulden, S. C. Wofsy, G. R. Shaver, J. M. Melillo, J. W. Munger, S. M. Fan, and K. J. Nadelhoffer. Modelling the soil-plant-atmosphere continuum in a Quercus-Acer stand at Harvard Forest: the regulation of stomatal conductance by light, nitrogen and soil/plant hydraulic properties. *Plant Cell Environ.*, 19:911–927, 1996.

M Williams, W Eugster, EB Rastetter, JP McFadden, and FS Chapin. The controls on net ecosystem productivity along an Arctic transect: a model comparison with flux measurements. *Glob. Change Biol.*, 6(1):116–126, 2000.

M Williams, BE Law, PM Anthoni, and MH Unsworth. Use of a simulation model and ecosystem flux data to examine carbon-water interactions in ponderosa pine. *Tree Physiol.*, 21(5):287–298, 2001.

S. D. Wullschleger. Biochemical Limitations to Carbon Assimilation in C3 Plants - A Retrospective Analysis of the A/Ci Curves from 109 Species. *Journal of Experimental Botany*, 44:907–920, 1993.